RESEARCH REPORT

HEALTH EFFECTS INSTITUTE

Number 110
December 2002

Particle Characteristics Responsible for Effects on Human Lung Epithelial Cells

Ann E Aust, James C Ball, Autumn A Hu, JoAnn S Lighty, Kevin R Smith, Ann M Straccia, John M Veranth, and Willie C Young

Includes a Commentary by the Institute's Health Review Committee

HEALTH
EFFECTS
INSTITUTE

The Health Effects Institute, established in 1980, is an independent and unbiased source of information on the health effects of motor vehicle emissions. HEI studies all major pollutants, including regulated pollutants (such as carbon monoxide, ozone, nitrogen dioxide, and particulate matter) and unregulated pollutants (such as diesel engine exhaust, methanol, and aldehydes). To date, HEI has supported more than 200 projects at institutions in North America and Europe and has published over 130 research reports.

Typically, HEI receives half its funds from the US Environmental Protection Agency and half from 28 manufacturers and marketers of motor vehicles and engines in the United States. Occasionally, funds from other public and private organizations either support special projects or provide resources for a portion of an HEI study. Regardless of funding sources, HEI exercises complete autonomy in setting its research priorities and in reaching its conclusions. An independent Board of Directors governs HEI. The Institute's Health Research and Health Review Committees serve complementary scientific purposes and draw distinguished scientists as members. The results of HEI-funded studies are made available as Research Reports, which contain both the Investigators' Report and the Review Committee's evaluation of the work's scientific quality and regulatory relevance.

HEI STATEMENT
Synopsis of Research Report 110

Effects of Metals Bound to Particulate Matter on Human Lung Epithelial Cells

INTRODUCTION

Inhaled particulate matter has been associated with both acute and chronic health effects. Concerns about these effects derive primarily from epidemiologic studies that associate short-term increases in particle concentration with increases in daily morbidity and mortality from respiratory and cardiovascular diseases. Over the past decade much research has been directed toward identifying plausible mechanisms linking particulate matter and pathophysiologic effects. Although progress has been made, many critical aspects are not understood. Thus, studies of the properties of particles that might induce pathologic effects are critical to establishing the mechanisms of particulate matter toxicity and to producing information necessary to target regulation of the sources that generate the most toxic particles.

Studies using laboratory animals have implicated metals associated with particulate matter in adverse health effects. Coal-fired power plants produce particulate residues called *fly ash*. Coal contains metals that vaporize during combustion and then condense on the surface of the ash. Inhaled coal fly ash could be a health hazard because metals solubilized from fly ash within lung cells may cause toxic reactions.

APPROACH

Dr Ann Aust and colleagues at Utah State University, the University of Utah, the University of California, Davis, and Ford Motor Company hypothesized that transition metals (metals that can participate in possibly toxic oxidative reactions) associated with particulate matter are released within lung epithelial cells and catalyze the formation of reactive oxygen species. Reactive oxygen species can stimulate epithelial cells to produce inflammatory mediators that contribute to lung inflammation and injury. The investigators focused their study on coal fly ash that was produced in the laboratory and separated into four size fractions. (They also performed experiments using particles from gasoline and diesel exhaust, natural soils, and ambient Utah air.) This multifaceted study focused mainly on the ability of iron (the major transition metal in coal fly ash) to produce reactive oxygen species and inflammatory mediators in cultured lung epithelial cells.

RESULTS AND INTERPRETATION

This study was performed by experienced investigators with demonstrated excellence in the area of metal-catalyzed oxidative stress and particle-associated injury. The study was of high scientific quality, was well conceived and executed, and adds substantially to our knowledge of the biologic properties of particles.

Aust and colleagues found that more iron was released from the smaller particles than from larger ones. They confirmed that soluble extracts of coal fly ash generated reactive oxygen species in vitro and that transition metals were likely responsible. Further, the smallest particles, which were rich in iron, were the most active. The investigators then examined the effects of coal fly ash on human lung epithelial cells in culture. First, they demonstrated that coal fly ash particles entered the cells and stimulated synthesis of the protein ferritin. Ferritin binds iron and is produced in response to increasing iron levels; thus, its presence indicates that iron was released intracellularly and that iron was available to provoke an inflammatory response by forming reactive oxygen species. The investigators obtained indirect evidence for formation of intracellular reactive oxygen species by demonstrating that lung epithelial cells exposed to coal fly ash synthesized the inflammatory mediator interleukin-8. Ferritin and interleukin-8 production were stimulated to a greater degree by smaller particles than by larger ones. Thus, the investigators provided a plausible connection among the intracellular

This Statement, prepared by the Health Effects Institute, summarizes a research project funded by HEI and conducted by Dr Ann E Aust of Utah State University, Logan UT. The following Research Report contains the detailed Investigators' Report and a Commentary on the study prepared by the Institute's Health Review Committee.

release of a transition metal from particles, formation of reactive oxygen species, and lung inflammation.

These findings may be important. To confirm their in vitro results, Aust and colleagues will measure ferritin levels in lung tissue and fluids from rats exposed to coal fly ash. The current results that smaller particles had greater effects supports the epidemiologic studies on the adverse effects of fine and ultrafine particles. Other components or properties of particles have also been proposed to cause lung injury; therefore, there may be multiple mechanisms by which inhaled particles produce adverse health effects. Further research to identify particle characteristics (and sources) responsible for particulate matter toxicity is important for developing increasingly effective and appropriate air quality regulations, as noted in HEI Perspectives, *Understanding the Health Effects of Components of the Particulate Matter Mix: Progress and Next Steps*.

Library of Congress Catalog Number for the HEI Report Series: WA 754 R432.
The paper in this publication meets the minimum standard requirements of the ANSI Standard Z39.48-1984 (Permanence of Paper) effective with Report 21 in December 1988; and effective with Report 92 in 1999 the paper is recycled from at least 30% postconsumer waste with Reports 25, 26, 32, 51, 65 Parts IV, VIII, and IX, 91 and 105 excepted. These excepted Reports are printed on acid-free coated paper.

HEI

CONTENTS

Research Report 110

HEALTH EFFECTS INSTITUTE

Particle Characteristics Responsible for Effects on Human Lung Epithelial Cells

Ann E Aust, James C Ball, Autumn A Hu, JoAnn S Lighty, Kevin R Smith, Ann M Straccia, John M Veranth, and Willie C Young

Department of Chemistry and Biochemistry, Utah State University, Logan, Utah; Institute of Toxicology and Environmental Health, University of California, Davis, California; Department of Chemical and Fuels Engineering, University of Utah, Salt Lake City, Utah; and Ford Motor Company Scientific Research Laboratory, Dearborn, Michigan

HEI STATEMENT

This Statement is a nontechnical summary of the Investigators' Report and the Health Review Committee's Commentary.

INVESTIGATORS' REPORT

When an HEI-funded study is completed, the investigators submit a final report. The Investigators' Report is first examined by three outside technical reviewers and a biostatistician. The Report and the reviewers' comments are then evaluated by members of the HEI Health Review Committee, who had no role in selecting or managing the project. During the review process, the investigators have an opportunity to exchange comments with the Review Committee and, if necessary, revise the report.

Continued

COMMENTARY Health Review Committee

The Commentary about the Investigators' Report is prepared by the HEI Health Review Committee and Staff. Its purpose is to place the study into a broader scientific context, to point out its strengths and limitations, and to discuss remaining uncertainties and implications of the findings for public health.

RELATED HEI PUBLICATIONS

Publishing History: This document was posted as a preprint on *www.healtheffects.org* and then finalized for print.

Citation for whole document:

Aust AE, Ball JC, Hu AA, Lighty JS, Smith KR, Straccia AM, Veranth JM, Young WC. 2002. Particle Characteristics Responsible for Effects on Human Lung Epithelial Cells. Research Report 110. Health Effects Institute, Boston MA.

When specifying a section of this report, cite it as a chapter of the whole document.

Particle Characteristics Responsible for Effects on Human Lung Epithelial Cells

Ann E Aust, James C Ball, Autumn A Hu, JoAnn S Lighty, Kevin R Smith, Ann M Straccia, John M Veranth, and Willie C Young

ABSTRACT

Some recent epidemiologic investigations have shown an association between increased incidence of respiratory symptoms and exposure to low levels of particulate matter (PM*) less than 10 µm or less than 2.5 µm in aerodynamic diameter (PM_{10} and $PM_{2.5}$, respectively). If particulates are causally involved with respiratory symptoms, it is important to understand which components may be responsible. However, increasing evidence suggests that transition metals present in particles, especially iron, generate reactive oxygen species (ROS) that may be involved in producing some of the observed respiratory symptoms.

The hypothesis for this study is twofold:

- bioavailable transition metals from inhaled airborne particulates catalyze redox reactions in human lung epithelial cells, leading to oxidative stress and increased production of mediators of pulmonary inflammation; and
- the size, transition metal content, and mineral speciation of particulates affect their ability to cause these effects.

This work focused on the relation between physical characteristics of particles (eg, size, bioavailable transition metal content, and mineral speciation) and their ability to generate hydroxyl radicals in cell-free systems and to cause oxidative stress, which results in the synthesis of mediators of pulmonary inflammation in cultured human lung epithelial cells. These relations were studied by comparing size-fractionated, chemically characterized coal fly ash (CFA) produced by combustion of three different coals to obtain milligram quantities of ash. One transition metal, iron, was studied specifically because it is by far the predominant transition metal in CFA. In addition, smaller quantities of particles from gasoline engines, diesel engines, and ambient air were studied.

Phosphate buffer soluble fractions from particles from all sources were capable of generating ROS, as measured by production of malondialdehyde (MDA) from 2-deoxyribose. This activity was inhibited over 90% for all particles by the metal chelator *N*-[5-[3-[(5-aminopentyl)hydroxycarbamoyl]propionamido]-pentyl]-3-[[5-(*N*-hydroxyacetamido)pentyl]carbamoyl]propionohydroxamic acid (desferrioxamine B, or DF), strongly suggesting that transition metal(s), probably iron, were responsible. Particles from coal or gasoline combustion had greater ability to produce ROS than particles from diesel combustion. Iron was mobilized by citrate (at pH 7.5) from particles of all sources tested; gasoline combustion particles were the only particles not analyzed for iron mobilization because there were not enough particles for the iron mobilization assay. CFA particles were size-fractioned; the amount of iron mobilized by citrate was inversely related to the size of particles and also depended on the source of coal. Iron from the CFA particles was responsible for inducing the iron-storage protein ferritin in cultured human lung epithelial cells (A549 cells). The amount of iron mobilized by citrate was directly proportional to the amount of ferritin induced in the A549 cells. Iron from the CFA was also responsible for inducing the inflammatory mediator interleukin (IL) 8 in A549 cells. Iron existed in several species in the fly ash, but the bioavailable iron was associated with the glassy aluminosilicate fraction, which caused ferritin and IL-8 to be induced in the A549 cells.

In crustal dust, another component of urban particulates, iron was associated with oxides and clay but not with aluminosilicates. The crustal dust contained almost

* A list of abbreviations and other terms appears at the end of the Investigators' Report.

This Investigators' Report is one part of Health Effects Institute Research Report 110, which also includes a Commentary by the Health Review Committee and an HEI Statement about the research project. Correspondence concerning the Investigators' Report may be addressed to Dr Ann E Aust, Department of Chemistry and Biochemistry, 300 Old Main Hill, Utah State University, Logan UT 84322-0300.

Although this document was produced with partial funding by the United States Environmental Protection Agency under Assistance Award R82811201 to the Health Effects Institute, it has not been subjected to the Agency's peer and administrative review and therefore may not necessarily reflect the views of the Agency, and no official endorsement by it should be inferred. The contents of this document also have not been reviewed by private party institutions, including those that support the Health Effects Institute; therefore, it may not reflect the views or policies of these parties, and no endorsement by them should be inferred.

no iron that could be mobilized by citrate. Iron could be mobilized from diesel combustion particulates, but at a much lower level than for all other combustion particles. Samples of ambient $PM_{2.5}$ collected in Salt Lake City over 5-day periods during one month varied widely in the amount of iron that could be mobilized.

If bioavailable transition metals (eg, iron) are related to the specific biological responses outlined here, then the potential exists to develop in vitro assays to determine whether particulates of unknown composition and origin can cause effects similar to those observed in this study.

INTRODUCTION

Some recent epidemiologic investigations have shown an association between exposure to ambient levels of PM_{10}, which is small enough to penetrate beyond the upper airways, and several statistics: increased incidence of respiratory symptoms (Dockery et al 1989; Pope 1989), increased rate of pulmonary-related hospitalizations (Dockery et al 1989; Pope 1991; Pope and Dockery 1992; Schwartz 1994a; Schwartz and Morris 1995), decreased pulmonary function (Dockery et al 1982; Pope and Dockery 1992), and increased daily mortality rates (Dockery et al 1993; Schwartz 1994b, 1994c). One comparison of daily mortality associated with fine particles ($PM_{2.5}$) or coarse particles (PM_{10}) measured in six eastern US cities over eight years showed the strongest association between $PM_{2.5}$ levels and increased daily mortality (Schwartz et al 1996). Deaths and monthly pollution levels are not always correlated, however, which indicates that the composition of pollution can vary (RMCOEH 1996). Many time-series studies have been criticized, however, because health effects are not always associated with daily PM_{10} increases or because they did not account for possible effects of confounding by other pollutants (Moolgavkar et al 1995; Health Effects Institute 1995, 1997; Moolgavkar and Luebeck 1996; Chen et al 1999). A recent study has shown that episodes of stagnant air pollution with a higher concentration of primary and secondary combustion-source particles correlated better with elevated mortality than did episodes of windblown dust with relatively higher concentrations of coarse crustal-derived particles (Pope et al 1999). If PM is shown to cause increased mortality, it will be very important to understand what factors may contribute to the toxicity of airborne particulates.

Particles vary in size, morphology, elemental composition, and chemical speciation. Fugitive dusts (including those from roads, agricultural operations, and wind erosion) are the predominant source of PM_{10} in the US, whereas emissions from manufacturing and combustion usually comprise only 6% to 9% by weight of total PM_{10} emissions (US Environmental Protection Agency [EPA] 1994). However, the latter emission sources may contribute more to toxicity than the fugitive dusts because (1) they comprise a large component of the fine ($PM_{2.5}$) fraction of PM_{10} (Houck et al 1990), which can reach the lower respiratory tract, and (2) some of its primary inorganic components (including sulfates and certain metals) potentially have greater toxicologic significance than the relatively inert minerals of fugitive dusts (Amdur et al 1978; Knecht et al 1985; Amdur et al 1986; Linn et al 1989; Doll 1990; Chen et al 1992; Benson et al 1995; Dusseldorp et al 1995).

Particles formed from combustion are affected by fuel composition and combustion conditions. The composition of particle emissions from fuels used for stationary combustion (eg, coal or residual fuel oil) contain larger amounts of inorganic components (including transition metals) than emissions from mobile sources, which burn distillate fuels. At least in coal combustion, metals appear to vaporize and then condense on submicron (PM_1) particles and therefore may be present at a higher relative proportion by weight on fine ($PM_{2.5}$) and ultrafine (PM_1) particles than on coarse particles (Linak and Wendt 1994). In addition, the speciation of metals, and in turn their solubility and reactivity, can be affected by combustion conditions. These differences may help determine the possible health effects of inhalation and other environmental effects of PM_{10}, $PM_{2.5}$, and PM_1 particles. One of the major impediments to studies of a toxicologic mechanism that may link particle characteristics to acute health effects is the difficulty of obtaining sufficient quantities of size-fractionated, chemically characterized particles in the respirable sizes of interest. In this study, methods were developed to generate enough CFA to compare the effects of coal sources and particle size on generation of ROS, the mobilization of iron in vitro and in cultured cells, and the induction of inflammatory mediators.

The remainder of the introduction reviews what is known about particles that contain transition metals, from both noncombustion and combustion sources. This review outlines the conditions leading to mobilization of the metals from the particles, the reactivity of the metals, and how this reactivity affects intact cells and whole animals.

ASBESTOS

Asbestos is a naturally occurring mineral fiber that contains iron. Much has been learned about the biochemical and biological effects of iron both from asbestos and from the environment. This work has yielded methods of

determining the amount of bioavailable iron and information about species of iron that release bioavailable iron. Asbestos is a family of two naturally occurring silicates that differ in crystalline structure: the amphiboles and the serpentines. Although fiber dimension and durability have been shown to be important in the carcinogenic process, the molecular mechanism by which asbestos causes cancer and other biological effects remains unknown. The chemical characteristics of the fibers' surface and the chemical reactions catalyzed by asbestos and other mineral fibers may contribute substantially to their pathologic effects. The amphiboles, crocidolite [$Na_2Fe^{III}_2(Fe^{II},Mg)_3Si_8O_{22}(OH)_2$] and amosite [$(Fe^{II},Mg)_7(Si_8O_{22})(OH)_2$] are more carcinogenic in humans than the serpentine, chrysotile [$Mg_3[Si_2O_5](OH_4)$]. The amphiboles contain about 27% iron by weight, whereas chrysotile contains only 2% to 3% iron as a structural substitute for magnesium. Iron mobilized from asbestos fibers has been found to be responsible for oxygen (O_2) consumption (Aust and Lund 1991; Lund and Aust 1991), $HO^{\bullet}$ generation (Weitzman and Graceffa 1984; Aust and Lund 1991; Kamp et al 1992), lipid peroxidation (Weitzman and Weitberg 1985; Gulumian and Wyk 1987), DNA oxidation (Takeuchi and Morimoto 1994), activation of Src kinase, induction of the inducible form of nitric oxide synthase (iNOS) (Chao et al 1996), and induction of breaks in single-strand DNA (Lund and Aust 1992). Iron was also mobilized from asbestos both in vivo (Holmes and Morgan 1967; Hart et al 1980) and in A549 cells, reaching an intracellular concentration of 1.4 mM in 24 hours (Chao et al 1994). The percentages of iron mobilized from crocidolite in these A549 cells over 24 hours was very similar to the percentage mobilized by citrate in vitro in the same time (Lund and Aust 1992). In the cell, the mobilized iron was found in proteins and in a low molecular weight (LMW) fraction (< 10,000 daltons) (Chao et al 1994). At a treatment dose of 6 µg crocidolite/cm^2, the intracellular concentration of iron mobilized into the low-molecular-weight fraction was 22 µM. Cytotoxicity of the crocidolite to the A549 cells was directly correlated with the amount of iron mobilized into this low-molecular-weight fraction, suggesting that this fraction contained active redox iron. Exposure to crocidolite fibers induced synthesis of the iron-storage protein ferritin if the fibers were endocytosed (Chao et al 1994).

In summary, the most carcinogenic asbestos fibers contain high levels of iron that can be mobilized from the fibers inside cells, leading to a variety of biological effects, including activation of phosphorylation signalling cascades, induction of iNOS, and DNA oxidation. Results from the studies discussed above strongly suggest that estimates of the amount of iron that can be mobilized by citrate in solution at pH 7.5 is a very good predictor of how much iron can be mobilized inside cells, as indicated by ferritin induction. Thus, these techniques may be useful for determining how much iron from other types of particles, including combustion particles, is bioavailable.

RESIDUAL OIL FLY ASH

Fuel oil combustion produces much less ash than coal combustion because coal contains high levels of crustal elements (aluminum, silicon, and calcium). However, ash from oil contains very high concentrations of alkali and transition metals (sodium, vanadium, iron, and nickel). Content of the latter three seems to be very important to the toxicity of the residual oil fly ash (ROFA) studied most recently (discussed in detail below). The sodium, vanadium, and nickel are concentrated in the heavier (higher boiling point) refinery streams, especially in residual oil left after distillation (Stultz and Kitto 1992). Residual oil sales have decreased since their peak in the 1970s because of improved refining technology and fuel substitution by customers. Many refineries no longer produce residual oil for fuel use. However, the unique composition of oil ash has been useful for identifying the mechanisms by which combustion particles affect cells.

The ROFA used in the studies discussed here was collected by researchers at the Southern Research Institute, Birmingham, Alabama, in a polytetrafluoroethylene (PTFE)-coated fiberglass filter placed downstream from the cyclone of a power plant in Florida that was burning low-sulfur #6 residual oil (Hatch et al 1985). Collected in this way, ROFA has a mean diameter of 0.5 µm and a high metal content. This particular ROFA is especially high in vanadium (19%) but also has high levels of iron (3.5%) and nickel (3.8%) (Pritchard et al 1996). Venezuelan fuel oils are typically high in vanadium, but the element is also found in other fuel oils and in coal. The concentration is usually at 1/10 or 1/100 the concentration of iron, but almost never at concentrations higher than iron. While the fuel oil used to produce this ROFA is not representative of most of the fuels currently used in the US, results from studies using this ROFA have been useful in identifying components of the oil that may cause pulmonary injury and disease.

Whole-Animal Studies

Intratracheal instillation of a relatively high dose (2.5 mg/animal) of ROFA in rats resulted in acute pulmonary injury characterized by neutrophilic alveolitis, edema, airway hyperreactivity, and increased susceptibility to microbial infections (Pritchard and Ghio 1993; Costa and Dreher 1997). The pulmonary injury induced by ROFA

seemed to be associated with its high content of transition metals (vanadium, nickel, iron). These metals are capable of generating ROS by reducing molecular oxygen and may be involved in the pathologic effects sometimes observed when the metals are present in the lung. More recent work supports the hypothesis that transition metals are involved in the toxic effects of ROFA in rodent lungs (Costa and Dreher 1997; Dreher et al 1997; Kodavanti et al 1997) and that the effects in some cases are mediated by ROS (Dye et al 1997). Transition metals in ROFA also seemed to be responsible for ROFA's adverse effects in a rat model of cardiopulmonary disease (pulmonary vasculitis and hypertension) induced by monocrotaline injection (Costa and Dreher 1997). An acid leachate of ROFA, containing predominantly iron, vanadium, and nickel, elicited the same responses when instilled in the lungs of rats as did the particulates before leaching (Dreher et al 1997). Solutions of iron, vanadium, and nickel prepared in the laboratory and instilled in the lungs of rats produced similar effects. After the metals were leached, however, the particles only minimally affected the rat lungs. These results suggest that transition metals in the particles play a key role in the pathology of the inhaled particles. When present at high levels, zinc also played a role (Gavett et al 1997) although the molecular mechanism by which zinc induces lung toxicity remains unknown. In summary, the results from experiments with rats strongly suggest that the transition metals vanadium, iron, and nickel are responsible for much of the acute pathology observed after instillation of ROFA.

Macrophages

Investigations of ROFA-induced effects on cell cultures have increased our understanding of how particles affect cells and, therefore, how these particles may affect the lung. Human epidemiologic data suggest that inhalation of air pollutants may be associated with an increased incidence and severity of acute respiratory infections. During investigations of whether particulate air pollutants alter pulmonary host defenses, Hatch and colleagues (1985) observed that relatively high doses of ROFA were very toxic to rabbit alveolar macrophages and induced high levels of mortality in mice exposed to a *Streptococcus* species. After examining ROFA and the other particulates, they concluded that the presence of metals or metal oxides in the particulates correlated with the toxicity to macrophages. These studies agreed with earlier work (Aranyi et al 1979; Mumford and Lewtas 1982). More recent studies, showed that the ROFA particles caused a rapid burst in respiration in human alveolar macrophages and became very toxic even after only 2 hours of exposure (Becker et al 1996). The ROFA induced little or no tumor necrosis factor (TNF) or IL-6 in human or rat macrophages. Thus, although the alveolar macrophage has long been assumed to be the cell type responsible for releasing mediators that result in inflammatory influx after particle exposure, this does not appear to be the case for rat and human alveolar macrophages exposed to ROFA particles in vitro.

In summary, the predominant impact of relatively high doses of ROFA on the alveolar macrophage is toxicity, which may lead to increased bacterial infection in rat lung.

Airway Epithelial Cells

There is growing recognition that airway epithelial cells not only serve as a critical air–blood barrier but also may play an important role in producing inflammatory mediators after stimulation by a variety of inhaled gases and particles. Following reports that airway epithelial cells produce inflammatory mediators (ie, IL-6, IL-8, and TNF) after having been exposed to ozone (Devlin et al 1994), there have been several investigations of ROFA-induced release of mediators from airway epithelial cells. Samet and colleagues (1996) observed the induction of prostaglandin H synthase 2 and increased secretion of prostaglandins E_2 (PGE_2) and $F_{2\alpha}$ ($PGF_{2\alpha}$) in ROFA-treated normal human airway epithelial cells and SV-40 transformed human bronchial epithelial cells. There were no increases in prostaglandin H synthase 1 or in the rate of arachidonic acid release, incorporation, or availability in ROFA-treated cells. Because PGE_2 sensitizes sensory neurons and mediates bronchodilation (Perl 1976) and vasodilation (Downey et al 1988), and because $PGF_{2\alpha}$ is a bronchoconstrictor (Downey et al 1988; Smith and DeWitt 1995), these findings suggest that prostaglandins may be involved in the toxicology of air pollution particle inhalation. The mechanism by which ROFA induces prostaglandin H synthase 2 was not explored but may be due to the generation of ROS catalyzed by the transition metals present in the particles. Prostaglandin H synthase 2 is induced by agents (eg, IL-1, TNF-α, and lipopolysaccharide) that mediate the production of prostaglandins by ROS in cells. The researchers speculated that ROFA activates the transcription factor called nuclear factor-κB (NF-κB) via phosphorylation signalling pathways. Vanadium, present in high concentrations in ROFA, is a potent inhibitor of the protein tyrosine phosphatase (Gordon 1991) that can activate the NF-κB signal transduction pathway (Schieven et al 1993; Imbert et al 1994).

ROFA also induced the expression of TNF, IL-6, and IL-8 in normal human bronchial epithelial cells (Carter et al 1997). The metal chelator DF and the radical scavenger dimethylthiourea (DMTU) inhibited this induction,

whereas vanadium, but not iron or nickel, appeared to be totally responsible for inducing it. Because the inhibition by DMTU suggests that ROS were involved in the cytokine induction, it was surprising that iron and nickel were not capable of causing these effects individually. However, Carter and colleagues (1997) rightfully emphasized that how these metals enter epithelial cells and what chelates are formed in the cells are not completely understood. Because the chelate determines the redox activity, iron and nickel chelates may not be as reactive as vanadium chelates. Vanadium also can directly inhibit tyrosine phosphatases by binding directly to the enzyme. Thus, vanadium may exert an effect beyond the catalysis of ROS that is important for cytokine induction in airway epithelial cells.

To better understand whether vanadium in ROFA affects phosphorylation signalling pathways, SV-40 transformed human bronchial epithelial cells (BEAS cells) treated with ROFA were analyzed for tyrosine kinase activity and phosphatase activity. ROFA and vanadium-containing solutions activated phosphorylation signalling pathways in BEAS cells, whereas solutions containing iron or nickel did not affect these pathways (Samet et al 1997). Tyrosine kinase activity appeared unaffected, but tyrosine phosphorylase activity was inhibited, supporting the additional role of vanadium in the activation of these pathways.

The effects of ROFA in primary rat lung epithelial cells have also been examined. The particles caused release of lactate dehydrogenase (LDH) and glutathione-associated enzymes from treated cells, and a decrease in intracellular total glutathione (Dye et al 1997). Cotreatment with a nitric oxide (NO) synthase inhibitor, *N*G-monomethyl-D-arginine, did not affect these parameters, suggesting that enzymatically generated NO had no role in these effects. However, cotreatment with DMTU inhibited both LDH release induced by ROFA and permeability changes in a dose-dependent manner. This result implicates ROS, probably hydroxyl radical, in the observed damage.

In summary, treatment of airway epithelial cells in culture with ROFA resulted in production of PGE_2 and $PGF_{2\alpha}$, TNF, IL-6, and IL-8. Vanadium in the ROFA probably induced TNF, IL-6, and IL-8 although this conclusion is subject to confirmation by further experiments.

COAL FLY ASH

Particle Formation

CFA formed in coal-fired boilers has a bimodal size distribution; most of the particles are large (PM > 10 µm in aerodynamic diameter [$PM_{>10}$]), and the rest are submicron particles (McCain et al 1975; McElroy et al 1982). The larger particles are similar in mineral composition to the parent coal (Sarofim et al 1977). CFA PM_1 particles are thought to be more environmentally relevant than $PM_{>10}$ for two reasons: Industrial scrubbing devices are least effective at removing particles 0.1 to 1 µm in diameter (Shendrikar et al 1983); and smaller particles are rich in toxic metals (Linak and Wendt 1994; Ratafia-Brown 1994). High temperatures in the boilers volatilize metals, thereby enriching the smaller particles in toxic metals through a process of vaporization, nucleation, condensation, and particle growth (Neville et al 1981). The different species deposit on particles as they cool while moving through the exhaust, which gives particles a layered structure (Neville and Sarofim 1982; Linak and Wendt 1994). In addition to metallic enrichment of the submicron particles, high-temperature combustion also increases formation of glassy aluminosilicates (Zeng 1998). The mineral composition of the parent coal determines which species are contained in the smaller particles (Quann and Sarofim 1982; Linak 1985).

Toxicity Studies

The CFA samples used in the studies reviewed here were from a variety of sources and the samples were poorly characterized. This incomplete description of CFAs in many studies does not allow accurate comparisons among coal types and combustion conditions. This remains a major problem in studies of many types of particles.

Intratracheal instillation of CFA (5–45 mg/animal) in rats resulted in only very mild to moderate fibrosis (Schreider et al 1985). The pathology observed was similar to those from other nuisance dusts at the same dose level. Extensive human epidemiologic studies of CFA are lacking, but studies based on electricity workers in the United Kingdom did not show convincing evidence of pneumoconiosis (Bonnell et al 1980). These studies did show, however, impairment of lung function and respiratory symptoms after prolonged, heavy exposures (Schilling et al 1988).

In vitro studies showed that CFA was toxic using a number of conventional tests with animal lung cells (Gormley et al 1979), human red blood cells (Liu et al 1986), and hamster ovary cells (Garrett et al 1981). In general, CFA was less toxic than crystalline silica, but significantly more toxic than negative controls (eg, TiO_2 or latex beads).

Almost no in vitro or in vivo data are available about the effects of CFA on markers recently shown to be important to ROFA toxicity. These include proinflammatory cytokines (TNF, IL-8), growth factors (tumor growth factor-β [TGF-β]), the generation of ROS (indicated by breaks in single strands of supercoiled DNA), and possibly

transition metals, especially iron, that may contribute to the pathologic effect of ROFA particles.

URBAN PARTICULATES

In Vitro Assays

Smith and Aust (1997) investigated the ability of urban particulates (Standard Reference Material [SRM] 1648 that contains 3.9% iron, collected in St Louis, Missouri, and SRM 1649 that contains 3% iron, collected in Washington DC) to release iron and generate ROS. Iron was mobilized from each particulate at pH 7.5 only in the presence of a chelator, either citrate or EDTA. More iron was mobilized from SRM 1649 than from SRM 1648 even though SRM 1648 contains more iron per unit mass. The particles produced ROS, as assessed by breaks in single strands of supercoiled DNA, only in the presence of citrate or EDTA along with ascorbate, a reductant. To determine whether iron was responsible for the generation of the ROS, the particles were incubated with DF for 24 hours before and 24 hours during the assay. This incubation inhibited activity completely, strongly suggesting that iron was responsible for the production of ROS because iron, but not other transition metals, is completely inhibited by DF. The researchers also determined that the iron was active after it was mobilized by citrate but not while it was on the particle.

Donaldson and colleagues (1997) also investigated whether PM_{10} (collected in Edinburgh, UK, at the Enhanced Urban Network sampling site) is capable of generating ROS that damages supercoiled plasmid DNA in vitro. The PM_{10} caused damage that appeared to be mediated by $HO^{\bullet}$; inhibition of the damage by DF strongly suggested that iron is involved. The PM_{10} contained large amounts of iron, and iron was leached from the particles, predominantly as Fe(III). Thus, the component of iron that generates radicals was released into solution and could be completely separated from the particles.

Ghio and colleagues (1996) examined whether humic-like substances, resulting from incomplete combustion, can bind transition metals present in urban particulates. They found these substances in combustion particulates produced from coal, diesel, oil, and wood, and there was some evidence that the substances were also in urban PM_{10}. Although the amount of humic-like substances present in urban PM_{10}, the amount of transition metals present, and the ability to generate ROS were weakly correlated, no data showed an actual interaction between the metals and the substances. Thus, speciation of the metals remained unclear. Ghio and colleagues (1999b) found that sulfate content and iron concentrations were correlated in acid extracts of 20 filters from Utah. In addition, laboratory-generated iron-sulfate complexes were water soluble and redox active. The authors concluded that the correlation between iron and sulfate content in the urban PM_{10} was likely the result of sulfate functioning as a ligand for the metal after it is mobilized from an oxide by photoreduction. However, this conclusion is highly speculative because there is no firm evidence for an iron-sulfate interaction in the PM_{10}. Firm evidence for this awaits Mössbauer analysis of urban particulate matter.

In summary, these studies by different investigators show that urban particles from a variety of sources can generate ROS and can induce inflammatory cytokines. Transition metals are probably responsible for the observed effects.

Cultured Cells

Human Lung Epithelial Cells Smith and Aust (1997) investigated whether iron associated with urban particulates (SRMs 1648 and 1649), which had been mobilized in vitro by citrate, could also be mobilized inside human lung epithelial cells. They found that iron was indeed mobilized, as determined by induction of the iron-storage protein ferritin. The amount of ferritin induced was directly related to the amount of iron mobilized by citrate in cell-free solution. As has been observed in the cell-free mobilization assays, the amount of iron mobilized in human cells did not correlate with the total iron content of the particles.

Frampton and colleagues (1999) examined aqueous extracts from PM_{10} filters for their ability to produce oxidants and toxic effects in BEAS-2B cells. The filters were obtained from the Utah Valley monitoring station a year before (year 1), during (year 2), and after (year 3) closure of the local steel mill. Samples from year 2 had the lowest concentration of transition metals. Dust from year 3 alone caused cytotoxicity (measured by LDH release), and dust from years 1 and 3 alone induced expression of IL-6 and IL-8.

Ghio and colleagues (1999a) determined that the ability of ambient particles (from North Provo UT) to induce oxidants and IL-8 in cultured respiratory epithelial cells correlated more strongly with content of ionizable metals than did total metal content.

Kennedy and colleagues (1998) found that particulates collected in Provo, Utah stimulated IL-6, IL-8, and intercellular adhesion molecule-1 synthesis in cultured BEAS-2B cells and stimulated IL-8 secretion in primary cultures of human bronchial epithelium. Cytokine secretion was preceded by NF-κB activation and was reduced in cultures containing superoxide dismutase, DF, or *N*-acetyl-L-cysteine, which boost intracellular glutathione levels. The

effects were replicated with copper(II) found in particle extracts. Mucin, present in lung lining fluid, inhibited these effects, whereas ceruloplasmin, a copper-containing protein, stimulated them. These results suggest that copper can induce inflammatory cytokines and that copper in particulates may contribute to observed biological effects.

Macrophages Hadnagy and Seemayer (1994) observed substantial inhibition of phagocytosis by human monocyte–derived macrophages treated with different extracts of airborne particulates collected in the highly industrialized Rhine-Ruhr area. This result was in good agreement with those from in vivo experiments on bronchoalveolar-lavaged macrophages from rodents (Kiell et al 1993). Neither the mechanism of inhibition nor the responsible component was identified.

Becker and colleagues (1996) investigated whether urban particles from St Louis (SRM 1648), Washington (SRM 1649), Dusseldorf, and Ottawa (EHC-93) were capable of activating human alveolar macrophages. A small but significant chemiluminescence response was observed after treating human macrophages with the particles from Dusseldorf and Ottawa. The particles may have induced TNF and IL-6 because they contain endotoxin, as the response was inhibited by polymyxin B. Holian and colleagues (1998) found that SRMs 1648 and 1649 induced apoptosis and caused a phenotypic shift to a higher state of immunoactivity in human alveolar macrophages. The researchers suggested that if this happened in vivo, lung inflammation and a possible increase in pulmonary and cardiovascular disease would result. Because it is now known that both SRMs are contaminated with endotoxin, however, it is not clear whether these effects were due to the particles themselves or to the endotoxin they contain.

IRON PARTICLES

Human Lung Epithelial Cells

The number of studies of iron-containing, noncombustion particles has increased over the past few years. Stringer and Imrich (1996) investigated whether A549 cells would take up particles including hematite (Fe_2O_3). The results indicate that the iron oxide particles were taken up, and that this uptake may have involved a receptor for a scavenger-like macrophage. Wesselius and colleagues (1996) found that alveolar macrophages removed by lavage from the lungs of rats after instillation of Fe_2O_3 contained increased amounts of iron and ferritin. Samet and colleagues (1998) conducted a more extensive investigation of several transition metals, including ferrous sulfate ($FeSO_4$), to determine whether they could activate mitogen-activated protein kinases (MAPKs) in BEAS-2B cells (Reddel et al 1988). Salts of arsenic, vanadium, zinc, and, to some extent, copper and chromium, induced MAPK. These metals also activated extracellular receptor kinase (ERK), c-Jun NH_2-terminal kinase (JNK), and p38, part of the MAPK signaling pathway. The substrates for the two kinases, activating transcription factor-2 (ATF-2) and c-Jun, were markedly phosphorylated. Interestingly, the presence of iron was not associated with increases in ERK, JNK, or p38. Because of the unusual chemical properties of iron salts, the manner in which the solutions were prepared may have led to precipitation of the iron as an oxide or an oxyhydroxide. The treatment times in the study were too short to allow sufficient time for any precipitate to be taken up by the cells.

Human Lung

In subsequent studies, Ghio and colleagues (1998) examined the effects of iron-containing particles generated from colloidal iron oxide on ferritin induction and the levels of transferrin, transferrin receptor, and lactoferrin receptor in human lungs. Although the majority of the iron in the generated particles was Fe_2O_3, a portion was an unidentified iron salt or an iron oxyhydroxide. They found that concentrations of ferritin in the lavage fluid increased significantly, that transferrin significantly diminished, and that lactoferrin and transferrin receptor concentrations were significantly elevated. The authors concluded that introduction of this iron-containing particle disrupted normal iron homeostasis.

Further studies using these particles (Lay et al 1999) showed that they induced transient acute inflammation in human lungs and in rats during the first day after instillation. The inflammatory response was resolved in 4 days. The authors concluded that the postexposure inflammation might be due in part to the ROS generated by the iron in the particles. They also determined that the Fe_2O_3 particles generated for these studies mobilized iron, but that commercially available forms of Fe_2O_3 did not. These results may be explained by incomplete formation of Fe_2O_3 during synthesis in the laboratory, resulting in contamination by ferric hydroxide, ferrihydrite or ferric oxyhydroxides. Any or all of these forms of iron might have been involved in the release of iron that likely triggered the inflammatory response observed. Thus, although the results strongly suggest that iron can cause lung inflammation, the responsible species is not known.

In summary, these studies suggest that iron particles can be taken up by cells and then iron from the particles released in the cells. In addition, iron may mediate inflammation in the lungs after particle instillation.

These studies also emphasize, however, a need to know what species of iron is being used because the species greatly impacts the bioavailability of iron and, therefore, its biological effects.

IRON SPECIES AND REACTIVITY

Iron (and other transition metals) in inhaled particulates can catalyze the formation of ROS as shown in the following reactions (for a review, see Halliwell and Gutteridge 1999):

$$Fe^{III} + \text{Reductant (n)} \longrightarrow Fe^{II} + \text{Reductant (n + 1)}$$
$$Fe^{II} + O_2 \longrightarrow Fe^{III} + O_2^{\bullet -}$$
$$O_2^{\bullet -} + HO_2^{\bullet} + H^+ \longrightarrow H_2O_2 + O_2$$
$$Fe^{II} + H_2O_2 \longrightarrow Fe^{III} + OH^- + HO^{\bullet}$$

The $HO^{\bullet}$ is the most reactive species in these reactions because it can react with all biological molecules. Thus, the presence of redox-active iron inside the cell may cause damage and create oxidative stress, which could lead to production of mediators such as $^{\bullet}NO$, prostaglandins, and interleukins. The rates of these reactions are controlled by the iron chelators and the availability of reducing agents and O_2, but the important point is that the reactions are cyclic: The metal is not consumed in the reaction and can continue to generate ROS until sequestered or removed. In addition, several enzymes can decompose ROS (eg, superoxide dismutase can decompose $O_2^{\bullet -}$, and catalase and glutathione peroxidase can decompose H_2O_2 [hydrogen peroxide]), which may decrease formation of $HO^{\bullet}$.

Excess iron in a cell is usually stored in the protein ferritin. Asbestos is the only particle in which this has been studied extensively; iron mobilized from asbestos was eventually sequestered in ferritin (Fang and Aust 1997). However, there was a constant pool of low-molecular-weight iron in the cell that was proportional to the amount of particulate with which the cell was treated. The size of this pool of iron correlated with the particulate's toxicity to the cell (Chao et al 1994). Iron was mobilized from the particles into the cells, probably into the low-molecular-weight pool, and was then incorporated into the ferritin. Thus, even though iron in ferritin is not reactive, it seemed to be reactive from the time it was mobilized until it was incorporated into ferritin.

Transition metals can also interact directly with proteins to affect their activity. Vanadium interacts with cysteines of phosphotyrosine phosphatase, resulting in its inhibition (Gordon 1991). We also have preliminary data that exposure to iron(III) activates Src kinase, a tyrosine kinase thought to be activated by oxidation of regulatory cysteines (Park and Aust, unpublished observation). Thus, certainly vanadium and likely other transition metals like iron, nickel and even zinc, bind or oxidize critical cysteines and thus activate or inhibit kinase and phosphatase activity, respectively. If specific phosphorylation signalling pathways are activated in turn, transcription factors such as NF-κB (Schieven et al 1993; Imbert et al 1994) or activation protein-1 (AP-1) may be activated, leading to transcription of a variety of genes, including those for inflammatory mediators.

Iron can exist in 16 different oxide forms, depending upon conditions during oxide formation. When studying particles that contain iron, it is critical to determine which form is responsible for the observed effects. Some oxides of iron, such as hematite (Fe_2O_3) and magnetite (Fe_3O_4), are relatively inert (Fang 1999) because the iron is nonreactive as a solid and thus is not easily mobilized from these particles. However, certain other forms are very reactive, such as some ferric oxyhydroxides (eg, ferrihydrite), or iron that interacts ionically with silicates (eg, asbestos [Hardy and Aust 1995], erionite [Eborn and Aust 1995], and other zeolites [Fubini et al 1999]); the iron in these materials is easily mobilized. Therefore, the speciation of the iron in a solid significantly affects the amount and reactivity of the iron once mobilized.

In many cases, soluble forms of iron are prepared to separate responses to iron from responses to particles in general. As discussed above in several examples, how solutions of iron are prepared determines iron's ultimate form in solution and, therefore, its reactivity. It is well accepted that iron(III) is hydrolyzed in aqueous solutions. Schneider (1984) discussed the formation of various ferric oxyhydroxide products from nucleation and polymerization of hydrolyzed iron(III) in solution. Some of these products are highly nonreactive, making it difficult to come to conclusions about the reactivity of soluble iron unless the researcher understands the nature of the prepared solution.

Thus, important requirements of all experiments involving iron are that solutions and particles must be prepared with great care and particles containing iron must be fully characterized to determine the species present.

SIGNIFICANCE

Airborne particulates, PM_{10}, have been associated with increased incidence of respiratory symptoms (Dockery et al 1989; Pope 1989), increased hospitalization related to pulmonary symptoms (Dockery et al 1989; Pope 1991; Pope and Dockery 1992; Schwartz 1994a; Schwartz and Morris 1995), decreased pulmonary function (Dockery et al 1982; Pope and Dockery 1992), and increased daily mortality rates (Dockery et al 1993; Schwartz 1994b, 1994c). $PM_{2.5}$ has also been more associated with increased daily

mortality than PM_{10} (Schwartz et al 1996). To date, however, there is no known mechanism by which particles, especially smaller ones, can elicit these effects. Although there has been speculation that combustion particles are the primary contributors to the adverse health effects, no mechanism has been elucidated to explain the difference between combustion particles and crustal dust (other than the organic components, which may or may not be involved in the acute health effects).

There is increasing evidence, however, that transition metals in the particles are responsible for a variety of pathologic effects. The experiments conducted in our study were designed to determine whether any pathogenicity of particles from specific combustion sources is due to differences in the chemistry of the particles' iron content. Such chemical differences could result from differences in the chemical composition of the combusted material, or from the mechanism of particle formation and from the iron speciation during and after combustion. Chemical differences could lead to pronounced differences in particles of different sizes from the same combustion source. If so, then the techniques developed as a result of this work (eg, mobilization of iron by citrate in vitro and ferritin induction in cultured human lung epithelial cells) can be used to identify the sources responsible for the production of readily bioavailable iron. Further, ferritin induction in the lung may be a biomonitor of human exposure to particulates that contain bioavailable iron.

SPECIFIC AIMS

The long-term objective of this research is to elucidate the mechanism(s) by which ambient air particulates contribute to respiratory disease and to identify the characteristics of particles that may be responsible for specific biological effects. Our hypothesis is twofold: (1) bioavailable transition metals from inhaled airborne particulates catalyze redox reactions in cultured human lung epithelial cells, leading to oxidative stress and increased production of mediators of pulmonary inflammation; and (2) these effects depend on the size, bioavailable transition metal content, and mineral speciation of the particulates. This work focused on the relation between the three particle characteristics and the ability of the particles to generate hydroxyl radicals in cell-free systems and to affect cultured human lung epithelial cells.

The effects of interest include the ability to cause oxidative stress in cultured human lung epithelial cells, resulting in the synthesis of mediators of pulmonary inflammation (eg, NO, PGE_2, and IL-8). These effects were studied by comparing size-fractionated, chemically characterized ash produced by combusting three different coals under conditions that yielded milligram quantities of ash necessary for these studies.

Iron, a transition metal, was studied specifically because it is by far the predominant transition metal in CFA. Although gasoline and diesel particulate and ambient particulate were collected in much smaller quantities than CFA, they were also compared with CFA in cell-free assays requiring only micrograms of material to determine whether particulates from different sources produce different amounts of oxygen radical species. If bioavailable transition metals (eg, iron) and the specific biological responses outlined above are related, then in vitro assays may be developed to determine whether particulates of unknown composition and origin are likely to cause specific health effects.

The specific aims of this study were to:

1. Determine whether CFA-associated iron is bioavailable in A549 cells and whether there is a relation between the bioavailability of iron and the source of the coal, the amount or speciation of iron in the ash, or the size of the respirable ash particles.
2. Determine whether the amount of iron mobilized from CFA by the biological chelator citrate in a cell-free system is an in vitro indicator of the relative amount of bioavailable iron in ash.
3. Determine whether mediators of pulmonary inflammation are produced in A549 cells exposed to CFA and whether there is a relation between production of mediators and the source of coal, the amount of bioavailable iron in the particles, or the size of respirable ash particles.
4. Determine whether the generation of hydroxyl radicals in a cell-free system by CFA is an in vitro indicator of the amount of bioavailable iron or of the production of mediators of pulmonary inflammation in A549 cells.
5. Determine whether automotive particulates from diesel or gasoline exhaust or ambient air particulates collected in Salt Lake City generate hydroxyl radicals and whether this generation is related to the amount of transition metals in the particulates.

METHODS AND STUDY DESIGN

These studies involve the collaborative efforts of three research groups. The combustion research group at the University of Utah generated and extensively characterized

CFA and crustal dust samples. The research group at Ford Motor Company examined ROS generation (specifically, formation of MDA from deoxyribose) by particles and transition metal salts. The biochemistry research group at Utah State University studied the mobilization of iron from particles, in vitro and in cultured human lung epithelial cells, and the induction of inflammatory mediators by particles in cultured human lung epithelial cells.

PARTICULATE SAMPLES

The generation of CFA and noncombustion mineral dust for use in iron mobilization and other toxicologic studies has been described by Veranth and colleagues (2000a). The samples used in this study were produced as described below.

Coal

Parent Coals The three coals used in the study are commercially important coals from the United States that have been used in numerous investigations of coal chemistry and combustion (Smith et al 1994). The Utah coal was a low-sulfur, low-ash, bituminous coal obtained from Deer Creek mine, Wasatch Plateau coal field in Huntington, Utah, operated by PacificCorp (Huntington UT). The Illinois coal was obtained from Consol mine, No 6 coal field, in Perry County, Illinois, operated by Consol (Library PA). This coal was bituminous with a high concentration of iron in the form of both included and excluded pyrite (FeS_2). Because of its high sulfur content, the Illinois coal produced an acidic ash. The North Dakota coal was obtained from Knife River mine, Beulah coal field in Beulah, North Dakota, operated by Knife River Mining (Beulah ND). This coal was a lignite with low iron content that produced an alkaline ash due to its high calcium and magnesium concentrations. The ash-forming elements in lignite were primarily ions bound to carboxyl groups. All coal was pulverized as described in Appendix A, and samples were analyzed by standard methods of the American Society for Testing and Materials (ASTM). Composition of the coal samples is shown in Table 1.

U-Furnace and Combustion Conditions A 30-kW, laboratory-scale, multifuel furnace, which simulates the time and gas-temperature history of a full-scale coal-fired boiler, was used to burn pulverized coals. Furnace details are described elsewhere (Spinti 1997) and in Appendix A.

The temperature of the furnace was maintained by burning natural gas whenever coal was not being burned. Pulverized coal was fed to the furnace at 7 to 12 lb/hr, depending on the coal type, to achieve an approximate burning rate of 90,000 BTU/hr. Approximately 15% excess air was added so the combustion products would contain 3.2 ± 0.5% oxygen. Temperature and exhaust gas composition were continuously monitored and recorded. Average furnace conditions for different runs are presented in Table 2.

Particle Collection Submicron particles were collected from the entire exhaust flow (35 m^3/hr) of the U-furnace using a submicron particle collection system, comprising two major components: a 20-jet preseparator and a virtual impactor. The 20-jet preseparator removes the coarse particles while the virtual impactor concentrates the gas flow that contains the fine particles. The preseparator is equipped with twenty nozzles 3/32 inch (2.38 mm) in diameter. Dilution air was adjusted to maintain a constant 3.2-psi drop in pressure through the preseparator. The submicron particles were collected in the preseparator on four PTFE filters that were removed regularly for particle recovery. The particles collected for this study are less than 1 µm in aerodynamic diameter (PM_1). Further details are in Appendix A.

The coarse-size fractions of CFA samples were collected with a 1-acfm (actual cubic feet per minute) Andersen cascade impactor (Graseby-Andersen, Smyrna GA). The impactor is a 10-stage conventional cascade impactor that runs at 1.7 m^3/hr (1 acfm) (Figure 1). The apparatus was set upstream of the submicron particle collection system. Approximately 5% of the total furnace flow was pulled through the cascade impactor by a diaphragm vacuum pump.

Material collected in the preseparator of the cascade impactor was rich in particles of aerodynamic diameter greater than 10 µm ($PM_{>10}$). Material collected on stages 1, 2, and 3 was rich in particles of aerodynamic diameter greater than 2.5 µm and less than 10 µm ($PM_{2.5–10}$). Material collected on stages 5, 6, 7 and on the final filter (Durapore membrane filter HVHP0950; Millipore, Bedford MA) was rich in $PM_{2.5}$. Further details are in Appendix A.

Particle Recovery Particles were recovered from each sample using either wet or dry recovery methods. PM_1 was wet-recovered from Teflo type RTPJ (PTFE) filters in the 20-jet preseparator. Each filter was submerged in a glass bottle containing 50 mL ethanol, placed in a water bath, and agitated ultrasonically for 2 minutes. The filters were removed from this wash solution, the bottle was placed in a vented oven at 80°C, the solvent was allowed to evaporate over night, and the ash was transferred to a clean glass bottle for storage. The $PM_{2.5}$ fraction collected from the cascade impactor was also recovered using ethanol in this manner.

The $PM_{2.5–10}$ and $PM_{>10}$ fractions were dry recovered from the cascade impactor and its preseparator, respectively. Dry recovery consisted of lightly brushing samples onto aluminum foil and transferring them to clean glass

Table 1. Analysis of Pulverized Coals[a]

	Utah	Illinois	North Dakota
Gross Components (% of total)			
Moisture	2.51	4.47	27.65
Volatile	40.97	29.86	28.51
Fixed carbon	46.59	59.86	32.95
CFA	9.93	5.81	10.89
Components (% of total)			
Carbon	69.89	70.76	45.90
Hydrogen	5.54	5.16	5.70
Oxygen	12.79	15.55	35.88
Nitrogen	1.33	1.65	0.62
Sulfur	0.52	1.07	1.01
CFA	9.93	5.81	10.89
Heat Value			
BTU/lb	12,338.00	12,748.00	7,532.00

[a] Ultimate and proximate analysis of coal used oxygen by difference. All values are on as receive basis. Analysis was performed by Huffman Laboratories (Golden CO).

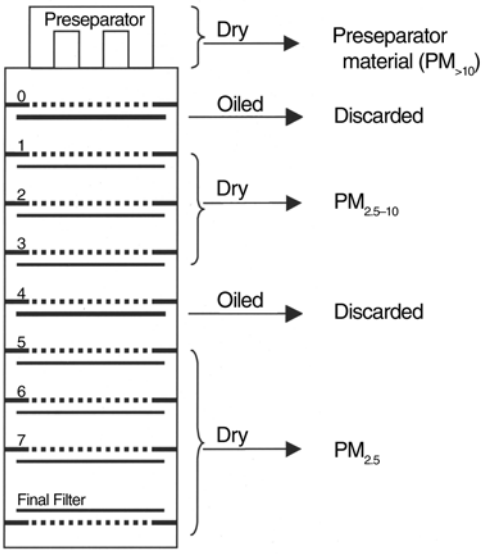

Figure 1. Andersen cascade impactor. Particles were collected on dry metal plates to avoid oil contamination that would interfere with biochemical and toxicologic experiments. Material collected on consecutive plates was combined to form a sample that was rich in particles of various size fractions. Oiled substrates were used between sections to prevent particles from bouncing.

Table 2. Coal Combustion Conditions[a]

	Utah		Illinois		North Dakota	
	PM_1	$PM_{2.5}$ $PM_{2.5–10}$ $PM_{>10}$	PM_1	$PM_{2.5}$ $PM_{2.5–10}$ $PM_{>10}$	PM_1	$PM_{2.5}$ $PM_{2.5–10}$ $PM_{>10}$
Conditions						
Feed rate (lb/hr)	7.00 ± 0.19	7.03 ± 0.28	8.05 ± 0.16	7.94 ± 0.08	12.35 ± 0.15	12.50 ± 0.28
High heat value (BTU/lb)	12,338	12,338	12,748	12,748	7,532	7,532
Low heat value (BTU/lb)	11,847	11,847	12,279	12,279	6,923	6,923
Energy (BTU/hr)	82,929	83,284	98,600	97,864	85,499	86,538
Combustion Gas						
% Oxygen	2.92 ± 0.20	2.86 ± 0.13	3.24 ± 0.15	3.17 ± 0.09	3.49 ± 0.11	3.23 ± 0.05
% Carbon dioxide	15.64 ± 0.26	15.65 ± 0.15	15.72 ± 0.25	15.87 ± 0.30	16.11 ± 0.24	15.43 ± 0.20
ppm Oxides of nitrogen	776 ± 27	796 ± 26	884 ± 12	886 ± 8	614 ± 11	542 ± 38
Furnace Temp (°F)						
S2-1	1421 ± 43	1381 ± 7	1372 ± 7	1383 ± 7	1621 ± 3	1623 ± 7
S4-1	1816 ± 51	1781 ± 20	1692 ± 23	1748 ± 22	1806 ± 20	1838 ± 11
Exit	1106 ± 31	1111 ± 35	1051 ± 15	1077 ± 9	1092 ± 13	1120 ± 2

[a] Conditions are averages of all runs ± SD.

vials for storage. Further details of both recovery methods are in Appendix A.

Size Validation Particle size distributions were analyzed to validate the operating conditions of the collection equipment. The size distribution of the sample was determined using the particle collection methods (the submicron particle collection system and the cascade impactor) and using scanning electron microscopy (SEM) imaging.

Mass Distribution and Morphology by SEM CFA samples were analyzed on a scanning electron microscope (model S240; Cambridge Research and Instrumentation, Woburn MA) at the University of Utah. SEM images were used to determine the mass distribution and morphology of each CFA sample. Approximately 1 mg of sample was suspended in 20 mL ethanol by ultrasonic agitation. An aliquot (4 to 8 mL) of the solution was filtered through a 47-mm polycarbonate membrane (GTTP047, Millipore). SEM samples for PM_1 and $PM_{2.5}$ and for $PM_{2.5–10}$ and $PM_{>10}$ were prepared with 0.115 to 0.173 and 0.231 to 0.346 μg filtrate/mm^2 filter, respectively. For each sample, a set of electronic images was taken on a structured pattern, not allowing the images to overlap each other.

To determine the mass distribution of each size fraction, the horizontal dimensions of approximately 1000 particles from each set of SEM images were manually measured using Scion Image software (Scion Corp, Frederick MD). In cases of ultrafine particle aggregates, the diameter of individual particles was measured. When particle diameter could not be determined, the diameter of the aggregate was measured.

SEM images were also used to identify particles based on their morphology. Less than 0.4% of particles in $PM_{>10}$ was identified as char, the porous, carbon-rich material that results from incomplete burning of coal particles. Char has high surface area (often > 100 m^2/g) but low mineral content (usually < 10% total weight) and low density (< 1 g/cm^3) due to its porosity. Thus, we assumed the char particles were an insignificant source of iron and excluded them from calculations of particle size distribution based on the SEM measurements.

Surface Area Determination and Elemental Analysis

The surface area of each sample fraction was determined using a single-point, nitrogen surface area measurement assuming monolayer adsorption. Each sample was analyzed on an MS-15 Quantachrome Monosorb Direct Reading Dynamic Flow Surface Area Analyzer (Quantachrome Instruments, Boynton Beach FL). Three adsorption and desorption cycles were completed for each sample.

Instrumental neutron activation analysis (INAA) was used to determine the elemental composition of CFA samples. Approximately 25 mg of each sample was placed in an acid-washed glass vial and shipped to the Environmental Research and Radiochemistry Department at the MIT Nuclear Reactor Laboratory (Cambridge MA) for INAA. In addition, Western Analysis (Salt Lake City UT) determined the carbon content of each sample using a carbon analyzer (model 521, Leco Corp, St Joseph MI).

Size Fractionation of Noncombustion Particles

Particle samples were generated in the laboratory from two natural soils (called desert dust and Mancos clay) representative of the surface of unimproved roads in rural desert areas and from the tailings produced by a metallurgic mill (called mine *tailings*). These are anthropogenic sources of noncombustion fine particles that contain major elements similar to those in CFA. The mine tailings were material left after the copper ore had been mechanically ground and sulfate minerals had been removed by flotation. The mine tailings were obtained wet and were oven-dried before size fractionation. The soil samples were sieved to remove gravel-sized rocks and organic debris. Samples were run through a jar mill with ceramic media to release the fine dust, which was carried by the air flow into a settling chamber and then into the Andersen cascade impactor. For the attrition-generated particles, the output from cascade impactor stages 5 and 6 were combined to produce a $PM_{2.5}$-rich fraction. Material from stage 7 and the final filter were combined to create a finer sample. The sample collection and size analysis are detailed by Veranth and colleagues (2000a). We compared the size distribution of the parent soils, determined by SEM examination of the sieved material, with the mass of submicron particles collected from the cascade impactor. The relative amounts of $PM_{2.5}$ and PM_1 in the parent material and the collected samples indicate that $PM_{2.5}$- and PM_1-rich samples were not solely composed of newly generated fine particles. The gentle grinding in the low-speed jar mill appears to have broken up aggregates and released preexisting fine particles.

The mine tailings, desert dust, and Mancos clay samples were digested with acid and the extracts analyzed by inductively coupled plasma mass spectrometry (ICP-MS). The samples were analyzed by Chemical and Mineralogical Services (Salt Lake City UT).

Gasoline and Diesel Combustion Particles

Exhaust particles from gasoline engines were collected from gasoline-operated vehicles in a dilution tunnel using rates of air flow and sampling sufficient for isokinetic

sampling. (See Siegl et al 1994 for a complete description of the dilution tunnel.) Vehicles were operated using the EPA Urban Dynamometer Driving Schedule, which includes a vehicle cold start on each of four consecutive days. Particles were collected using 25-µm ultrathin PTFE-membrane filters (2-µm PTFE, Gelman Sciences, Ann Arbor MI) and were weighed in a room with controlled temperature and humidity (20°C, 50% humidity).

Exhaust particles from diesel engines were collected from a 1994 inline, 6-cylinder, turbocharged, intercooled, on-highway diesel engine. The engine was operated at 220 rpm at 100% load, generating 420 lb-ft torque and 175 hp brake power. The exhaust was mixed with dilution air in a partial dilution system. Particulate filters were collected over 2.5 hours using isokinetic sampling rates and were weighed in a room with constant temperature and humidity (20°C, 50% humidity).

SRM Particulates

Samples of SRM 1648, 1649, 1650, and 2975 were obtained from the US National Institute of Standards and Technology (NIST, Gaithersburg MD). SRM 1648 is PM from urban air collected over 2 years (from 1974 to 1976) in St Louis, Missouri; SRM 1649 is dust and organics from urban air collected over a year (from 1975 to 1976) (Washington DC). Approximately 50% and 30% of the particulates in SRMs 1648 and 1649 are PM_{10} (B MacDonald, NIST, personal communication). Results of elemental analysis of SRM 1648 (Gladney et al 1984) and SRM 1649 (May et al 1992) are available. Several laboratories, including ours, have shown these samples to be contaminated by endotoxin. SRM 1650 and SRM 2975 are diesel particulate samples. No information is available on their elemental composition.

Urban Particles from Salt Lake City

Ambient particles were collected from an industrialized area of Salt Lake City near the interstate highway. A modified Anderson Hi-Vol sampler PM_{10} inlet was used to separate out $PM_{>10}$. The 34 m^3/hr flow of air was directed through the rectangular slot virtual impactor described above. The concentrated particulate in the minor flow was collected using stages 4 and 7 of an Andersen cascade impactor to collect $PM_{2.5–10}$ and $PM_{2.5}$, respectively. The submicron material was deposited on a bank of PTFE final filters downstream of the impactor. This system was a prototype designed to demonstrate a method of collecting ambient particulate sufficient for iron mobilization studies and other biochemical studies.

Particles were collected four consecutive times for 5 days each time in August and September 1999. The PM_1 was prepared for mobilization studies by incubating the collection filters for 24 hours in 50 mM sodium chloride (NaCl), pH 7.5, in the presence of 1 mM citrate. The concentration of iron in the supernatant was determined using the iron chelator 3-(2-pyridyl)-5,6-diphenyl-1,2,4-triazine-*p,p′*-disulfonic acid (or ferrozine).

IRON MOBILIZATION DETERMINATIONS

Sodium chloride and sodium citrate were obtained from Mallinckrodt (Paris KY). We removed contaminating metals from 50 mM NaCl using chromatography with Chelex 100 (Bio-Rad Laboratories, Richmond CA). All remaining solutions were prepared using this Chelex-treated NaCl under incandescent red lights and were stored in the dark. Ferrozine, which forms a colored complex of high molar absorbtivity with iron(II), was obtained from Aldrich Chemical Company (Milwaukee WI). The iron chelator DF, which forms a colored complex of high molar absorptivity with iron(III), was obtained from Ciba-Geigy Corporation (Summit NJ).

CFA particles supplied in glass bottles were weighed and suspended in the appropriate solution. The diesel exhaust particles were carefully scraped from the PTFE filters with a plastic spatula and were combined to yield a sample large enough for iron mobilization and ferritin induction. The particles were also weighed and suspended in the appropriate solution.

Mobilization by Citrate

The mobilization of iron from particulates by citrate was determined using a spectrophotometric total iron assay, which utilizes ferrozine to quantify both iron(II) and iron(III) as a result of the addition of the reductant ascorbate, as previously described (Lund and Aust 1990). The concentration of iron (nanomoles of iron per milligram of particulate) mobilized by citrate was plotted against time.

The particles used in these studies included CFA from Utah, Illinois, and North Dakota, $PM_{2.5}$, $PM_{2.5–10}$, and $PM_{>10}$, diesel exhaust particulate, ambient air particulate from Salt Lake City, Utah, $PM_{2.5}$ and $PM_{>10}$, and the non-combustion particulates, Mancos clay, desert dust and mine tailings, $PM_{2.5}$. Because CFA is basic, the 50 mM NaCl added to it was adjusted to pH 4.5 so the final pH of the CFA suspension (1 mg/mL) was near 7.5. The pH was also adjusted after the particles were fully suspended to maintain the pH at 7.5 throughout the experiment. The amount of iron mobilized from CFA was determined over periods of increasing duration with a maximum of 24 hours.

Because diesel exhaust particles are acidic, the 50 mM NaCl added to it was adjusted to pH 9.5 so the final pH of the diesel exhaust particle suspension (1 mg/mL) was near

7.5. The concentration of iron mobilized by citrate (nmol iron/mg diesel exhaust particles) was determined after a 24-hour incubation.

Iron(II) Mobilization by Ferrozine

$PM_{2.5}$ from Utah, Illinois, or North Dakota CFA was suspended in pH-adjusted 50 mM NaCl. Ferrozine was added for a final concentration of 1 mM. After 24 hours, we determined the amount of iron(II) mobilized as the ferrozine:iron(II) complex by measuring absorbance of the supernatant at 562 nm, as previously described (Lund and Aust 1990).

Solubility of Metals Under Various Conditions

The $PM_{2.5}$ of Utah CFA was incubated at a concentration of 1 mg/mL for 24 hours under four different conditions: (1) in water at pH 2.5 (the pH of many ambient PM suspensions in water); (2) in water at pH 10 (the pH of CFA suspended in water without pH adjustment); (3) in 50 mM NaCl at pH 7.5 without added chelators; and (4) in 50 mM NaCl at pH 7.5 with 1 mM citrate. The suspensions were centrifuged at 3750*g* for 30 minutes and the concentrations of metals in the supernatants were analyzed using ICP (Soil Testing Laboratory, Utah State University, Logan UT).

DETECTION OF HYDROXYL RADICALS BY DEOXYRIBOSE OXIDATION AND MDA FORMATION

Chelex Treatment of Buffer

Metals were removed from 0.1 M phosphate buffer, pH 7.0, using 5 to 10 g Chelex 100 chelating ion exchange resin (Biorad, Melville NY) per 100 mL buffer (Schaich 1990). The mixture was shaken for one hour, filtered through a 0.2-µm sterile nylon membrane (Gelman Sciences), and stored in a polypropylene bottle. This Chelex-treated buffer ranged from pH 7.1 to 7.2. The buffer was checked for contaminating metals by measuring the oxidation of ascorbic acid over time (Buettner 1990), and all remaining solutions were prepared using this Chelex-treated buffer. All glassware and plastic labware were soaked overnight in 0.1N HCl (ultrapure, metal certified; Fisher Scientific, Pittsburgh PA) and rinsed with deionized water (18 $M\Omega/cm^{-1}$).

Phosphate-Buffer Extraction of Particles from Filters and ICP-MS Analysis

PTFE filters containing particles from gasoline and diesel engines were shaken overnight in 3.0 mL 0.1 M phosphate buffer (pH 7.2) at 37°C. The aqueous extract was poured through 0.8-µm and 0.45-µm filters (Versapor Acrodisc, Gelman Sciences). Extracts of blank filters were filtered in the same fashion. The filtered solutions were assayed for their ability to produce MDA in the presence of 2-deoxyribose and ascorbic acid.

PTFE filters containing particles from the exhaust of gasoline engines only were shaken overnight in 3.0 mL 0.1-M phosphate buffer (pH 7.2) at 37°C. The samples were filtered and the extracts were sent to Clayton Environmental Services (Novi MI) for ICP-MS analysis of the transition elements cobalt, copper, iron, nickel, vanadium, and zinc. A buffer sample containing no PM was sent as a control. The amount of each metal in the control was subtracted from that found in the particulate samples. The ICP-MS instrument was calibrated using standard metal concentrations prepared in 0.1 M phosphate buffer (pH 7.2). The limits of detection (nanogram per filter) was 20, 50, 50, 60, 100, and 250 for cobalt, vanadium, zinc, copper, nickel, and iron, respectively.

Quantification of MDA Using 2-Thiobarbituric Acid

The ability of pure transition metal sulfates and extracts of complex particulate mixtures to generate ROS depends solely on the presence of a biological reducing agent (ascorbic acid) and atmospheric oxygen. We made no assumptions about chemical intermediates that might be formed during generation of ROS. This is in contrast to many studies that add H_2O_2 to their assay system (Ghio et al 1996; Pritchard et al 1996), which means that only the Fenton reaction—the ability of transition metals to cleave H_2O_2 into hydroxyl radicals—is being measured. Because the concentration of H_2O_2 in lungs is not generally known, we wanted to examine the ability of metals and particulates to generate their own, possibly unique ROS (Aust et al 1985; Minotti and Aust 1987).

Aqueous extracts of gasoline and diesel particles collected on filters were prepared by incubating the filters in 0.1 M phosphate buffer, pH 7.2, overnight at 37°C with continuous shaking. At the end of the incubation, any suspended particles were removed by filtration using 0.8 µm first and then 0.45 µm. Extracts of blank filters were prepared and incubated in the same way and were used as a negative control. Each filtrate in 0.1 M phosphate buffer, pH 7.2, containing a final concentration of 1 mM ascorbic acid and 1.0 mM 2-deoxyribose, was vigorously shaken for 24 hours at 37°C. Each incubation was analyzed for MDA as described below. Utah, Illinois, and North Dakota CFA, $PM_{<1}$, $PM_{2.5}$, $PM_{2.5-10}$, and $PM_{>10}$, and SRM particulate were added directly to a solution containing 0.5 mM 2-deoxyribose and 1.0 mM ascorbic acid in 0.1 M phosphate buffer (pH 7.2) and was vigorously shaken for specified times at 37°C. At the conclusion of each time period, the particulate sample was filtered through a 0.8-µm and a

0.45-μm filter. Appropriate blanks were filtered in the same fashion. The resulting solution was then assayed for MDA.

The effect of DF on the formation of MDA was determined using phosphate-buffered aqueous extracts of gasoline and diesel filter samples and SRM particulate samples. DF (final concentration 1 mM) was added to the filtered extracts and incubated for 1 hour before adding concentrated stock solutions of 2-deoxyribose and ascorbic acid (final concentration 1.0 mM and 0.5 mM ascorbic acid for the engine samples and SRM samples, respectively, and 1 mM 2-deoxyribose for all samples). This solution was shaken vigorously for 24 hours at 37°C. Appropriate positive and negative controls were also prepared.

To determine the amount of MDA in the solutions, 1 mL of each sample was incubated with 0.67% 2-thiobarbituric acid in 2 mL 1.0N acetic acid for 1 hour at 100°C. The solutions were then cooled on ice to stop the reaction. We quantified the presence of pink chromophore by determining the absorbance at 532 nm of the sample solutions using a PerkinElmer Lambda 6 UV-VIS spectrometer (PerkinElmer, Boston MA), from which the absorbance of the blank was subtracted. A concentrated MDA solution was prepared by heating a solution of MDA bis(dimethyl acetal) (Aldrich Chemical Co) in water containing a catalytic amount of HCl; the molar absorptivity of the pink chromophore at 532 nm was 141,000 ± 8,000 cm^{-1} M^{-1} (n = 23).

CELL CULTURE AND TREATMENTS

Culture Medium, Cell Culture, and Endotoxin Assay

Ham F12 cell culture medium, 0.5% trypsin (with 0.2% EDTA), and 0.25% trypsin were obtained from Life Technologies (Grand Island NY). Gentamicin (50 μg/mL) was obtained from BioWhittaker (Walkersville MD). Fetal bovine serum was obtained from Summit Biotechnology (Fort Collins CO) and Hyclone Laboratories (Logan UT). Human-liver ferritin and cytochalasin D were obtained from Calbiochem (San Diego CA) and bicinchoninic acid from Sigma Chemical Company (St Louis MO).

Complete growth medium was composed of Ham F12 cell culture medium, 50 μg/mL gentamicin, 10% fetal bovine serum, and 1.176 g sodium bicarbonate ($NaHCO_3$) per L medium for a final pH of 7.4.

We used the human lung epithelial cell line A549, which has characteristics of alveolar epithelial type-II cells in experiments. The A549 cells (ATCC CCL185) were obtained from American Type Culture Collection (Rockville MD). Cells were cultivated in complete growth medium in a water-jacketed incubator (model 3326, Forma Scientific, Marietta OH) at 37°C in an atmosphere of 5% carbon dioxide (CO_2) and 95% humidity. Some cells were dislodged with 0.5% trypsin plus 0.2% EDTA before they had reached confluence, resuspended in complete growth medium, and plated as stock cultures.

Culture medium containing the particulates or other chemicals was examined for the presence of endotoxin by the *Limulus* amebocyte assay (BioWhittaker) according to the manufacturer's instructions. The results were expressed as endotoxin units per milliliter medium.

Treatment of Cells with Particle Suspension

Immediately before use, Utah, Illinois, and North Dakota CFA of all size fractions were suspended in sterile 14 mM $NaHCO_3$ (pH 7.4) and diesel exhaust particles were suspended in Ham F12 cell culture medium without fetal bovine serum (pH 7.4). These mixtures were vortexed for 1 minute and diluted to the appropriate concentration with complete growth medium for a final pH of 7.5.

A549 cells were cultured in flasks until about 75% confluent, dislodged with trypsin-EDTA, resuspended in complete growth medium, counted using a cell counter (Coulter Electronics, Hialeah FL), and plated at a culture density of 20,000 cells/cm^2. The cells were allowed to recover for 24 hours.

Some cells were treated with the CFA or diesel exhaust particle solutions for 24 hours, after which we removed the complete growth medium, which contained particles that were not associated with the cells, and assayed it for IL-8. For the other cells, in a single experiment, the growth medium was removed and replaced with medium containing 10 μM cytochalasin D. After one hour, CFA or ferric ammonium citrate (FAC) was added directly to the medium and the cells were incubated for 24 hours. FAC (1.5 mM iron) was used for comparison because it is a soluble form of iron that is taken into cells by a mechanism other than endocytosis. This culture medium was then removed from the cells and assayed for IL-8.

Cells from all treatments were rinsed once with 0.15 M phosphate-buffered saline (pH 7.4) and dislodged with 0.25% trypsin without EDTA because EDTA may mobilize iron from ambient particulates (Smith and Aust 1997). The cells were stored in 1 mL double-distilled, deionized water containing 0.1 mM phenylmethanesulfonyl fluoride and frozen at −80°C for ferritin determinations at a later time.

Quantification of Intracellular Ferritin

The frozen cells were lysed as previously described (Chao et al 1994) and the concentration of intracellular ferritin was determined using a sandwich enzyme-linked immunosorbent assay (ELISA) as previously described (Hornbeck 1994; Fang and Aust 1997). The standard curve

describing absorbance at 450 nm per unit human-liver ferritin (0 to 7.5 ng) was linear. Total protein in the cell lysate was determined using bicinchoninic acid. The results were expressed as nanograms of ferritin per microgram total protein.

Quantification of IL-8 and PGE_2 in Culture Medium

IL-8 in the culture medium removed from cells treated with CFA or FAC was quantified by solid-phase sandwich ELISA (BioSource International, Camarillo CA). The assay was performed according to manufacturer's instructions; the results were expressed as picograms IL-8 per milliliter culture medium.

PGE_2 in culture medium removed from cells treated with CFA was quantified by using a competitive enzyme immunoassay (EIA; Cayman Chemical Co, Ann Arbor MI). The assay was performed according to the instructions provided with the EIA.

Incubation of Cells with DF-Pretreated CFA and Tetramethylthiourea or DMSO, or FAC

In some experiments, we examined the role of iron in inducing IL-8 production by incubating cells with CFA from which iron had been removed by DF. Utah CFA PM_1 (1 mg/mL) was incubated for 14 days in 50 mM NaCl (pH 7.5) containing 1 mM DF. The 1 mM DF was changed after approximately 1 day and about every 2 days thereafter. To confirm that a component of CFA, other than iron and responsible for inducing IL-8 was not being washed away in the DF treatments, Utah CFA PM_1 (1 mg/mL) was also incubated in 50 mM NaCl without DF. To determine which metals were present, ICP was performed on the supernatant removed from both untreated and DF-treated CFA PM_1. The CFA was washed five times with sterile, distilled water, dried, and stored at room temperature. The DF treatment removed approximately 24% of the total iron from the particles. The particles were resuspended immediately before use.

To determine the contribution of free radicals to CFA-induced IL-8 secretion, the radical scavengers tetramethylthiourea (TMTU) or DMSO was dissolved in culture medium and added to A549 cells. One hour later, resuspended Utah CFA PM_1 (20 μg/cm^2) was added to the culture medium covering the cells.

To determine whether a soluble form of iron can mimic the effects of CFA, a stock solution of FAC was prepared in 14 mM $NaHCO_3$ (pH 7.4) immediately before use. FAC was diluted to the appropriate concentration by complete growth medium, for a final pH of 7.5. Cells we treated with the indicated concentrations of FAC for 24 hours. Supernatants were assayed for IL-8 production and cells were analyzed for ferritin.

RT-PCR Analysis for IL-8 mRNA

Relative levels of IL-8 messenger RNA (mRNA) were estimated using a Multiplex PCR kit (BioSource International, Camarillo CA). The reverse transcriptase–polymerase chain reaction (RT-PCR) was performed according to manufacturer's instructions. The specific primers for iNOS and glyceraldehyde-3-phosphate dehydrogenase (GAPDH) were obtained from Clontech Laboratories (Palo Alto CA).

Cells were lysed directly in the culture flask by adding 5 mL TRIZOL reagent (Gibco BRL, Grand Island NY) per 25 cm^2 of culture flask surface area. Isopropanol-precipitated RNA was resuspended in double-distilled water and stored at −80°C until use.

Total RNA (1 μg) was reverse-transcribed using AMV (avian myeloblastosis virus) reverse transcriptase (Sigma Chemical Co). The reverse transcription for cytokine mRNA was performed as follows: 10 minutes at 77.5°C, 15 minutes at 25°C, and 50 minutes at 42°C. Then the PCR was conducted as follows: 2 cycles of 1 minute of initial denaturation at 96°C, 1 more minute at 96°C, and 4 minutes at 56°C; 33 cycles of 1 minute at 94°C and 2.5 minutes at 57°C; and 10 minutes at 70°C for final extension. The complementary DNA (cDNA) amplification products obtained from the RT-PCR were separated on a 2% agarose gel by electrophoresis, stained with ethidium bromide, transilluminated with UV light, and photographed. The negatives were then analyzed by integrated scanning densitometry. The area under the peak for each cytokine's mRNA was used to calculate the percentage of cytokine mRNA relative to GAPDH mRNA. Results were expressed as the fold increase over the value obtained for the untreated control cells.

The specific primers for iNOS and GAPDH were purchased from Clontech Labs (Palo Alto CA). The cDNA obtained from RT-PCR was analyzed on a 2% agarose gel by electrophoresis and visualized with ethidium bromide, as previously described by Chao and colleagues (1996).

SPECIATION OF IRON IN CFA USING MÖSSBAUER SPECTROSCOPY

Approximately 200 mg of each sample was placed in a standard Mössbauer holder. The spectra were each run for a number of days in order to obtain a statistically reasonable spectrum. Simultaneous with each sample reading, a calibration spectrum from a thin metallic foil was accumulated at the opposite end of the Mössbauer driving unit in order to calibrate the velocity (energy) scale of the spectrum of the sample and to locate the zero-velocity point. Each spectrum was analyzed using a least-squares fitting procedure based on a Lorentzian peak shape. Iron-bearing phases in the samples were identified on the basis of

isomer shift, quadrupole splitting, and magnetic hyperfine splitting with the help of interpretive experience gained from analysis of previous coal and combustion ash samples (Huffman and Huggins 1978; Huffman et al 1981). The best match of the observed spectra to known iron species was reported.

Interpretation of Mössbauer spectra of CFA is less precise than that of spectra from pure crystalline minerals because of variability in glass composition and because the elemental composition of CFA varies among particles. The phase data were categorized as oxides and iron in glass, based on the fact that iron in glass lacks magnetic hyperfine splitting. Experimental error for these determinations was within 5% of the total iron concentration.

STATISTICAL METHODS AND DATA ANALYSIS

Analysis of Variance

We assessed how CFA size class and source affected MDA formation, iron mobilization by citrate, concentration of ferritin in A549 cells, and concentration of IL-8 in culture medium for three doses of CFA of ferritin, of citrate, and of MDA using two-way factorial analysis of variance (ANOVA) in a completely randomized design. Each variable was analyzed individually. IL-8 concentration data were natural-log transformed before the analysis to better conform to assumptions of normality and homogeneity of variance. Where appropriate, we used Tukey multiple comparisons test to make posthoc pairwise comparisons among size class means and among source means. PROC GLM in SAS Release 7.0 (SAS Institute, Cary NC) was used for all computations.

Pearson Correlation Analysis of Various Parameters

The relations among MDA, copper, zinc, iron, ferritin, citrate, IL-8, and two measures of surface area were assessed visually using scatterplots and were quantified using Pearson correlation coefficients. Each datum was the mean of three subsamples. PROC CORR in SAS Release 7.0 (SAS Institute) was used for all computations. We used the Bonferroni method to adjust the significance level per comparison so that the experimentwise error rate was at most 0.10.

Regression Analysis of Ferritin and FAC

The degree to which ferritin levels could be explained by FAC was modeled using linear regression. Because each FAC value had several replicates, we could test for deviation from linearity (Zar 1996). The REG and GLM procedures in SAS Release 7.0 (SAS Institute) was used for the computations.

Uncentered, Piecewise Linear Regression Between IL-8 and Ferritin for FAC

We compared the dependence of IL-8 and ferritin on FAC and on CFA by joining two piecewise linear regressions with separate, unknown breakpoints. IL-8 was the dependent variable, and ferritin was the independent variable. Each datum was the mean of three replicates. PROC NLIN in SAS Release 7.0 (SAS Institute) was used with the secant iterative method and a grid of initial parameter estimates.

RESULTS

SOLUBLE TRANSITION METAL SALTS

Because our focus was to begin evaluating whether transition metals are responsible for the biological effects of combustion particulates, we assessed the ability of first-row transition elements to generate ROS using the production of MDA from 2-deoxyribose. Sulfate salts were used whenever possible because of their high purity and aqueous solubility. Six metals—iron(II) sulfate, copper(II) sulfate, vanadium(IV) sulfate, cobalt(II) sulfate, nickel(II) sulfate, and zinc(II) sulfate—catalyzed the time-dependent formation of MDA, each at a different rate (Figure 2). For example, MDA formation catalyzed by copper(II) sulfate was concentration-dependent, with a steep increase followed by a plateau or slight decrease in MDA yield. Vanadium(IV) sulfate, on the other hand, shows a more gradual rise in MDA concentration over time.

These curves are difficult to interpret for several reasons: (1) there are many reactions that can occur during this assay's incubation period; (2) MDA, the reaction product of interest, can be oxidized during the assay, rendering it undetectable; and (3) the actual ROS (eg, hydroxyl radicals or an oxymetal complex) that oxidizes 2-deoxyribose may depend upon the metal used.

DF is a metal chelator that has been traditionally used to determine the participation of iron in redox reactions because it completely inhibits the reaction of iron(III) with most common reductants and therefore prevents further reactions with O_2. However, DF can also bind other transition metals; it inhibited formation of ROS catalyzed by the six transition metals, except nickel(II) (Table 3). Each metal was incubated with DF for 1 hour prior to the addition of 2-deoxyribose and ascorbic acid. DF inhibited formation of reactive oxygen by varying degrees. The percentage of the formation of ROS inhibited by DF was greatest (100%) for iron and zinc and least for vanadium and nickel.

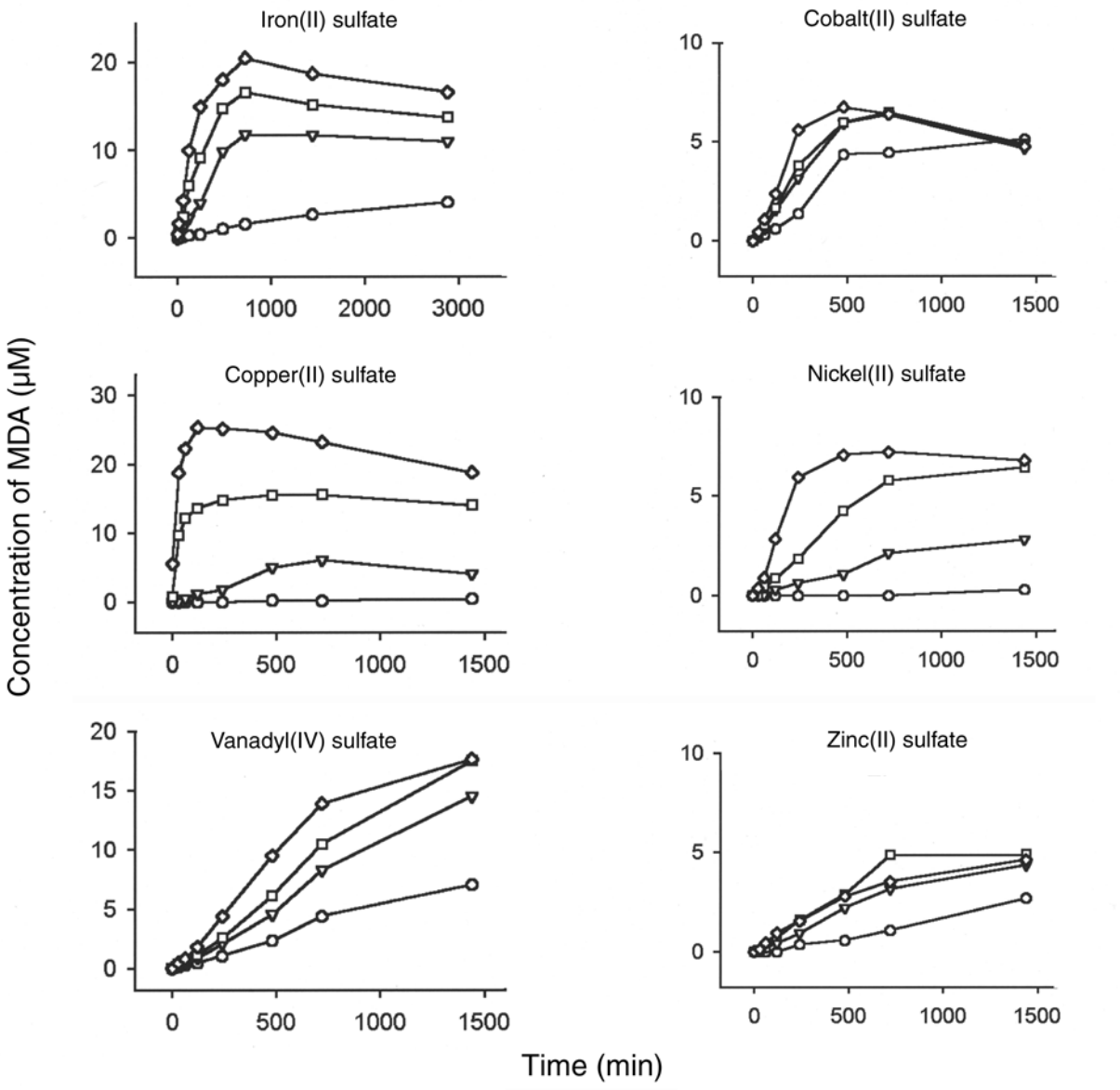

Figure 2. Time-dependent formation of MDA via metal sulfates. Various concentrations of iron(II) sulfate, copper(II) sulfate, vanadyl(IV) sulfate, cobalt(II) sulfate, nickel(II) sulfate, and zinc(II) sulfate were used: ○, 1.0 μM; ▽, 5 μM; □, 10 μM; ◇ 50 μM.

Table 3. Effect of DF on Transition Metal–Catalyzed Formation of MDA

Transition Metal Sulfate[a]	MDA[b] (μM)	MDA (μM) (+ 1 mM DF)[c]	Inhibition of MDA by 1 mM DF (%)
Iron(II) sulfate	13.2	0.0	100
Copper(II) sulfate	17.7	8.1	54
Vanadyl(IV sulfate)	17.7	11.6	34
Nickel(II) sulfate	7.6	8.0	−5
Cobalt(II) sulfate	7.4	1.2	84
Zinc(II) sulfate	4.0	0.0	100

[a] Each sulfate contained 50 μM transition metal.

[b] Transition metal sulfates were incubated for 24 hours at 37°C with 1 mM ascorbate and 1 mM deoxyribose. The amount of MDA formed was determined by further incubation with 2-thiobarbituric acid.

[c] Transition metal sulfates were incubated for 1 hour with 1 mM DF before incubating for 24 hours at 37°C with 1 mM ascorbate and 1 mM deoxyribose. The amount of MDA formed was determined by further incubation with 2-thiobarbituric acid.

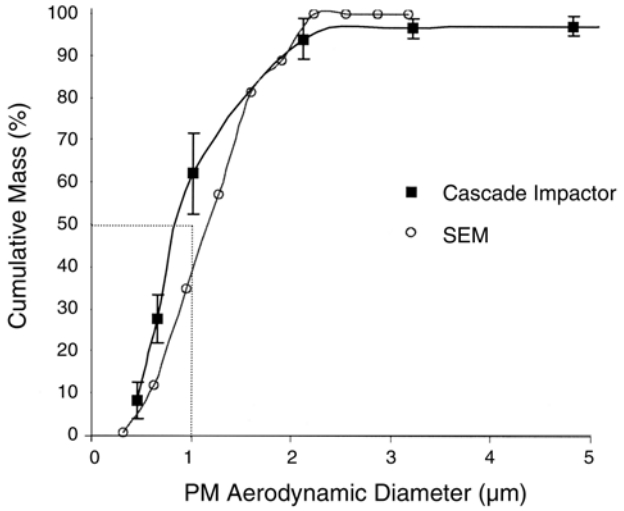

Figure 3. Size distribution as determined by cascade impactor and SEM analysis mass. Distribution of Utah CFA obtained from 6 cascade-impactor samples taken downstream of the virtual impactor and one SEM analysis of material collected on the submicron filters. Collection equipment operated with twenty 3/32-inch nozzles in the preseparator and a pressure drop of 3.2 psi. Optical diameters obtained from SEM were converted to aerodynamic diameters using 2.5 g/cm^3 particle density without adjustment for nonspherical particles.

COAL FLY ASH

Generation of Ash

Size Validation and Morphology The mass distributions obtained for Utah CFA by cascade impactor sampling and by electron microscopy are shown in Figure 3. As indicated by the distribution, PM_1 made up more than 50% of the sample mass. The SEM images of the size-fractionated samples are shown for Utah, Illinois, and North Dakota in Figures 4 through 6. The char particles are the remnants of incomplete combustion of coal particles, and they have an irregular, porous structure. The mineral ash particles are formed from compounds that have gone through vaporization and condensation, and they have a spherical shape. As indicated by the SEM images, material in all size fractions was composed mostly of ash particles that were smooth spheres, mixed with a very small amount of char particles that had a porous lacy structure. PM_1 fractions also contained ultrafine particle aggregates that were sometimes difficult to resolve. $PM_{2.5}$ and PM_1 contain spherical particles. The lack of fragments or irregular particles in PM_1 and $PM_{2.5}$ indicates that the ultrasonic agitation used to remove the deposits from the cascade impactor collection surface did not fracture the spherical particles of mineral ash which are formed as the molten

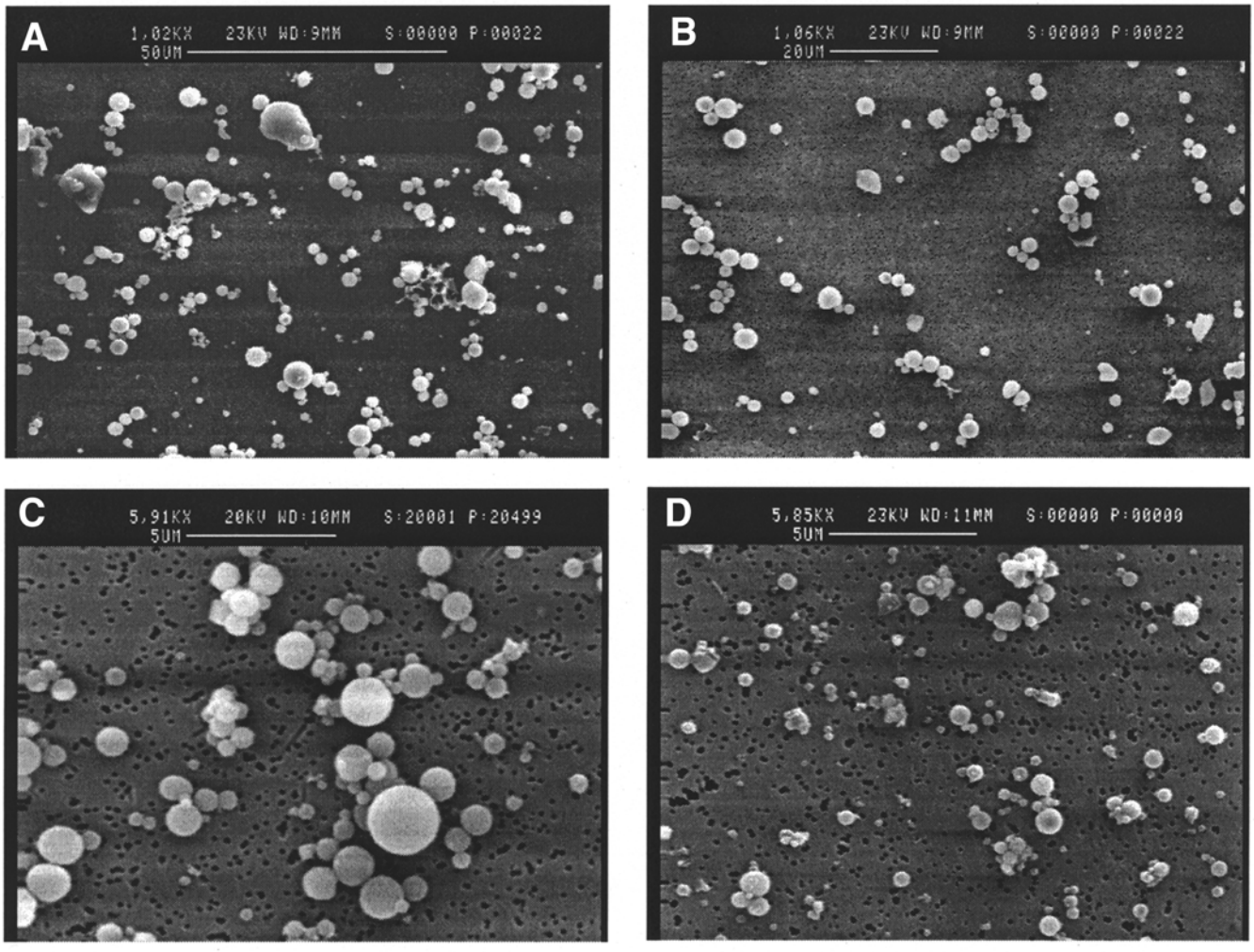

Figure 4. SEM images of the 1998 size-fractionated Utah CFA. ***A***. $PM_{>10}$ at ×1000 magnification; ***B***. $PM_{2.5–10}$ at ×2000 magnification; ***C***. $PM_{2.5}$ at ×6000 magnification; and ***D***. PM_1 at ×6000 magnification. The spherical particles are mineral ash; the irregular particles are char; the black circles are pores in the polycarbonate substrate.

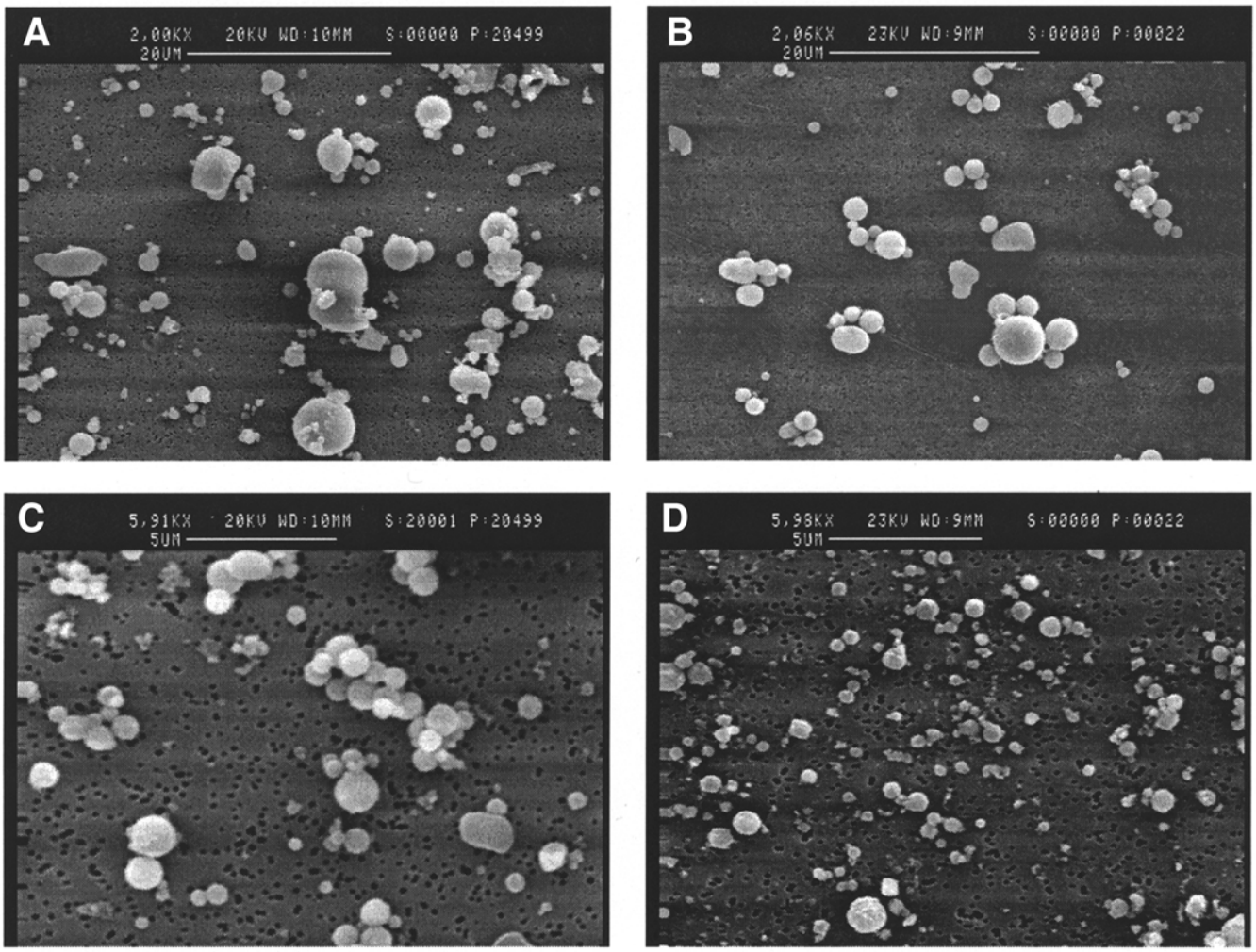

Figure 5. SEM images of the 1998 size-fractionated Illinois CFA. ***A***. $PM_{>10}$ at ×2000 magnification; ***B***. $PM_{2.5–10}$ at ×2000 magnification; ***C***. $PM_{2.5}$ at ×6000 magnification; and ***D***. PM_1 at ×6000 magnification. The spherical particles are mineral ash; the irregular particles are char; the black circles are pores in the polycarbonate substrate.

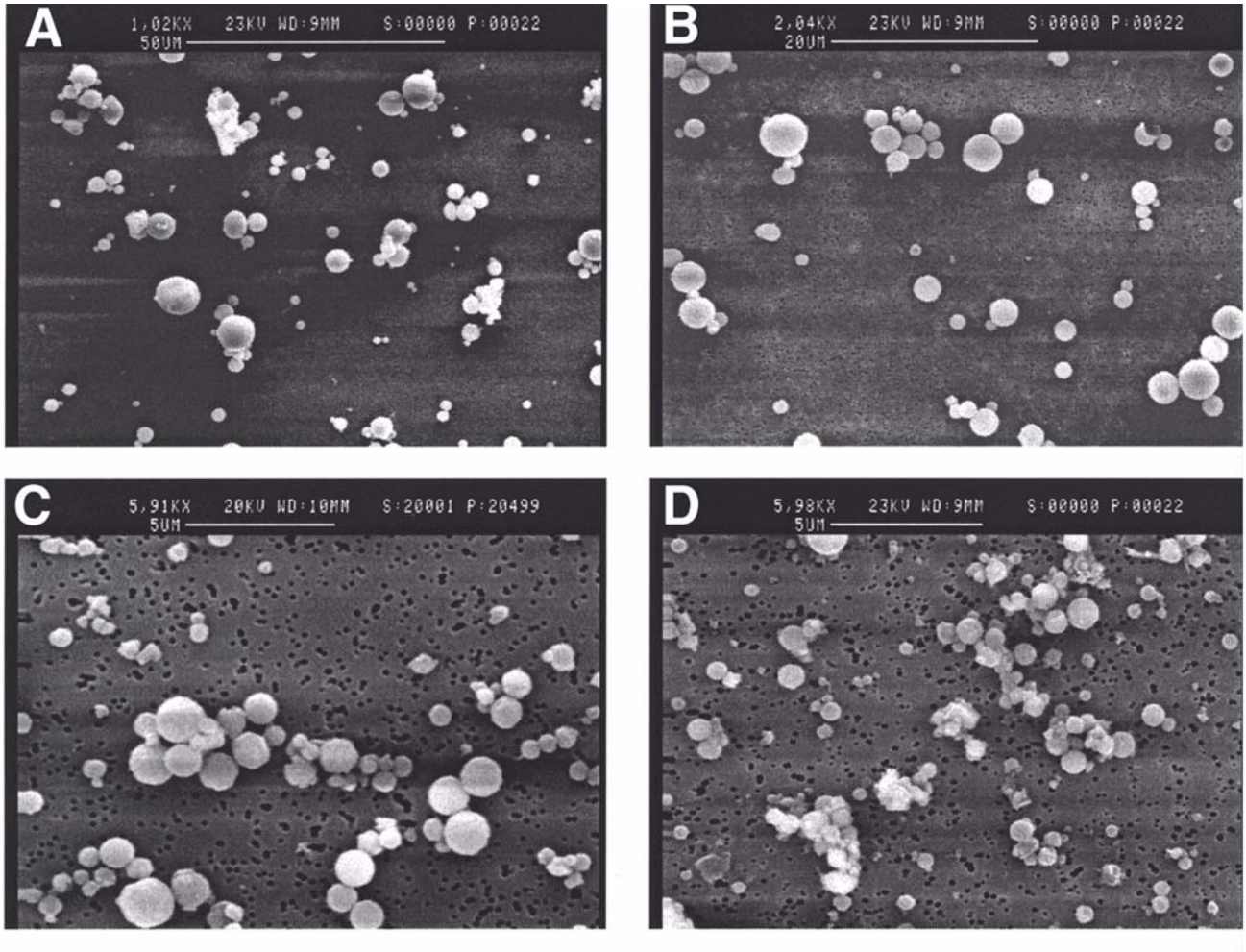

Figure 6. SEM images of the 1998 size-fractionated North Dakota CFA. ***A***. $PM_{>10}$ at ×1000 magnification; ***B***. $PM_{2.5–10}$ at ×2000 magnification; ***C***. $PM_{2.5}$ at ×6000 magnification; and ***D***. PM_1 at ×6000 magnification. The spherical particles are mineral ash; the irregular particles are char; the black circles are pores in the polycarbonate substrate.

ash cools and freezes after leaving the combustion zone. The method used to handle the $PM_{2.5}$ and PM_1 was considered unlikely to affect the particle surface area for either iron mobilization or for the surface measurement by nitrogen adsorption.

Collection Rates Table 4 summarizes the nominal rate at which size-fractionated samples were collected from either the virtual impactor (PM_1) or the cascade impactor ($PM_{2.5}$, $PM_{2.5–10}$, $PM_{>10}$). Over the course of the experiment, the time required to collect gram-size samples of submicron particles decreased from about 13 days to 2 days, demonstrating that the method can generate samples sufficient for replicating particle characterization and biochemical assays.

Determination of Mass Distribution and Surface Area The mass distributions of size-fractionated Utah, Illinois,

Table 4. Collection Rates of Size-Fractionated CFA

Sample	Mass Collected (g)	Total Collection Time (hr)	Collection Rate (mg/hr)	Collection Time (days)[a]	Number of Runs[a]	Run Times (min/run)
Utah						
PM_1	0.771	—	126[b]	13	22	30–60
$PM_{2.5}$	1.763	8.5	207	5	9	60
$PM_{2.5–10}$	1.618	8.5	190	5	9	60
$PM_{>10}$	7.143	8.5	840	5	9	60
Illinois						
PM_1	1.107	6.5	171[b]	3	6	60–90
$PM_{2.5}$	0.378	4.3	88	4	4	60–70
North Dakota						
PM_1	1.017	4.1	248[b]	2	6	40–60
$PM_{2.5}$	0.840	1.8	467	2	5	20–30
$PM_{2.5–10}$	0.765	1.8	425	2	5	20–30
$PM_{>10}$	0.750	1.8	417	2	5	20–30

[a] Collection time decreased from 13 days with 22 runs for the first sample to 2 days with 5 runs for the last samples. Efficiency reflects improvements in equipment and procedures during the project.

[b] Average collection rates when 4 filters were used in the submicron particle collection system.

and North Dakota CFA samples are shown in Figures 7 through 9, respectively. The number-weighted, surface-weighted, mass-weighted, and aerodynamic mean diameters of each sample are presented in Table 5.

The surface area of the CFA samples determined by nitrogen adsorption ranged from 0.85 m^2/g for $PM_{>10}$ to 6.72 m^2/g for PM_1 (Table 6). The area-weighted mean particle diameters determined by SEM analysis were used to calculate the SEM surface area of spherical particles with a density of 2.5 g/cm^3. The ratios of nitrogen adsorption surface area to SEM surface area show that surface areas determined by nitrogen adsorption analysis were 1 to about 4 times larger than the SEM surface area, with the difference generally increasing with particle size (Table 6). This result suggests that the particles contain micropores that were not detected at the magnification used for SEM imaging.

Elemental Analysis The metals that were greater than 5000 µg/g in the CFA were sodium, magnesium, aluminum, calcium, titanium, potassium, and iron (Table 7). The iron

Table 5. Mean Diameters (in microns) of 1998 CFA Samples

	Number Weighted[a]		Surface Weighted[b]		Mass Weighted[c]		Aerodynamic[d]
Sample	d_g	σ_g	d_{gs}	σ_{gs}	d_{gm}	σ_{gm}	D
Utah							
PM_1	0.38	1.55	0.57	1.63	0.75	1.80	1.19
$PM_{2.5}$	0.47	1.91	0.97	1.73	1.27	1.64	2.02
$PM_{2.5–10}$	1.40	2.01	2.67	1.57	3.19	1.49	5.04
$PM_{>10}$	1.37	1.92	3.28	2.06	5.82	2.15	9.20
Illinois							
PM_1	0.30	1.77	0.56	1.74	0.77	1.82	1.22
$PM_{2.5}$	0.40	1.95	0.79	1.62	0.96	1.49	1.52
$PM_{2.5–10}$	0.96	2.12	2.31	1.81	3.30	1.83	5.22
$PM_{>10}$	0.78	2.23	2.89	1.94	3.94	1.59	6.23
North Dakota							
PM_1	0.39	1.68	0.68	1.76	0.97	1.87	1.53
$PM_{2.5}$	0.46	2.06	0.91	1.62	1.12	1.54	1.77
$PM_{2.5–10}$	1.33	1.94	2.35	1.53	2.74	1.43	4.33
$PM_{>10}$	1.30	2.18	3.53	1.92	5.43	1.94	8.58

[a] The number-weighted geometric mean diameter (d_g) and geometric standard deviation (σ_g) are calculated according the following equations:

$$d_g = \frac{\sum n_i \ln d_i}{N} \qquad \ln\sigma_g = \left[\frac{\sum n_i(\ln d_i - \ln d_g)^2}{N-1}\right]^{1/2}$$

where the variable n_i is the number of particles in group i having a midpoint diameter d_i, and N is the total number of particles.

[b] The surface-weighted geometric mean diameter (d_{gs}) and geometric standard deviation (σ_{gs}) are calculated according to the following equations:

$$d_{gs} = \frac{\sum S_i \ln d_i}{S} = \frac{\sum \pi n_i d_i^2 \ln d_i}{\sum \pi n_i d_i^2} = \frac{\sum n_i d_i^2 \ln d_i}{\sum n_i d_i^2} \qquad \ln\sigma_{gs} = \left[\frac{\sum S_i(\ln d_i - \ln d_g)^2}{S-1}\right]^{1/2} = \left[\frac{\sum n_i d_i^2(\ln d_i - \ln d_g)^2}{\sum n_i d_i^2}\right]^{1/2}$$

where S is the total surface area of all particles and S_i is the total surface area of particles in group i.

[c] The mass-weighted geometric mean diameter (d_{gm}) and geometric standard deviation (σ_{gm}) are calculated according to the following equations:

$$d_{gm} = \frac{\sum M_i \ln d_i}{M} = \frac{\sum (\pi\rho/6) n_i d_i^3 \ln d_i}{\sum (\pi\rho/6) n_i d_i^3} = \frac{\sum n_i d_i^3 \ln d_i}{\sum n_i d_i^3} \qquad \ln\sigma_{gm} = \left[\frac{\sum M_i(\ln d_i - \ln d_g)^2}{M-1}\right]^{1/2} = \left[\frac{\sum n_i d_i^3(\ln d_i - \ln d_g)^2}{\sum n_i d_i^3}\right]^{1/2}$$

where M is the total mass of particles, M_i is the total mass of particles in group i, and ρ is particle density.

[d] The aerodynamic diameter (D) was calculated as $D = d_{gm}\sqrt{2.5}$, where 2.5 g/cm^3 is the assumed particle density.

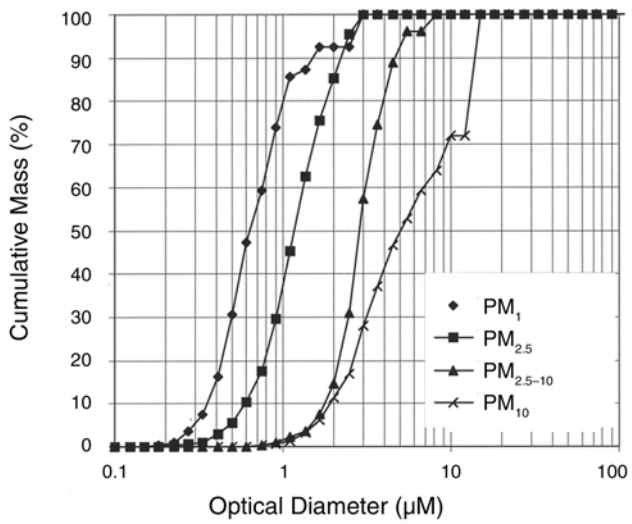

Figure 7. Mass distribution of size-fractionated Utah CFA. The size of the particles was determined by SEM measurements of individual particles.

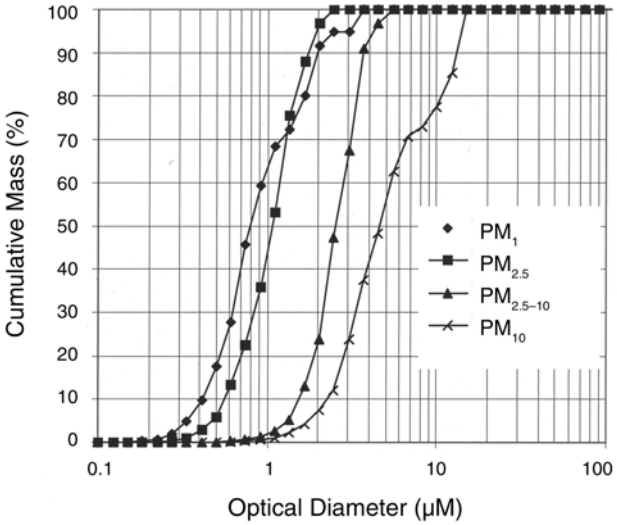

Figure 9. Mass distribution of size-fractionated North Dakota CFA. The size of the particles was determined by SEM measurements of individual particles.

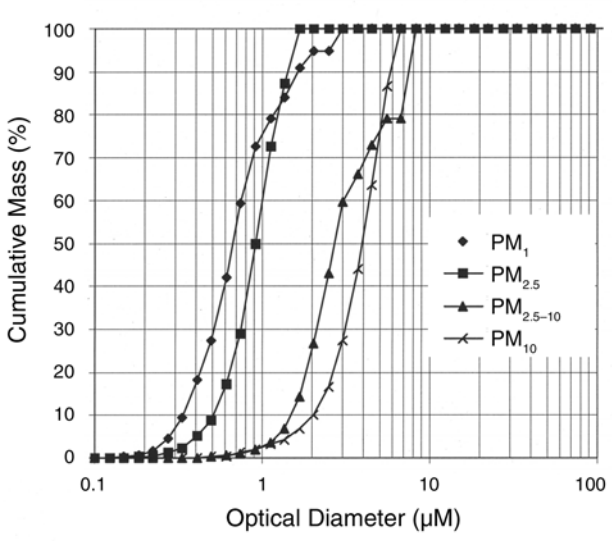

Figure 8. Mass distribution of size-fractionated Illinois CFA. The size of the particles was determined by SEM measurements of individual particles.

Table 6. Comparison of Surface Area Estimates (m^2/g) Obtained Using SEM and Nitrogen Adsorption

Sample	N_2 Adsorption Surface Area	SEM Dp,a[a]	SEM Surface Area[b]	N_2 Adsorption/ SEM Surface Areas
Utah				
PM_1	6.50	0.65	3.67	1.77
$PM_{2.5}$	3.00	1.12	2.15	1.40
$PM_{2.5–10}$	2.20	2.92	0.82	2.68
$PM_{>10}$	2.01	4.35	0.55	3.64
Illinois				
PM_1	5.17	0.65	3.67	1.41
$PM_{2.5}$	3.14	0.88	2.74	1.15
$PM_{2.5–10}$	1.77	2.75	0.87	2.03
$PM_{>10}$	ND[c]	3.44	0.70	ND[c]
North Dakota				
PM_1	6.72	0.80	2.98	2.25
$PM_{2.5}$	3.14	1.01	2.36	1.33
$PM_{2.5–10}$	1.04	2.55	0.94	1.10
$PM_{>10}$	0.85	4.37	0.55	1.55

[a] Dp,a = surface-weighted mean particle diameter (in microns) obtained from analysis of SEM images.

[b] SEM surface area was calculated for particles assuming a density of 2.5 g/cm^3. Area/mass = $6/2.5 \times$ Dp,a.

[c] ND = not determined.

Table 7. Elemental Analysis by INAA for CFA[a]

	Utah[b]				Illinois[b]	
Element	PM_1	$PM_{2.5}$	$PM_{2.5–10}$	$PM_{>10}$	PM_1	$PM_{2.5}$
Na	35,000±2,400	39,000±270	32,000±2,200	34,000±2,200	24,000±1,700	22,000±1,600
Mg	120,000±2,600	15,000±3,000	12,000±2,600	8,000±1,500	8,800±2,200	7,400±1,800
Al	90,000±3,700	110,000±4,800	93,000±4,000	90,000±3,600	100,000±4,600	110,000±5,000
Ca	—[c]	< 29,000	< 49,000	—[c]	< 7,700	< 6,200
Ti	6,100±630	6,600±750	5,100±560	5,500±560	8,000±910	7,800±940
K	10,000±3,100	4,900±1,500	16,000±3,200	18,000±3,400	25,000±4,700	29,000±5,500
Fe	65,000±6,400	38,000±2,500	38,000±2,600	58,000±4,200	140,000±6,800	130,000±6,400
Cl	380±84	94±46	350±67	2,900±200	160±58	64±61
V	400±23	270±18	120±8.2	130±7	740±47	570±37
Cr	320±65	160±24	130±18	220±39	200±19	250±22
Mn	85±1.8	86±1.7	84±1.6	91±1.7	360±5.8	340±5.6
Sc	32±0.2	17±1.1	18±1.2	27±1.8	38±2.5	35±2.2
Co	77±11	41±4.3	37±4.6	47±5.8	150±11	150±11
Zn	370±140	210±99	130±71	420±110	1,500±400	1,400±360
Ga	120±52	110±96	72±45	< 43	210±170	170±130
As	100±10	41±4.1	22±2.2	27±7.9	1,200±120	710±71
Se	< 26	7.5±7.4	8±7.4	< 12	37±36	< 14
Br	21±6.3	2±1	3.6±1.2	71±20	21±6.1	3.2±1.5
Rb	< 600	< 160	< 350	130±110	< 47	130±83
Sr	700±140	680±150	470±110	690±130	750±170	690±180
Mo	84±29	24±8.2	21±6.7	24±10	110±24	58±13
Cd	< 1.5	< 4.1	< 0.75	< 0.11	< 10	< 6.4
In	350±210	< 0.88	< 0.26	240±230	< 2.2	< 1.6
Sb	12±1.2	3.7±0.42	2.5±0.26	4.5±0.53	150±12	67±5.5
Cs	20±15	13±5.7	8.5±4.3	8.8±6.4	31±7	32±7.2
Ba	2,300±200	1,700±140	1,500±140	1,800±160	550±72	520±87
La	130±8.1	78±5	76±4.8	100±6.6	100±6.4	96±6.1
Ce	210±26	110±9.4	110±8.6	150±16	180±12	180±12
Nd	40±14	43±14	41±11	38±9.7	72±19	89±19
Sm	15±1.3	9±0.76	9.2±0.86	12±1.1	16±1.4	15±1.3
Eu	< 7.6	0.17±0.069	0.18±0.052	2.7±1.6	< 0.65	3.9±1.3
Yb	6.2±2.5	3.8±1	3±0.83	8.1±2	5.9±1.3	5.6±1.3
Lu	600±240	0.46±0.14	0.39±0.11	0.78±0.2	0.59±0.14	0.99±0.23
Au	0.064±0.033	< 0.0051	0.0051	0.038±0.019	< 0.022	< 0.021
Hg	< 0.041	< 2.4	< 1.9	< 0.041	< 1.9	< 1.8
Th	33±4.3	13±1.3	15±1.4	22±2.4	24±2.4	25±2.2
U	86±12	16±1.9	10±1.3	8.8±2.4	23±1	14±0.68

Table continues next page

[a] INAA was performed by Environmental Research & Radiochemistry, MIT Nuclear Reactor Laboratory, Cambridge MA. Four samples of NIST 1633b fly ash were used as standards; the SD for the samples was 0.54 weight percentage (5,354 µg/g).

[b] All values are micrograms per gram particle.

[c] Not detected because amounts were less than lower limit of detection.

Table 7 (*continued*). Elemental Analysis by INAA for CFA[a]

Illinois[b]		North Dakota[b]				
$PM_{2.5–10}$	$PM_{>10}$	PM_1	$PM_{2.5}$	$PM_{2.5–10}$	$PM_{>10}$	Element
21,000±1,400	19,000±1,300	21,000±1,400	75,000±5,200	76,000±5,200	63,000±4,200	Na
7,500±1,900	6,900±2,100	5,200±1,100	18,000±3,700	23,000±4,800	44,000±8,400	Mg
130,000±5,700	120,000±5,400	130,000±5,300	80,000±3,400	83,000±3,600	83,000±3,500	Al
< 8,600	< 13,000	—[c]	< 97,000	< 100,000	—[c]	Ca
7,200±890	6,800±1,100	7,000±780	3,100±660	2,200±690	4,600±740	Ti
25,000±4,700	23,000±5,600	26,000±3,400	7,600±1,900	7,500±2,100	8,300±3,500	K
81,000±4,600	98,000±5,400	62,000±4,100	20,000±3,000	16,000±2,800	40,000±11,000	Fe
230±74	6,300±530	240±72	550±120	500±210	2,100±230	Cl
300±19	310±22	310±160	110±8.8	82±8.3	84±7.7	V
210±22	250±33	90±14	26±23	77±27	150±92	Cr
240±4.3	240±4.5	240±3.9	500±7.9	510±8.1	530±8.8	Mn
33±2.1	39±2.5	27±1.8	13±0.85	14±0.94	20±1.5	Sc
91±7.7	140±11	71±7.3	34±4.6	42±6.1	41±13	Co
800±250	4,200±880	500±160	180±150	140±130	< 310	Zn
200±110	< 140	< 43	< 140	< 140	< 43	Ga
280±28	350±35	230±23	190±18	140±14	130±13	As
47±44	49±33	< 4.5	23±19	< 7	< 14	Se
16±5.1	120±33	15±4.4	< 4.4	< 4	38±13	Br
58±48	< 270	110±66	280±110	130±110	< 11,200	Rb
370±140	280±210	480±120	6,500±1,100	5,300±960	4,300±590	Sr
25±6.8	60±25	37±14	34±17	39±18	< 20	Mo
< 3.7	< 4.6	3.2±2.7	1.4±0.41	< 14	< 4.6	Cd
0.67±0.64	< 0.4	730±510	< 0.39	< 0.28	350±260	In
27±2.3	36±3	24±2.1	13±1.2	6.9±0.73	5.8±1.2	Sb
10±3.8	18±5.4	15±9.4	< 11	4.5±3.8	< 18	Cs
360±100	560±170	320±98	13,000±990	9,600±710	11,000±790	Ba
72±4.6	85±5.5	62±4	34±2.2	32±2.1	42±2.9	La
120±12	150±18	130±16	72±14	62±16	91±39	Ce
53±16	91±31	38±20	< 55	< 70	< 74	Nd
12±1.3	15±1.3	11±0.92	4.9±0.43	5.1±0.45	6.6±0.6	Sm
1.2±0.78	4.7±2	4.8±3.6	3.6±2.5	3±2.5	< 18	Eu
4.3±1.1	5.6±2	3.9±0.97	3.1±1.5	3.6±1.7	< 3.6	Yb
0.7±0.17	1.4±0.35	0.7±0.19	0.19±0.11	0.59±0.18	0.6±0.37	Lu
< 0.0066	0.012±11	0.012±0.0061	< 0.018	< 0.0051	0.0098±0.0064	Au
< 1.8	1.9±1.4	< 1.8	< 2.6	< 3.2	< 3.9	Hg
21±2.2	25±3.3	16±2.1	12±2.1	8.7±2.4	7.3±6	Th
8.5±0.7	15±0.89	9.1±1.5	5.7±0.52	5.5±0.58	19±2.5	U

[a] INAA was performed by Environmental Research & Radiochemistry, MIT Nuclear Reactor Laboratory, Cambridge MA. Four samples of NIST 1633b fly ash were used as standards; the SD for the samples was 0.54 weight percent (5,354 µg/g).

[b] All values are micrograms per gram particle.

[c] Not detected because amounts were less than lower limit of detection.

content is summarized in Figure 10. Utah CFA contained 3.8% to 6.5% iron by weight; Illinois CFA, 8.1% to 14.0%, and North Dakota CFA, 1.6% to 6.2%. The PM_1 fly ash fraction was richer in iron than the coarser fractions of the same coal for all three mines (Figure 10). The carbon content for all the samples was 2.05% to 3.1% by weight.

Analysis of CFA Reactivity

Mobilization of Iron from CFA by Citrate and Ferrozine Size-fractionated CFA was selected for these studies because of the need for additional information on the biological effects of the different size fractions of inhalable air particulates. We used citrate, a physiologically relevant chelator, because previous studies have shown that the amount of iron mobilized from crocidolite asbestos by citrate in vitro indicated the amount of iron mobilized from crocidolite in A549 cells (Chao et al 1994). Although no iron was mobilized from CFA incubated in 50 mM NaCl (pH 7.5) in the absence of metal chelators (data not shown), iron was mobilized by citrate from the three larger size fractions of CFA (Figure 11). (We did not use PM_1 in these assays because the amount of sample available was limited.)

The method of collecting $PM_{2.5}$, using ethanol and ultrasonic agitation, may have altered the particles in a way that changed the rates of iron mobilization. However, differences in iron mobilization from particles collected dry and those collected in ethanol with ultrasonic agitation

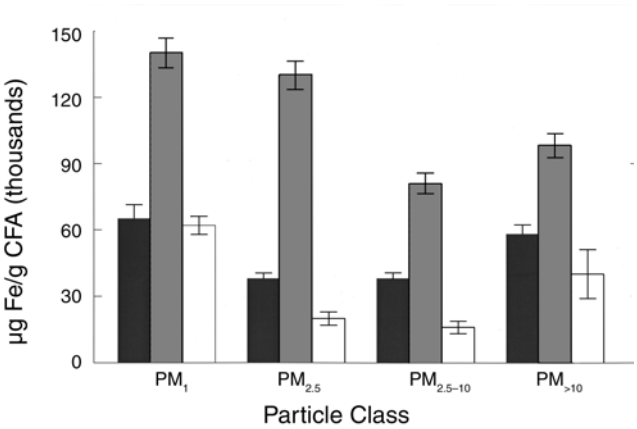

Figure 10. Iron content in size-fractionated CFA determined by INAA. The CFA from different sources of coal designated as follows: Utah, black bars; Illinois, gray bars; North Dakota, white bars.

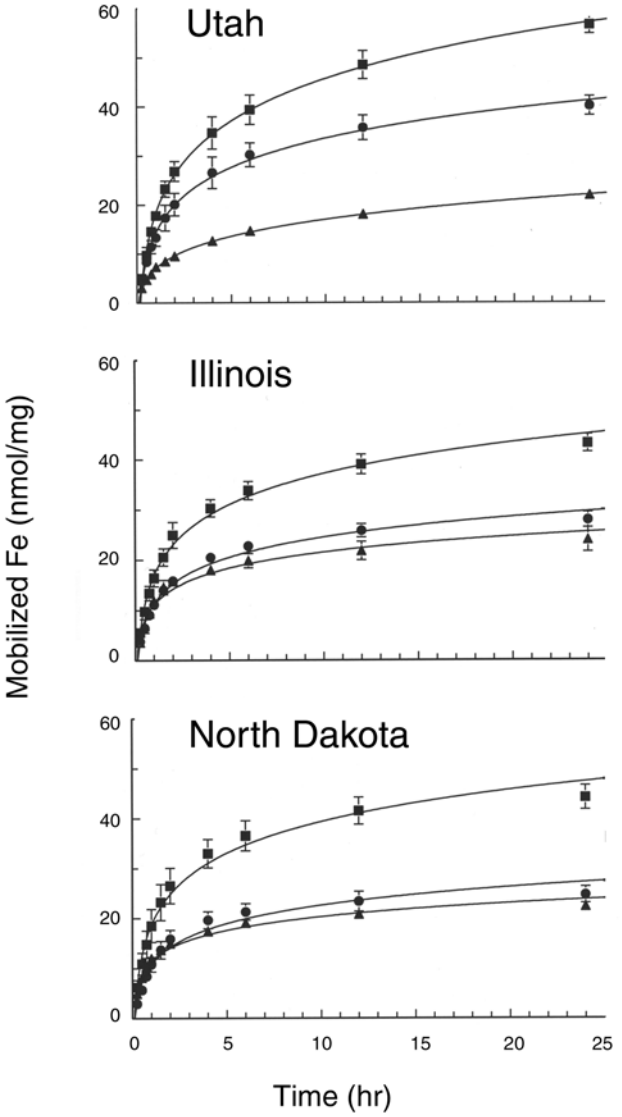

Figure 11. Iron mobilization from CFA by citrate. Samples (1 mg/mL) of CFA $PM_{2.5}$ (■); $PM_{2.5–10}$ (●); and $PM_{>10}$ (▲) produced from Utah, Illinois, or North Dakota coal were incubated in 50 mM NaCl (pH 7.5) with 1 mM citrate for 24 hours. Each symbol represents the mean (n = 3); each error bar represents 1 SD. The absence of error bars indicates that the SD is contained within the symbol.

were well within the limits of normal variation among replicate samples (typically 2–4 nmol/mg particle). Thus, it appeared that using ethanol had little, if any, effect on iron mobilization. Particles collected in ethanol were used for the remainder of the experiments. The amount of iron mobilized after 24 hours is summarized in Figure 12. (For statistical analysis of the data, see Table B.1.) For every coal type, more iron was mobilized from CFA $PM_{2.5}$ than from larger-diameter particles. In addition, more iron was mobilized from Utah CFA $PM_{2.5}$ than from Illinois CFA $PM_{2.5}$, even though the Illinois CFA contained almost 3 times more iron.

We also compared the amount of iron mobilized by citrate in 24 hours among the CFA samples, crocidolite, diesel exhaust particles, the urban air particulates SRM 1648 and SRM 1649, the soil and mine tailings samples, and two iron oxides often present in crustal dust samples, hematite and magnetite (Table 8). Clearly, CFA and urban particulates release considerably more iron in the presence of citrate

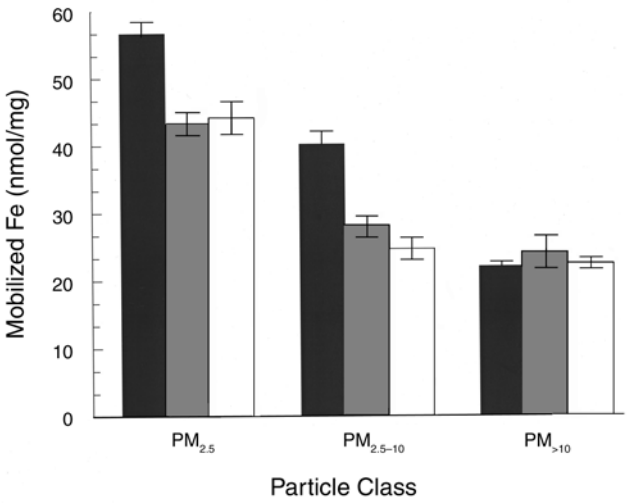

Figure 12. Mobilization of iron from CFA by citrate in 24 hours. These data were taken from Figure 11. The CFA from different sources of coal is designated as follows: Utah, black bars; Illinois, gray bars; North Dakota, white bars. Each bar represents the mean (n = 3); each error bar represents 1 SD.

Table 8. Mobilization of Iron from Particulates[a] and Biological and Biochemical Effects of Particulates

Particulate (1 mg/mL)[b]	Fe Content (nmol/mg particle)	Fe (nmol/mg particle) Mobilized by Citrate in 24 Hours[c]	Fe Mobilized by Citrate in 24 Hours (%)	Ferritin (ng/μg protein)[c]	IL-8 (pg/mL medium)[c]
Utah CFA $PM_{2.5}$	892	56.7 ± 1.8	6.4	0.95 ± 0.07	402 ± 45
SRM 1649	536	52.9 ± 2.4[d]	9.9	1.51 ± 0.09[d]	ND[e]
North Dakota CFA $PM_{2.5}$	554	44.1 ± 2.4	8.0	0.38 ± 0.03	127 ± 6
Illinois CFA $PM_{2.5}$	2679	43.3 ± 1.8	1.6	0.75 ± 0.09	279 ± 35
Utah CFA $PM_{2.5–10}$	786	40.2 ± 1.9	5.1	0.61 ± 0.08	278 ± 16
Crocidolite	4821	37.7 ± 2.9[f]	0.8	0.54 ± 0.08[f]	ND
Illinois CFA $PM_{2.5–10}$	1964	27.9 ± 1.5	1.4	0.52 ± 0.09	216 ± 35
SRM 1648	696	24.9 ± 0.8[d]	3.6	1.15 ± 0.16[d]	ND
North Dakota CFA $PM_{2.5–10}$	1054	24.6 ± 1.6	2.3	0.33 ± 0.05	103 ± 8
Illinois CFA $PM_{>10}$	1964	24.0 ± 2.4	1.2	0.36 ± 0.03	120 ± 10
North Dakota CFA $PM_{>10}$	1268	22.3 ± 0.8	1.8	0.14 ± 0.03	106 ± 9
Utah CFA $PM_{>10}$	875	22.0 ± 0.7	2.5	0.23 ± 0.03	103 ± 10
Mine Tailings	554	20	3.6	ND	ND
DEP	ND	17.1	ND	0.33	ND
Magnetite (10 mg/mL)	12,857	7.8 ± 1.2[g]	<0.1	0.30 ± 0.02[g]	ND
Mancos Clay	518	4	0.8	ND	ND
Desert Dust	536	2	0.4	ND	ND
Hematite (10 mg/mL)	12,500	0[g]	0	0.13 ± 0.03[g]	ND

[a] Listed in order of decreasing amount of iron mobilized.

[b] Unless otherwise noted.

[c] Values are mean ± SD.

[d] Data taken from Smith and Aust 1997.

[e] ND = not determined.

[f] Data taken from Fang and Aust 1997.

[g] Data taken from Fang 1999.

than the iron oxides; in fact, hematite appeared to release none.

Incubation of CFA $PM_{2.5}$ from all 3 coal sources with ferrozine did not result in any detectable mobilization of iron(II) (data not shown).

Solubility of Metals from CFA Under Various Conditions Because of the developing interest in the role of transition metals in the biological effects of inhaled particulates, we compared our method of measuring metal bioavailability using citrate with methods that use water, which are commonly employed by other research groups. The solubility of different metals in CFA $PM_{2.5}$ only in the presence or absence of citrate at different pHs is shown in Table 9. Iron was approximately 4 times more soluble at pH 2.5 in the absence of citrate than at pH 7.5 in the presence of 1 mM citrate. Iron was not detected in the supernatant from CFA $PM_{2.5}$ incubated in 50 mM NaCl at pH 7.5. These results suggest that both pH and the presence of a chelator are important when determining the bioavailability of metals from PM. Further, the method of determining metal solubility by simply suspending metal-containing particles in water is not likely to reflect what may occur in the lungs at a pH near 7.5. For example, vanadium, iron, and nickel from ROFA suspended in water may be soluble at pH 2.8, but not necessarily at the pH of the lung. Thus, it is important to select a pH and chelator(s) that most closely mimic those in the lungs and in lung cells exposed to PM.

MDA Formation Catalyzed by CFA Size-fractionated CFA particles extracted with phosphate buffer were used to catalyze the formation of MDA (see Figure 13 for assay results and Table B.1 for statistical results). PM_1 extracts from Illinois coal and from Utah coal generated more MDA than PM_1 extracts from North Dakota coal. The $PM_{2.5}$ and $PM_{2.5–10}$ fractions from all coal sources catalyzed about the same amount of MDA. The $PM_{>10}$ fraction of North Dakota coal generated less MDA than the other two sources of coal particles from the same size fraction.

ICP-MS analysis of the metal content of phosphate-buffer CFA extracts from all three mines detected only

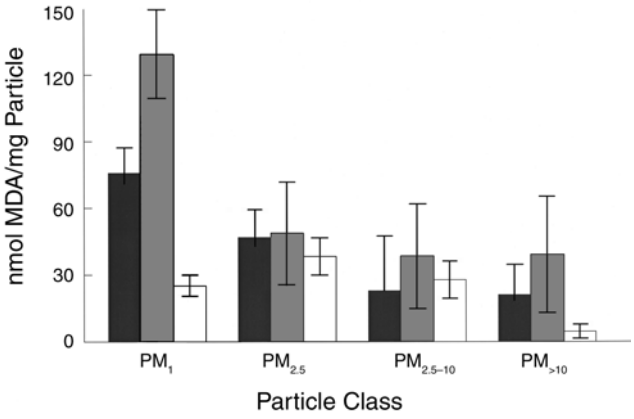

Figure 13. CFA-catalyzed production of MDA. Phosphate-buffer extracts from a 24-hour incubation with size-fractionated CFA particles were mixed with ascorbic acid (1 mM final concentration) and 2-deoxyribose (1 mM final concentration) with or without 1 mM DF and were shaken vigorously for 24 hours at 37°C. The solutions were analyzed for MDA with 2-thiobarbituric acid. The CFA from different sources of coal are designated as follows: Utah, black bars; Illinois, gray bars; North Dakota, white bars. Each bar represents the mean (n = 3); each error bar represents 1 SD.

Table 9. Solubility of Metals from Utah CFA $PM_{2.5}$ at Different pHs, With and Without Citrate[a] (nmol metal/mg CFA)

	Al	Cr	Cu	Fe	Mg	Pb	Si	Sr	Zn
Solution									
Water (pH 2.5)	1931±33	1±0.1	2±0	107±4	251±4	0.5±0.0	1064±14	8±0.2	3±0.3
Water (pH 10.1)	56±7	1±0.0	ND[b]	ND	37±1	ND	85±7	2±0.1	ND
50 mM NaCl (pH 7.5)	ND	1±0.0	ND	ND	37±0.8	ND	36±4	2±0.1	ND
50 mM NaCl + 1 mM Citrate (pH 7.5)	63±1	1±0.1	ND	27±0.7	53±0.9	ND	89±11	3±0.1	3±0.2
Reporting Limits	4	0.6	0.8	0.9	8	0.2	2	0.6	0.8

[a] 1 mg/mL $PM_{2.5}$ was incubated in solution for 24 hours at room temperature. The metals present in the supernatant were determined by ICP. Each value is mean ± SD (n = 3).

[b] ND = not detected.

copper and zinc (Table 10). The Illinois and Utah CFA PM_1 extracts showed higher MDA-forming activity, which is reflected qualitatively by their higher concentrations of copper and zinc extracts. However, solubilization of copper and zinc was not associated with particle size within a coal source. The high detection limit for iron (Table 10) suggests that iron could have been present in these samples at a concentration high enough to generate MDA, but too low to be detected by ICP-MS. Preincubation of the buffer extracts with 1 mM DF inhibited 78% or more of MDA formation from the four CFA PM fractions from each mine, further suggesting that transition metals were responsible for MDA formation.

Modeling Iron Mobilization The rate of the mobilization of iron from CFA in vitro is consistent with solid-phase, diffusion-limited mass transfer, and the differences in total amount of mobilized iron are consistent with size-dependent differences in chemical speciation (Veranth et al 2000b). (For a more specific discussion of these studies, see Appendix C.)

Effect of CFA or FAC on Ferritin Concentration in A549 Cells To determine whether iron was mobilized from CFA in A549 cells, cellular ferritin levels were measured in cells after 24 hours of exposure to CFA and compared with those of untreated controls. Ferritin levels were inversely proportional to the size of the CFA particles for each coal source, and ferritin levels differed by coal source (highest in Utah and lowest in North Dakota). Ferritin levels in A549 cells treated with Utah CFA PM_1, $PM_{2.5}$, $PM_{2.5–10}$, and $PM_{>10}$ were 16.1, 11.9, 7.6, and 2.9 times greater, respectively, than levels in untreated controls (Figure 14). (For statistical results, see Table B.1.) Similarly, ferritin

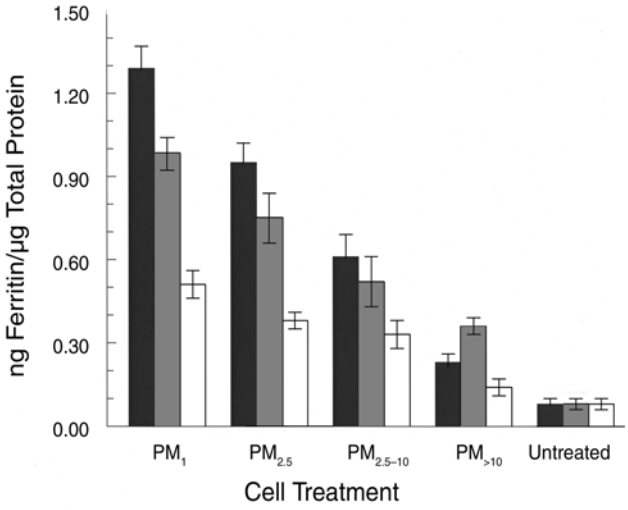

Figure 14. Effect of CFA on the concentration of ferritin in A549 cells. A549 cells were plated in complete growth medium and treated with CFA (20 µg/cm^2). Cells were harvested 24 hours later and the concentration of ferritin was determined. The CFA from different sources of coal is designated as follows: Utah, black bars; Illinois, gray bars; North Dakota, white bars. Each bar represents the mean (n = 3); each error bar represents 1 SD.

Table 10. Soluble Transition Metal Content of Phosphate-Buffered CFA Extracts

Sample	Mass (mg)	Content (mg/kg)[a,b]		Concentration (µM)	
		Cu	Zn	Cu	Zn
Utah					
PM_1	0.64	42	258	0.22	0.84
$PM_{2.5}$	0.72	54	133	0.28	0.49
$PM_{2.5–10}$	0.20	< 75	< 75	< 0.079	< 0.076
$PM_{<10}$	0.20	< 75	< 75	< 0.079	< 0.076
Illinois					
PM_1	0.51	206	394	0.63	1.0
$PM_{2.5}$	0.26	69	< 58	0.17	< 0.076
$PM_{2.5–10}$	0.40	158	< 38	0.41	< 0.076
$PM_{<10}$	0.10	< 75	300	< 0.079	0.23
North Dakota					
PM_1	0.85	11	133	0.13	0.72
$PM_{2.5}$	0.65	69	58	0.33	< 0.076
$PM_{2.5–10}$	0.70	39	< 21	0.22	< 0.076
$PM_{<10}$	0.80	< 19	< 19	< 0.079	< 0.076

[a] Iron, cobalt, vanadium, and nickel were not detected by ICP-MS.

[b] Iron detection limit was <1.8 mg/kg by ICP-MS.

levels in cells treated with Illinois CFA PM_1, $PM_{2.5}$, $PM_{2.5–10}$, and $PM_{>10}$ were 12.3, 9.4, 6.5, and 4.5 times greater than untreated control cells; corresponding values for North Dakota were 6.4, 4.8, 4.1, and 1.8 times greater. The relation between ferritin levels and CFA PM size shown by these data generally agree with the relation between amounts of iron mobilized by citrate and CFA PM size (for $PM_{2.5}$, $PM_{2.5–10}$, and $PM_{>10}$; PM_1 was not assayed in the iron mobilization studies).

To determine whether a soluble form of iron can increase intracellular iron levels, A549 cells were treated with FAC and the amount of induced ferritin was measured. Cells treated with 0 to 10 mM FAC showed dose-dependent increases in ferritin (Figure 15; for statistical results, see Tables B.2 and B.3). Treatment with 10 mM FAC induced the greatest amount of ferritin, 18.9 times the amount in untreated control cells cultured in the same medium. The response appears to be linear, although ferritin levels may have begun to plateau at FAC concentrations greater than 8 mM.

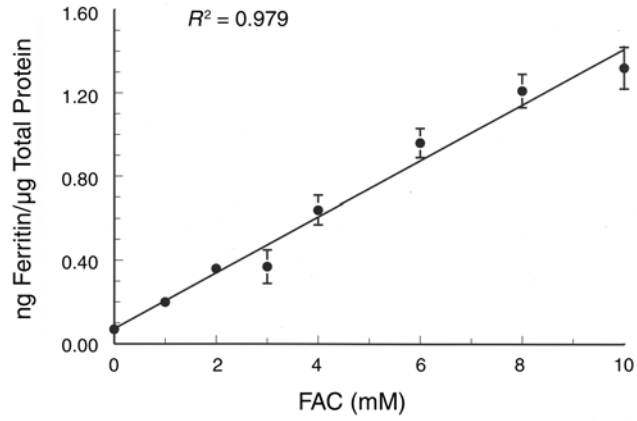

Figure 15. Effect of FAC on the concentration of ferritin in A549 cells. A549 cells were plated in complete growth medium and treated with FAC (0–10 mM). Cells were harvested 24 hours later and the concentration of ferritin was determined. Each symbol represents the mean (n = 3); each error bar represents 1 SD. The absence of error bars indicates that the SD is contained within the symbol.

Ferritin Induction in A549 Cells in the Presence of Cytochalasin D To determine whether iron is mobilized from CFA intracellularly, FAC and Utah CFA $PM_{2.5}$ were each incubated with A549 cells for 24 hours in the presence or absence of cytochalasin D, which inhibits actin filament polymerization and thus prevents endocytosis. Ferritin levels were measured and compared between the treated and untreated cells in each experiment. Utah CFA $PM_{2.5}$ was used because adequate sample was collected and substantial amounts of iron were mobilized from this particular coal and fraction. Ferritin levels in A549 cells treated with FAC (1.5 mM iron), a soluble source of iron, in the presence of 10 µM cytochalasin D did not differ significantly from those in cells not treated with cytochalasin D (Figure 16). Thus, cytochalasin D did not seem to affect ferritin induction by iron that enters the cell by a mechanism other than endocytosis. Ferritin levels in A549 cells treated with Utah CFA $PM_{2.5}$ in the presence of 10 µM cytochalasin D, however, were 82% lower than those in untreated cells. This finding strongly suggests that CFA particles must be endocytized for the iron they contain to be mobilized because, like the results for FAC, if iron mobilized outside rather than inside the cells induced ferritin production, ferritin levels would have been unaffected.

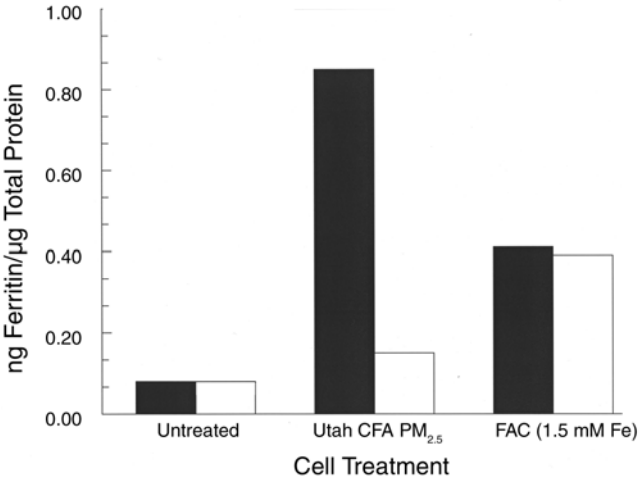

Figure 16. Effect of cytochalasin D on ferritin induction by CFA. A549 cells were plated in complete growth medium with (□) or without (■) 10 µm cytochalasin D; 1 hour later, Utah CFA $PM_{2.5}$ (20 µg/cm^2) or FAC (1.5 mM Fe) was added. Media were removed 24 hours later and ferritin levels were determined. Each bar represents the result from a single determination.

Effect of CFA or FAC in A549 Cell Medium on IL-8 Concentration IL-8 increased according to dose in A549 cells treated with Utah, Illinois, and North Dakota CFA

PM_1, $PM_{2.5}$, and $PM_{2.5–10}$ (Figure 17; for statistical results, see Table B.1). Treatment with CFA $PM_{>10}$ from each coal source did not result in a dose-dependent increase in IL-8. IL-8 levels increased as much as 3.3-, 5.6-, or 8.0-fold over untreated control cells (for the 10, 20,and 40 μg/cm^2 Utah CFA treatments, respectively). IL-8 levels also depended on the source of coal. The 20 μg/cm^2 CFA PM_1 treatment resulted in IL-8 levels that were higher by 1.2-fold and 3.6-fold in cells treated with Utah CFA than those treated with Illinois and North Dakota CFA, respectively. In addition, IL-8 levels were inversely dependent on particle size within a given CFA. Treatment with 20 μg/cm^2 of Utah, Illinois, or North Dakota CFA PM_1 resulted in IL-8 levels 1.6-, 1.9- or 1.4-fold higher than those from $PM_{2.5}$ of the same coal types, respectively.

Endotoxin stimulates IL-8 production and is a frequent PM contaminant. Most particulates were assayed for the presence of endotoxin and none was detected. SRM 1648 and 1649 were heavily contaminated, however, and could not be used as standards for these assays.

To determine whether a soluble form of iron could increase IL-8 levels, A549 cells were treated with FAC (0–10 mM) and the IL-8 in the medium was measured. This treatment resulted in a dose-dependent increase in IL-8 (Figure 18; for statistical results, see Tables B.4 and B.5). IL-8 increased the most in cells treated with 10 mM FAC, wherein its concentration was 6.3-fold higher than untreated control cells cultured in the same medium. IL-8 concentrations increased only at FAC concentrations of greater than 2.6 mM, after which the increase was approximately linear. The IL-8 level may have begun to plateau after approximately 8 mM FAC.

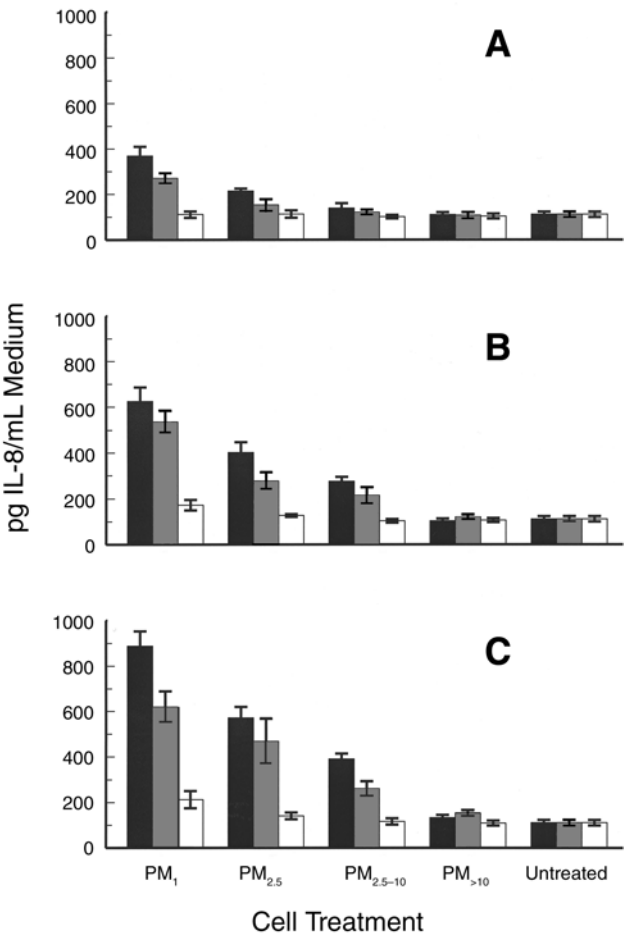

Figure 17. Effect of CFA on IL-8 response in A549 cells. A549 cells were plated in complete growth medium and treated with 10 μg/cm^2 CFA (***A***), 20 μg/cm^2 CFA (***B***), or 40 μg/cm^2 CFA (***C***). Media were harvested 24 hours later, and the concentration of IL-8 was determined. CFA from different sources of coal is designated as follows: Utah, black bars; Illinois, gray bars; and North Dakota, white bars. Each bar represents the mean (n = 3); each error bar represents 1 SD.

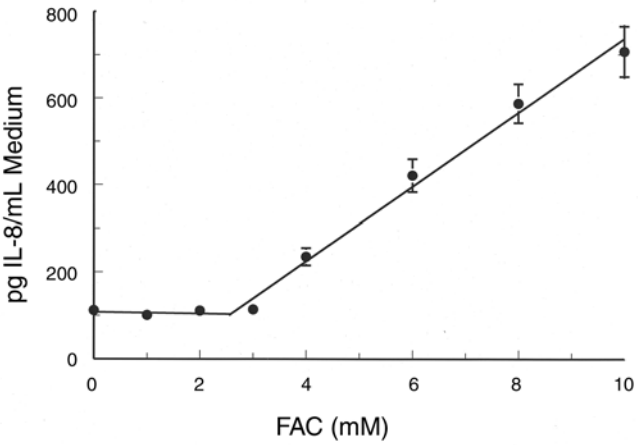

Figure 18. Effect of FAC on IL-8 response in A549 cells. A549 cells were plated in complete growth medium and treated with FAC (0–10 mM). Media were harvested 24 hours later, and the concentration of IL-8 was determined. Each circle represents the mean (n = 3); each error bar represents 1 SD. The absence of error bars indicates that the SD is contained within the symbol. We used PROC NLIN in SAS 7.0 with the secant iterative method and a grid of initial parameter estimates to fit the lines. The equations for the best-fit line before the breakpoint is [IL-8] = 108 − 0.7 × [FAC] and for after the breakpoint is [IL-8] = −112 + 85 × [FAC].

Effect of CFA on IL-8 mRNA Levels Treatment of A549 cells with Utah CFA PM_1 (20 μg/cm^2) for 4 hours resulted in a 2.6-fold increase in IL-8 mRNA levels, over those of untreated control cells (Figure 19). The cytokine IL-1β (0.2 ng/mL), known to increase the levels of IL-8 mRNA (Standiford et al 1990), was used as a positive control. Cells treated with IL-1β had IL-8 mRNA levels 3.6-fold greater than those of untreated control cells. In contrast, A549 cells treated with Utah CFA PM_1, which had been incubated with DF for 14 days to remove the easily mobilized iron, yielded IL-8 mRNA levels that were similar to those of the untreated control cells. No increases in iNOS mRNA were observed under any of the treatment conditions.

Effect of TMTU or DMSO on IL-8 Induction by CFA Utah CFA PM_1 was incubated in the presence of TMTU or DMSO to determine whether oxidative stress is involved in IL-8 production in A549 cells treated with CFA. These antioxidants inhibited IL-8 secretion in a dose-dependent manner (Figure 20). IL-8 levels were reduced to those of untreated control levels when CFA was incubated with A549 cells in the presence of 50 mM TMTU or 140 mM DMSO.

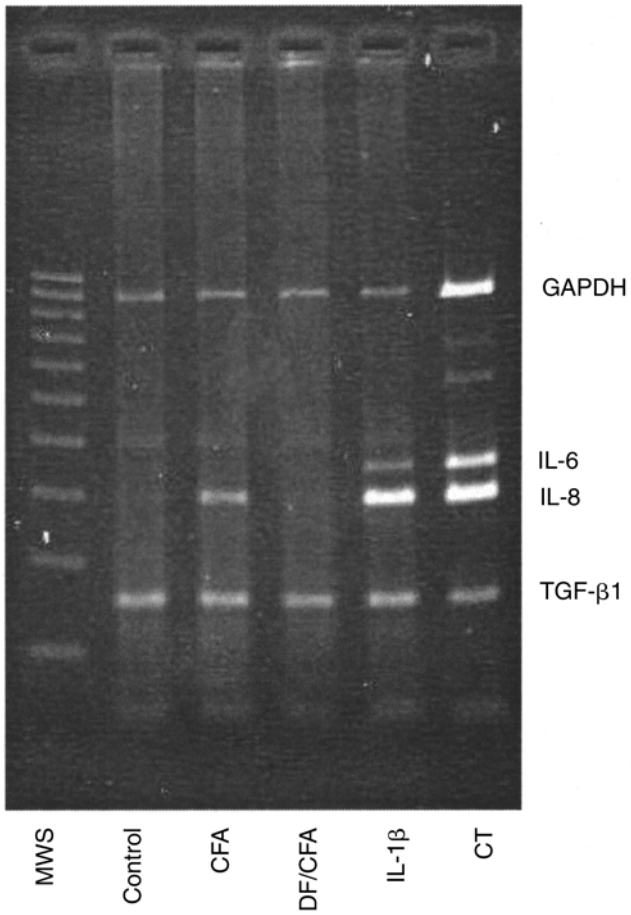

Figure 19. Induction of IL-8 mRNA in CFA-treated A549 cells. A549 cells were cultured in complete growth medium exposed to 20 μg/cm^2 CFA for 4 hours. The cells were removed and the total RNA was isolated and analyzed for IL-8 or GAPDH mRNA using a multiplex PCR kit. MWS lane, molecular weight standards. Control lane, GAPDH and IL-8 in untreated A549 cells. CFA lane, GAPDH and IL-8 in CFA-treated A549 cells. DF/CFA lane, GAPDH and IL-8 in DF/CFA-treated A549 cells. IL-1β lane, GAPDH and IL-8 in A549 cells treated with IL-1β. CT lane, control (cytokine cDNA; Biosource International, Camarillo CA).

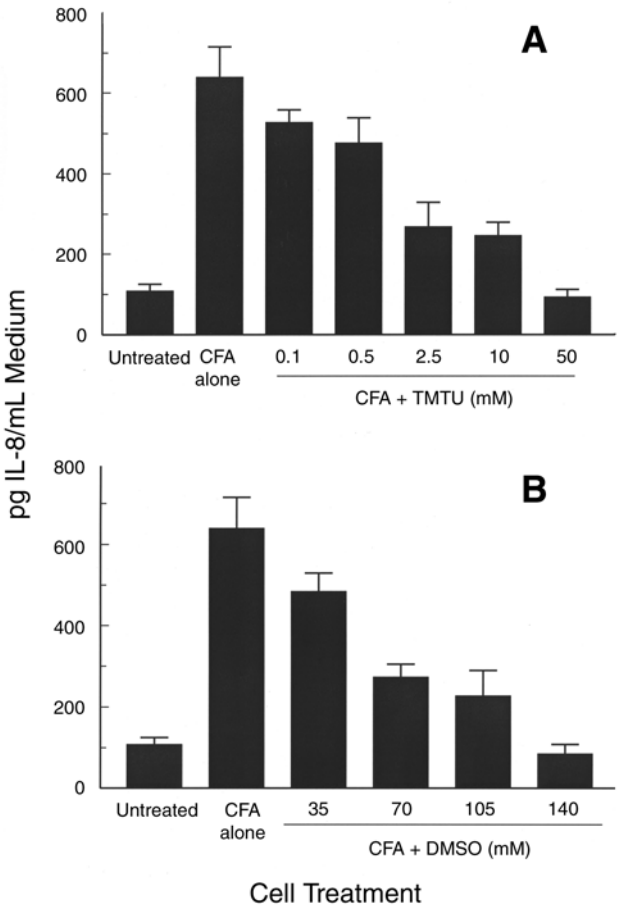

Figure 20. Effect of TMTU or DMSO on CFA-induced IL-8 response in A549 cells. Cells were plated in complete growth medium (untreated), treated with 20 μg/cm^2 Utah CFA PM_1 (CFA alone), or treated for 1 hour with the indicated dose of TMTU (***A***) or DMSO (***B***) and then treated with 20 μg/cm^2 Utah PM_1 CFA. Media were harvested 24 hours later and the concentration of IL-8 was determined. Each bar represents the mean (n = 3); each error bar represents 1 SD.

Effect of CFA or FAC on PGE_2 Levels Treatment of A549 cells with Utah CFA PM_1 (20 μg/cm^2) or with 10 mM FAC for 24 hours resulted in an apparent increase in PGE_2 levels in the extracellular medium. However, after running the appropriate controls, medium with CFA or FAC but without cells, it was clear that CFA and FAC interfered with the assay such that the results were false positives. Therefore, we concluded that CFA and FAC treatment did not increase PGE_2 levels in extracellular medium. Because there was no evidence of increased PGE_2 levels, we did not conduct a Western blot analysis for cyclooxygenase 2.

Relation Between IL-8 Induction and Intracellular Iron Levels in A549 Cells Treated with CFA or FAC To determine whether iron released from CFA was involved in IL-8 induction, we indirectly compared IL-8 levels with intracellular iron levels by using ferritin levels induced by CFA or FAC. The relations between IL-8 production and ferritin levels in cells treated with 20 μg/cm^2 of Utah, Illinois, and North Dakota CFA PM are shown in Figure 21. Ferritin levels increased after CFA exposure and FAC exposure, but IL-8 concentrations increased linearly only after the breakpoint of 0.34 ng ferritin/μg total protein (CFA) and 0.48 ng ferritin/μg total protein (FAC). Estimation of the breakpoint for ferritin in cells treated with FAC was problematic because of a gap in the data in the general region of the breakpoint. The reported value reflects the best statistical fit with the current data. Ferritin levels, which represent intracellular iron levels, and IL-8 induction are strongly correlated for both the CFA and FAC treatments. In addition, the curves for each treatment did not seem to differ. These similar results suggest that intracellular iron levels and the stimulation of IL-8 production are very strongly correlated, whether the iron is from a particle or a soluble source.

Utah CFA PM_1 was incubated for 2 weeks in 50 mM NaCl (pH 7.5) with or without 1 mM DF. The particles incubated with 50 mM NaCl and DF failed to stimulate the A549 cells to produce IL-8, whereas those incubated with 50 mM NaCl alone stimulated IL-8 production as much as untreated CFA (Figure 22). The two incubation solutions were saved and examined by ICP to determine what other reactive transition

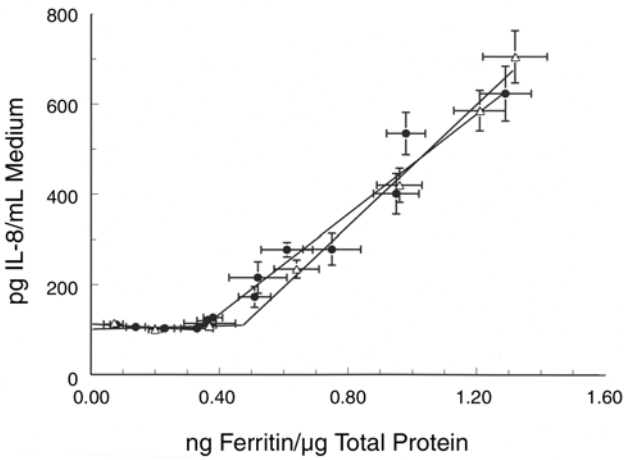

Figure 21. Relation between IL-8 in medium and ferritin levels in A549 cells treated with CFA (●) or FAC (△). Each symbol represents the mean (n = 3); each error bar represents 1 SD. The absence of error bars indicates that the SD is contained within the symbol. We used PROC NLIN in SAS 7.0 with the secant iterative method and a grid of initial parameter estimates to fit the lines. The equations for the best-fit line for IL-8 induction after FAC treatment before the breakpoint is [IL-8] = 107 + 11 × [ferritin] and for following the breakpoint is [IL-8] = −210 + 675 × [ferritin]. The equations for the best fit line for IL-8 induction after CFA treatment before the breakpoint is [IL-8] = 112 −30 × [ferritin] and for after the breakpoint is [IL-8] = −89 + 560 × [ferritin].

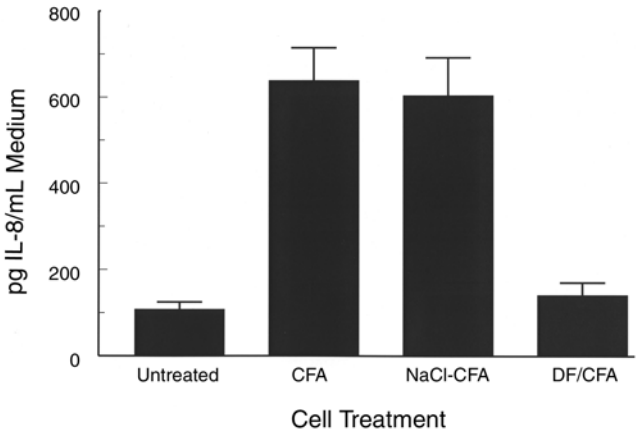

Figure 22. IL-8 production in A549 cells. Cells were plated in complete growth medium containing 1 mg/mL Utah CFA PM_1 (CFA), PM_1 preincubated with NaCl alone (NaCl/CFA), or PM_1 preincubated with NaCl and DF (DF/CFA). Media were harvested 24 hours later and the concentration of IL-8 was determined. Each bar represents the mean (n = 3); each error bar represents 1 SD.

metals might have been removed from the particles (Table 11). The transition metals copper and vanadium were the only others that were mobilized. DF appears to have enhanced the solubilization of copper and vanadium, but only such that about twice the amount of these metals were solubilized in the absence of DF. In contrast, DF enhanced iron solubilization 25 fold. Because copper and vanadium were removed from particles in the NaCl solution without DF and these particles induced levels of IL-8 in cells similar to those in untreated cells, copper and vanadium probably were not involved in induction of IL-8 by CFA. This conclusion further supports the involvement of iron from these particles in the induction of IL-8.

Speciation of Iron in CFA using Mössbauer Spectroscopy Previous work (Smith et al 1998) suggests that iron speciation could help explain the amount of iron mobilized from CFA. Utah CFA had low iron content but high iron mobilization, Illinois CFA had higher iron content but lower iron mobilization, and desert dust had low iron content and low iron mobilization (Table 8). Total iron content and the amount of iron mobilized after 24 hours did not correlate (Figure 23). Citrate mobilized very little or no iron from the pure iron oxides, hematite and magnetite, even though these compounds contain the greatest amounts of iron. These results imply that some iron compounds in CFA are more biochemically reactive than others.

Iron in CFA is usually found in magnetite-based spinels, hematite, or glassy aluminosilicates (Bancroft 1973; Hansen et al 1981; Huffman et al 1981). Mössbauer spectroscopy analysis of ash samples of coal from two different

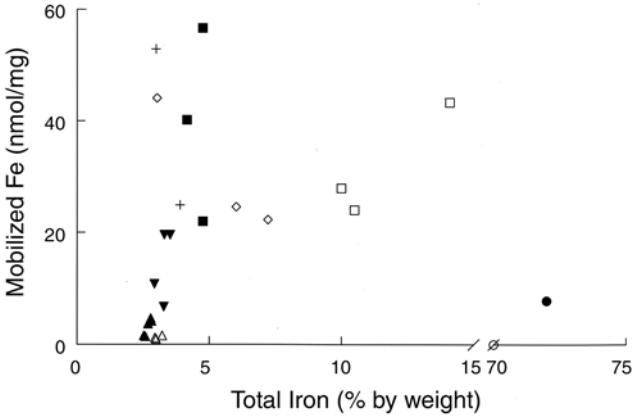

Figure 23. Amount of iron mobilized by citrate in vitro versus total iron in various particulates. Utah CFA (■), Illinois CFA (□), North Dakota CFA (◇), Mine Tailings (▼), Mancos Clay (▲), Desert Dust (▽), and SRMs (●).

sources shows that CFA larger than 10 µm nominal size contained 43% to 47% iron in an aluminosilicate glass phase (n = 2 samples), whereas CFA smaller than 2.5 µm contained 62% to 75% iron in the glass phase (n = 2). The balance of the iron in CFA was in the form of mixed oxides. Table 12 shows the iron content, iron mobilized by citrate, and iron speciation for several particle samples. Crustal dust samples analyzed for this study had similar elemental composition to CFA, but most of the iron was in clay minerals with no glass phase detected. The amount of iron mobilized from the crustal dust was substantially lower than that from the CFA particles.

Table 11. Solubility of Metals from Utah CFA PM_1[a]

	nmol metal/mg CFA (% removed)						
Solution	Aluminum	Copper	Iron	Manganese	Nickel	Silicon	Vanadium
50 mM NaCl	1616 (48.4)	0.9 (ND[b])	10.7 (0.9)	<0.4 (<23.5)	<2.6 (ND)	1164 (ND)	4.5 (57.5)
50 mM NaCl + 1 mM DF	1957 (58.7)	1.9 (ND)	272.2 (23.4)	<0.4 (<23.5)	<2.6 (ND)	1392 (ND)	7.3 (92.5)

[a] 1 mg/mL PM_1 was incubated in solution for 14 days at room temperature. The metals present in the supernatant were determined by ICP.

[b] ND = not determined.

Mössbauer spectra were determined for PM_1-rich Utah CFA before and after treatment with DF for 14 days (Figure 24). Each spectrum was least-squares fitted to a model based on four iron-bearing species (the spectra were interpreted by Dr Frank Huggins, University of Kentucky). Hematite and magnetite (iron oxide) had two six-peak magnetic components; the nonmagnetic iron in glass had two two-peak quadrupole components. The intensity of the iron oxides was essentially unchanged, but the intensity of the two peaks associated with iron in glass was reduced by treatment with DF. The iron in glass phase in Utah CFA PM_1 was 62% before treatment with DF and only 44% afterward. The amount of iron mobilized from the Utah CFA PM_1 samples by DF (272 nmol/mg particle) (Smith et al 2000) was consistent with the decrease in glass-phase iron (210 nmol/mg particle) and was within the experimental error (5%) of the total iron determined from the Mössbauer spectra (Veranth et al 2000c). This result strongly suggests that the iron removed by DF was from the glass phase.

According to previous reports, citrate mobilizes 22 to 57 nmol iron/mg CFA particles, depending on the size of the particles and the source of the coal (Smith et al 1998; Veranth et al 2000b). Citrate mobilized 1 to 4 nmol iron/mg particles of three size fractions of crustal dust derived from material collected at two geologically distinct sites in Utah (Veranth et al 2000a). Citrate mobilized 4 nmol iron/mg Utah CFA particles treated with DF, which is less iron than was mobilized from other Utah CFA samples. This finding indicates that the iron in glass, which was removed by the DF treatment, is the source of iron mobilized by citrate.

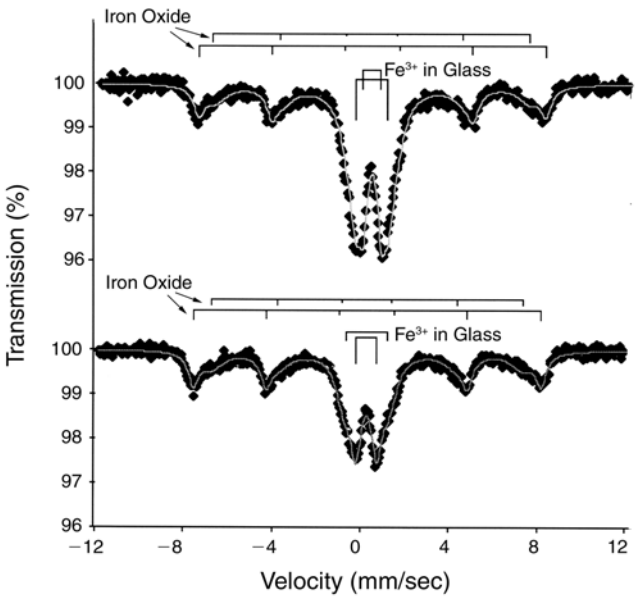

Figure 24. Mössbauer spectra of Utah CFA PM_1 before (top) and after (bottom) treatment with DF for 14 days. Bottom spectrum is offset by 5% for better visualization. The white line through each spectrum is the convergent model envelope that fits the data (each datum indicated by a black diamond) with the lowest χ^2 statistic, using the four components and 18 degrees of freedom. The line graphs above the spectra indicate the individual components used for fitting; the height of each bar reflects the relative intensity of the peak it represents.

Table 12. Comparison of Iron Speciation and Iron Mobilization for Selected PM Samples[a]

Sample	Total Iron[b] (% by weight)	Iron in Glass[c] (% by weight)	Iron in Clay[c] (% by weight)	Iron Mobilized[d] (nmol/mg particle)
Utah CFA $PM_{>10}$	4.8 ± 0.2	47	0	22 ± 0.7
Crustal dust $PM_{2.5–10}$	3.0 ± 0.1	0	91	1.2 ± 0.3
Utah CFA PM_1	6.5 ± 0.6	62	0	ND[e]
Utah CFA PM_1 (pretreated with DF)	ND[e]	44	0	4.2

[a] Values are mean ± 1 SD.

[b] Total iron was determined by INAA analysis.

[c] Iron in glass and clay was determined by Mössbauer spectroscopy; the remainder (not shown) was iron in various iron oxides.

[d] These data are taken from Smith and colleagues (1998) and reflect the amount of iron mobilized from the particles into 50 mM NaCl (pH 7.5) containing 1 mM citrate over 24 hours at 22°C.

[e] ND = not determined.

Relations Among Biochemical and Biological Endpoints and Physical Characteristics of CFA We compared the various biochemical and biological endpoints of CFA and its various physical characteristics to determine whether any of these variables are related. The comparisons were analyzed using Pearson correlation coefficients (Table 13). Because copper and zinc were the only two transition metals detected in the phosphate-buffer extractions of the CFA particles, these metals were used to conduct the MDA assays. The amounts of copper and zinc in the extractions did not correlate significantly with each other, with the MDA generated by ROS produced from the extracts, or with any of the other biochemical or cellular measurements taken (Table 13).

Table 13. Pearson Correlation Coefficients for CFA Endpoints and Characteristics[a]

					Particle Surface Area		Iron Mobilization by Citrate	Total Iron
	Copper	Zinc	Ferritin	IL-8	Nitrogen	SEM		
MDA								
Correlation coefficient	0.745	0.713	0.743	0.799	0.562	0.737	0.624	0.642
P value	0.034	0.177	0.0056	0.0018	0.072	0.0063	0.0726	0.024
Sample size	8	5	12	12	11	12	9	12
Copper								
Correlation coefficient		0.6015	0.175	0.346	−0.076	0.104	−0.163	0.415
P value		0.3985	0.679	0.401	0.857	0.806	0.7935	0.307
Sample size		4	8	8	8	8	5	8
Zinc								
Correlation coefficient			0.648	0.722	0.571	0.976	1.000	0.336
P value			0.237	0.169	0.429	0.0045		0.5805
Sample size			5	5	4	5	2	5
Ferritin								
Correlation coefficient				0.957	0.671	0.782	0.8618	0.3736
P value				<0.0001	0.0239	0.0027	0.0028	0.2315
Sample size				13	11	12	9	12
IL-8								
Correlation coefficient					0.6327	0.744	0.833	0.3959
P value					0.0367	0.0056	0.0053	0.2027
Sample size					11	12	9	12
Particle Surface Area$_{Nitrogen}$								
Correlation coefficient						0.888	0.845	0.383
P value						0.0003	0.0082	0.245
Sample size						11	8	11
Particle Surface Area$_{SEM}$								
Correlation coefficient							0.8145	0.4056
P value							0.0075	0.1904
Sample size							9	12
Iron Mobilization by Citrate								
Correlation coefficient								−0.0596
P value								0.8789
Sample size								9

[a] Shaded squares indicate a significant correlation (Pearson correlation coefficient >0.5; P <0.005).

MDA levels did, however, correlate with IL-8 induction in A549 cells (Table 13). This result seems consistent with what we know of the mechanisms for production of MDA and IL-8. The IL-8 induction was apparently the result of reactive radicals induced by iron, and MDA formation is apparently a measure of ROS production. A concern about drawing too many conclusions with this correlation is that although iron was responsible for IL-8 induction in A549 cells, it may or may not have been responsible for MDA formation.

The intracellular mobilization of iron from CFA indicated by induction of ferritin was significantly correlated with mobilization of iron from CFA by citrate in aqueous solution (Table 13). This correlation is consistent with what we have observed previously for other types of particles. Ferritin levels also correlated significantly with IL-8 production by A549 cells. This correlation seems reasonable because both factors were measured in treated A549 cells and because IL-8 induction appears to depend on increased iron levels in cells.

The correlation is less strong between ferritin levels and the surface area of the particles, determined by SEM analysis (Table 13). If no other factors were involved in the mobilization of iron, this correlation should have been significantly high. In fact, other factors, such as the speciation of the iron, may determine the amount of iron that is mobilized; this is consistent with the Mössbauer analysis of the species of iron that were present in different particles and those that were mobilized. The determination of particle surface area using nitrogen adsorption surface analysis correlated significantly only with the particle surface area determined by SEM. Because nitrogen adsorption surface analysis uses nitrogen (N_2) binding to indicate surface area, it measures the uneven surfaces and invaginations in which N_2, but perhaps not larger molecules, can fit. In fact, the surface areas measured using nitrogen adsorption surface analysis were larger than those measured using SEM. The discrepancy between the two estimates may indicate that the small areas are accessible only to N_2 and are thus not relevant to the chelators that remove iron, for example.

An important outcome of these comparisons is that the total iron content of the CFA particles did not correlate with any other parameter. This result emphasizes the importance of measuring the bioavailable iron in particles to determine whether iron is related to the possibly pathologic effects of the particles.

NONCOMBUSTION PARTICLES

Mobilization of Iron from Noncombustion Particles by Citrate

The rate at which iron is mobilized from size-fractioned, noncombustion particles, which occur in ambient PM, was compared to that from combustion particles. Iron was mobilized from all noncombustion particle samples from Mancos clay, desert dust, and mine tailings (Figure 25). The amount of iron mobilized generally decreased as the PM increased in diameter. The least iron was mobilized over 24 hours from desert dust samples (1.0–1.6 nmol iron/mg particle), followed by Mancos clay samples (1.6–4.7 nmol iron/mg particle); the most iron was mobilized from the mine tailing samples (6.7–19.6 nmol iron/mg particle). For all the samples, less iron was mobilized from $PM_{>10}$ than from smaller-size PM.

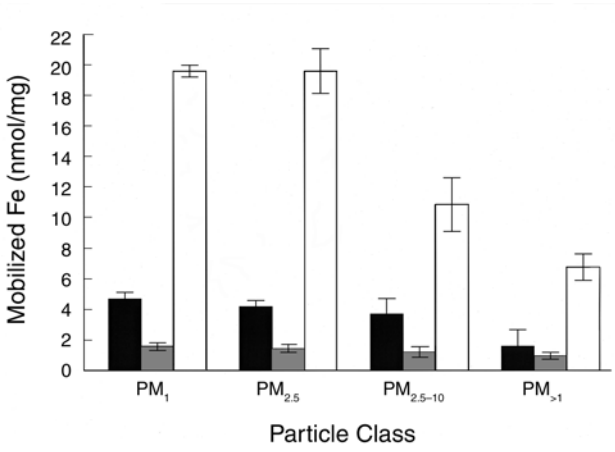

Figure 25. Iron mobilization by citrate from noncombustion particulates. Samples of Mancos clay (black bars), desert dust (gray bars), and mine tailings (white bars) were suspended in flowing air by rotating a jar mill. The suspended particles were passed through a settling chamber and then into an Andersen cascade impactor for size fractionation. The size-fractionated particles were suspended in 50 mM NaCl (pH 7.5) with 1 mM citrate for 24 hours. The particle-free supernatants were analyzed for iron. Each bar represents the mean (n = 3); each error bar represents 1 SD.

ENGINE EXHAUST PARTICLES

MDA Formation Catalyzed by Particles from Gasoline- and Diesel-Engine Exhaust

The formation of MDA catalyzed by phosphate-buffer extracts of filters containing particles from gasoline engines or diesel engines is summarized in Table 14. From 28 to 154 nmol MDA was formed per 1 mg particle of gasoline-engine exhaust compared with 15 nmol MDA per particle from the one diesel sample, a much less effective catalyst. The levels of MDA formation catalyzed by CFA PM_1 and $PM_{2.5}$ (26–148 nmol MDA/mg particle; Figure 13) are within the range of those catalyzed by gasoline-exhaust particles.

DF affected the ability of gasoline and diesel particle extracts to generate MDA formation (Table 14). In 5 of the 9 samples, DF inhibited MDA formation by over 90%, suggesting that transition metals (primarily iron) were involved in the reactions that yielded MDA. DF only partially inhibited (by 45% and 46%) the formation of MDA from two of the gasoline particle samples, perhaps because the transition metals involved in MDA formation (eg, copper) were only partially inhibited by DF. We cannot unequivocally identify the metal(s) responsible for the production of MDA, however, because we cannot measure the metal content of these samples.

From 50 to 200 µg PM was collected on filters from gasoline engines. Iron, cobalt, copper, vanadium, nickel, and zinc were not detected in phosphate-buffer extracts of these filters. The mass of particulate collected from the diesel engine (about 2–3 mg) was sufficient to measure the concentration of zinc (± SE): 4.1 ± 0.6 µM (or 610 ± 6 mg) zinc/kg diesel PM (n = 2). However, no other transition metal (iron, copper, cobalt, vanadium, and nickel) was detected above the background level of blank filters.

Mobilization of Iron from Diesel Exhaust Particles by Citrate

Diesel exhaust particles (1 mg/mL) incubated in 50 mM NaCl (pH 7.5) for 24 hours without citrate resulted in no detectable release of iron compared with those incubated with citrate, which resulted in the mobilization of 17.1 nmol iron/mg diesel exhaust particles.

Effect of Diesel Exhaust Particles on Ferritin Concentration in A549 Cells

To determine whether iron was mobilized from diesel exhaust particles used to treat A549 cells, we compared ferritin levels between treated and untreated controls after 24 hours of treatment. A549 cells treated with 20 µg diesel exhaust particles/cm^2 produced 0.33 ng ferritin/µg total protein compared with 0.11 ng ferritin/µg total protein in untreated control cells. This result suggests that iron was released from the diesel exhaust particles in the cells.

Table 14. Formation of MDA from Particles Collected from Gasoline and Diesel Engines[a]

Engine	Fuel	Mean MDA (nmol/mg particle ± SE)	Mean MDA (nmol/mg particle ± SE) with DF	Inhibition of MDA Formation by DF (%)
Gasoline				
1	Reformulated gasoline 305	117 ± 12 (4)[b]	22.4 ± 2.0 (4)[b]	81
8	Reformulated gasoline 305	154 ± 22 (4)	19.2 ± 4.6 (4)	97
2	Indolene clear	44.1 ± 2.7 (4)	24.2 ± 0.9 (4)	45
5	Indolene clear	54.0 ± 4.4 (2)	2.1 ± 0.1 (2)	96
6	Indolene clear	45.5 ± 3.3 (4)	3.5 ± 0.3 (4)	92
7	Reformulated gasoline 309	78.1 ± 3.5 (4)	5.8 ± 0.1 (4)	93
3	Reformulated gasoline 309	69.3 ± 4.4 (6)	24.1 ± 1.6 (6)	65
4	Reformulated gasoline 309	28.3 ± 4.7 (4)	15.4 ± 0.6 (4)	46
Diesel				
	Low-sulfur fuel	14.6 ± 1.5 (4)	0.38 ± 0.01 (4)	97

[a] Particles were extracted from engine filters using 0.1 M phosphate buffer (pH 7.2).

[b] Sample size is indicated in parantheses.

SRM PARTICLES

MDA Formation Catalyzed by SRM Particles

We used SRM samples in this study in part because they contain enough particulate for metals analysis of the buffer solutions in which the samples are incubated. Such analysis provides a better idea of what metals may be involved in MDA formation. The metals analyses showed that several metals were mobilized from SRM samples after 24 hours in phosphate buffer (Table 15).

The MDA assays were conducted somewhat differently for SRM samples than for the CFA, gasoline, and diesel particulates discussed earlier. The SRM particles were incubated with the deoxyribose and then removed, and the amount of MDA in the supernatant was determined in two independently conducted experiments (Table 16). SRM 1649 catalyzed about 2 times the MDA catalyzed by SRM 1648. This result is consistent with the relative levels of $HO^{\bullet}$ produced by these SRM samples in the presence of chelators (citrate and ascorbate) in a different assay (Smith and Aust 1997). Both of the diesel particulate samples (SRM 1650 and 2975) catalyzed the production of less MDA than the urban samples; in particular, a sample of SRM 2975 10 times the volume of the other samples was

Table 15. Metals Removed from SRM Samples[a]

Metal (nmol/mg particle ± SD)	Particulate			
	SRM 1648[b]	SRM 1649[c]	SRM 1650[d]	SRM 2975[e]
Cobalt	0.007 ± 0.008	0.005 ± 0.006	ND[f]	0.0017 ± 0.0017
Copper	1.110 ± 0.170	0.47 ± 0.016	0.048 ± 0.034	0.014 ± 0.009
Iron	0.07 ± 0.016	0.08 ± 0.11	0.360 ± 0.460	—[g]
Nickel	0.190 ± 0.020	0.390 ± 0.002	0.110 ± 0.030	0.008 ± 0.012
Vandium	0.250 ± 0.060	1.510 ± 0.120	0.010 ± 0.014	—[g]
Zinc	0.540 ± 0.120	0.250 ± 0.060	2.620 ± 0.380	0.250 ± 0.060

[a] Amount solubilized in 24 hours in phosphate buffer (pH 7.2). Values are mean ± SD.

[b] Urban dust from St Louis MO.

[c] Urban dust from Washington DC.

[d] Diesel PM.

[e] Diesel PM from a forklift engine.

[f] ND = not determined.

[g] Not detected because amount was less than lower limit of detection.

Table 16. Effect of DF on MDA Formation Catalyzed by SRM Particulates[a]

Particulate	Sample Volume	MDA (nmol/mg particle)		Inhibition by DF (%)
		Without DF	With DF	
SRM 1648[c]	160 µg/mL	59, 57[b]	5.6, 4.4[b]	91, 92[b]
SRM 1649[d]	160 µg/mL	100, 94	11, 8.8	89, 91
SRM 1650[e]	160 µg/mL	26, 25	0.81, 0.00	97, 100
SRM 2975[f]	1600 µg/mL	5.5, 5.4	0.48, 0.46	91, 91

[a] Samples were incubated with or without 1 mM DF for 1 hour before deoxyribose was added for the final 24-hour incubation at 37°C. The supernatants were analyzed for MDA.

[b] Results from two independent experiments are reported.

[c] Urban dust from St Louis MO.

[d] Urban dust from Washington DC.

[e] PM from diesel-engine exhaust.

[f] Diesel exhaust particles from a forklift engine.

required to produce detectable amounts of MDA. DF inhibited production of MDA in the presence of each of the four samples by 89% or more (Table 16). This finding strongly suggests that transition metals are involved in the formation of ROS, which in turn leads to MDA formation. Because several metals were mobilized, it is not clear which metal or metals may be involved. However, the degree of inhibition by DF is consistent with that expected if iron were involved, even though iron was not detected in all SRM samples.

Solubility of Metals Under Various Conditions

The solubility of iron depends on the solutions used to incubate the source particles. For example, in this study, SRM particles were incubated in phosphate buffer at pH 7.0 or in citrate solution at pH 7.5. Incubation in citrate solution for 24 hours mobilized on average 52.9 and 24.9 nmol iron/mg particle from SRM 1649 and SRM 1648 (Table 8), respectively. These amounts of iron are equivalent to 660 and 356 times the mean amount recovered from the same samples in phosphate-buffer incubations in the MDA assay (Table 15). This finding is consistent with previous reports of iron mobilized from asbestos, where phosphate actually inhibited iron mobilization (Lund and Aust 1990). Thus, it is important to consider not only the pH, but also the chelators and buffers that are used in these types of studies.

MOBILIZATION OF IRON FROM URBAN PARTICLES

To compare the amount of iron that can be mobilized from urban particles, we concentrated and collected particles from ambient air in Salt Lake City during four 7-day periods that spanned 3 weeks in 1999. The four $PM_{2.5}$ samples and one PM_{10} sample were incubated with citrate and NaCl (pH 7.5) and analyzed for rates of iron mobilization (Figure 26). In slight contrast to the other iron mobilization experiments in this study, the entire filter on which the particles were collected was incubated for the entire 24-hour period, because too little particulate was collected to remove enough material otherwise. Considerable amounts of iron were mobilized from the $PM_{2.5}$ samples, and the amount varied by collection date. The greatest amount of iron mobilized from these Salt Lake City samples were in the range of the greatest amount of iron mobilized from particles using this mobilization assay (56 nmol iron/mg Utah CFA particle). The Salt Lake City PM_{10} sample yielded less iron than the $PM_{2.5}$ samples.

These assays show that it is feasible to collect urban particles in amounts sufficient to conduct careful studies of iron mobilization with the ultimate goal of determining the iron species responsible for the mobilization.

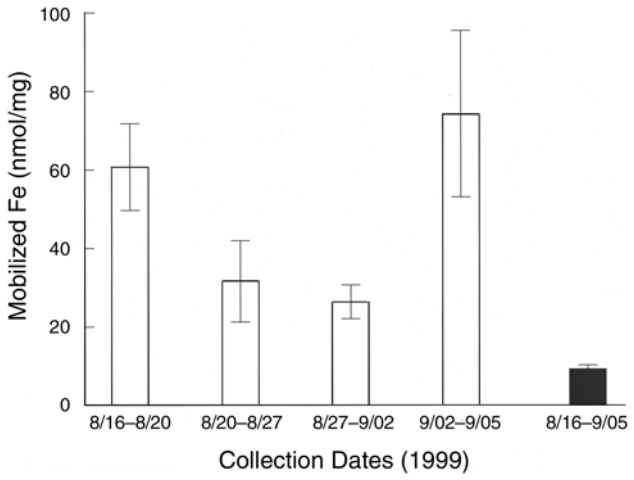

Figure 26. Iron mobilized by citrate from ambient air particles collected in Salt Lake City, Utah. Ambient air particles were concentrated and size-fractionated. $PM_{2.5}$ (white bar) and PM_{10} (black bar) were suspended in 50 mM NaCl (pH 7.5) with 1 mM citrate for 24 hours, and the particle-free supernatants were analyzed for iron.

DISCUSSION AND CONCLUSIONS

Our results show that one or more components from urban particulates, gasoline combustion particulates, diesel combustion particulates, and CFA can generate ROS and that the responsible component(s) is probably one or more transition metals. In most of the cases in which we could clearly distinguish the participation of different metals, iron, the predominant transition metal, appeared to be responsible. Treatment of A549 cells with SRMs (Smith and Aust 1997) or CFA (Smith et al 1998) led to the induction of ferritin, the iron-storage protein, which indicates that bioavailable iron was released. The generation of ROS by CFA led to induction of the inflammatory mediator, IL-8, in A549 cells (Smith et al 2000). Iron, or other transition metals, is also thought to be involved in health effects of particles other than those used in this study. Considerable work has addressed how relatively high doses of ROFA particles exacerbate health effects in rats, and a number of transition metals appear to be involved in these processes. Two naturally occurring crystalline mineral fibers, asbestos (Hardy and Aust 1995) and erionite (Eborn and Aust 1995), have also been studied extensively to determine the role that iron may play in acute and chronic health effects. Asbestos contains 27% iron by weight and can also acquire iron from solution; erionite contains little iron naturally but can readily acquire it from solution. The iron carried by asbestos fibers into cultured lung cells is associated with ROS generation,

DNA damage, and induction of cellular mediators. Therefore, a pattern emerging for a variety of particle types suggests that iron released into cells at sufficiently high concentrations can cause intracellular iron overload, which in turn causes a variety of biological effects.

The amount of bioavailable iron released from CFA depends on the source of the parent coal and is inversely related to the particle size (Smith et al 1998, 2000). This relation may be important if the epidemiologic observations that smaller particles are associated with health effects in humans are shown to be true. We showed that particles had to be endocytosed by cultured A549 cells before bioavailable iron was released. This is likely because the concentration of chelators is much higher inside the cell than outside. Although the nature of intracellular chelators is unknown, it would not be surprising if they were organic acids, such as citrate, because they are at millimolar concentrations in the cell. The amount of the iron-storage protein ferritin was a reliable, indirect indicator of the amount of iron released in the cells and correlated strongly with the amount of iron mobilized by citrate in cell-free suspension. Thus, measuring ferritin induction or iron mobilization by citrate or both for particles of unknown origin may help determine whether the particles can release iron and generate ROS in the lung.

The rate of iron mobilization from CFA in vitro is consistent with solid-phase, diffusion-limited mass transfer, and the differences in total amount of iron mobilized are consistent with size-dependent differences in chemical speciation (Veranth et al 2000b). Size-dependent differences in CFA composition are expected because fine CFA particles are formed by a different process than large particles. Submicron fumes, formed by mineral vaporization, nucleation, and condensation, result in a layered structure rich in certain elements (Neville and Sarofim 1982; Linak and Wendt 1994). Because CFA derives from minerals codeposited with organic material, it comprises predominantly aluminum, silicon, calcium, magnesium, and iron. The ash, which contains iron in aluminosilicate glass, is produced by high-temperature combustion followed by rapid cooling from high temperatures, whereas crustal dusts are produced by weathering and attrition. Although both particle types have a similar total iron composition, iron is mobilized from them at different rates (Smith et al 1998). Thus, the speciation of the iron is likely the most important determining factor for whether iron is bioavailable.

The results presented here show that iron associated with aluminosilicate glass in CFA is much more readily mobilized by citrate or ferrozine, in vitro or by cultured human lung epithelial cells, than iron associated with other fractions, predominantly iron oxides (Veranth et al 2000c). In addition, a noncombustion source particulate, crustal dust, did not contain iron associated with aluminosilicate glass and showed much lower rates of iron mobilization than did the CFA particulates. Zeng (1998) observed that the amount of iron associated with glassy aluminosilicates in CFA increased with decreasing particle size. Our studies implicated this iron as the species that causes IL-8 induction and demonstrated that smaller CFA particles were more active than larger ones. The biochemical and biological data are consistent with the epidemiologic observations of an association between fine particles and adverse health effects.

The ability to produce large amounts of well-characterized, size-fractionated CFA allowed us to compare various chemical and physical characteristics with specific biological effects in cultured human lung epithelial cells. An important goal of these studies was to elucidate what characteristics were related to the bioavailability of iron. Particle surface area and iron bioavailability appeared to be weakly correlated. Surface area estimated by nitrogen adsorption surface analysis was 2 to 4 times larger than that estimated using SEM. This discrepancy suggests that the particles may have contained micropores that were not detected at the magnification used in SEM imaging.

The results presented here show that neutral phosphate-buffer extracts of 4 sources of particles (urban air, coal, gasoline engines, and diesel engines) contained transition metals sufficient to generate ROS, as indicated by the formation of MDA from 2-deoxyribose. The inhibitory effect of DF provided strong support for the role of transition metals, especially iron, in the generation of these reactive species, even though the metal content of many of these extracts was too low to be detected by ICP-MS. DF inhibited the generation of ROS by iron (100%) much more strongly than by copper (54%). However, DF's inhibitory effect on mixtures of transition metals has not been investigated. In most cases for particles from all four sources, DF inhibited MDA formation by more than 90%. Although iron was not detected in any of the neutral phosphate-buffer extracts, a concentration of 1 μM (which is below the detection limit of 1.8 μM) would have yielded a significant amount of MDA over 24 hours, as evidenced by the data presented for solutions of the pure metal salts (Table 3). Extracts of SRM samples had detectable levels of cobalt, copper, iron, nickel, vanadium, and zinc; only copper and zinc were detected in extracts of CFA; and only zinc was detected in extracts from diesel engine exhaust particles. No transition metals were detected in extracts from particles generated by gasoline-fueled engines. Thus, although we cannot identify which transition metal or metals were responsible for the observed activity, transition metals

were clearly responsible for the generation of ROS and in turn the formation of MDA from 2-deoxyribose.

Combustion particles from gasoline and diesel engines are essentially all PM_1. Thus, combustion engine particles can be compared with CFA PM_1. Because extracts of CFA and gasoline-engine exhaust particles catalyzed formation of similar ranges of MDA (28–154 nmol MDA/mg particle), these 2 classes of particles may generate ROS to a similar degree. In contrast, the diesel-engine exhaust sample, generated from a single engine for these experiments, catalyzed formation of considerably less MDA (about 15 nmol MDA/mg particle). This difference may be due to the higher concentration of oil or unburned fuel that is typical of diesel-engine exhaust particles and that would dilute the amount of metal per total particle mass. Additional samples from diesel-engine exhaust need to be examined before firm conclusions can be made.

If whole-animal and human studies continue to support a role for transition metals in health effects of particles, then the ability to estimate the levels of metals that are bioavailable using in vitro techniques will be important. The results reported here show clear evidence that the conditions used in solubility studies greatly influence their outcome. This is particularly true for iron, which is not soluble to any measurable extent at neutral pH in the absence of a chelator. At least for iron, for which we could assess the amount mobilized in cells using ferritin induction, conditions of 50 mM NaCl (pH 7.5) plus 1 mM citrate most closely approximated the conditions under which intracellular mobilization occurs. Iron was not mobilized under these conditions in the absence of citrate. Because chelators are not present at millimolar levels in extracellular lung fluid, it is unlikely that iron will be mobilized appreciably in the lining fluid. More likely, the iron will be mobilized intracellularly after the particles are phagocytized or endocytized. Thus, the methods used here to mobilize iron by citrate may help estimate the bioavailability of iron in uncharacterized particles.

In conclusion, our findings indicate that iron, and in some cases other transition metals, from combustion and ambient particles are bioavailable and capable of generating ROS. The amount of bioavailable iron in those CFA samples from which enough particles were isolated depended on the source of coal and the size of the particles. That the smallest particles were the most active supports some epidemiologic work suggesting that adverse health effects are related to the mass of fine particles present in the air. Mobilization of iron from CFA, especially the smallest CFA particles, and generation of ROS led to the induction of the inflammatory mediator IL-8 in cultured human lung epithelial cells. An important outcome of our study is that the species of iron present in the particles determined whether the iron was bioavailable. Iron associated with glassy aluminosilicate in CFA seemed to be the most bioavailable. Because of the possible implications of these studies, future work should include particles from a wider range of combustion and geologic sources to better understand and identify individual species that may contribute significantly to health effects in humans. This study also emphasizes the need for large amounts of well-characterized particles in chemical, biochemical, and biological experiments.

ACKNOWLEDGMENTS

We thank Dick Chase, Gary Duszkiewicz, and Dezi Lewis of the Vehicle Emission Research Laboratory of Ford Motor Co for producing and collecting gasoline combustion particulates. For the diesel combustion particles, we thank Bob Waytulonis of the Department of Mechanical Engineering at the University of Minnesota. We thank several people from the University of Utah: Denise Chirban for assistance with the SEM imaging of CFA particles, Dana Overacker and Sara L Dansie for furnace operation, and James B Griffin for constructing the particle sampling train for CFA particle collection. From the Department of Chemistry and Biochemistry, Utah State University, we owe Matthew L Huggins and Ruihua Fang for iron mobilization studies with noncombustion particles and James Rohrbough for iron mobilization studies with the urban air particles collected in Salt Lake City, Utah. We thank Susan Durham, system analyst from the Fisheries and Wildlife Department of Utah State University, for her assistance with statistical analysis. We also thank Ryan Ball, Department of Chemistry and Biochemistry of Utah State University, for his editorial assistance in preparing the manuscript.

REFERENCES

Amdur MO, Bayles J, Ugro V, Underhill DW. 1978. Comparative irritant potency of sulfate salts. Environ Res 16:1–8.

Amdur MO, Sarofim AF, Neville M, Quann RJ, McCarathy JF, Elliott JF, Lam HF, Rogers AE, Conner MW. 1986. Coal combustion aerosols and SO_2: An interdisciplinary analysis. Environ Sci Technol 20:138–145.

Aranyi C, Miller FJ, Andres S, Ehrlich P, Fenters J, Gardner DE, Waters MD. 1979. Cytotoxicity to alveolar macrophages of trace metals absorbed on fly ash. Environ Res 20:14–23.

Aust AE, Lund LG. 1991. Iron mobilization from crocidolite results in enhanced iron-catalyzed oxygen consumption and hydroxyl radical generation in the presence of cysteine. In: Mechanisms in Fibre Carcinogenesis (Brown RC, Hoskins JA, Johnson NF, ed). Plenum Press, New York NY, pp 397–406.

Aust SD, Morehouse LA, Thomas CE. 1985. Role of metals in oxygen radical reactions. J Free Radic Biol Med 1:3–25.

Bancroft GM. 1973. Mössbauer Spectroscopy: An Introduction for Inorganic Chemists and Geochemists. John Wiley & Sons, New York NY.

Becker S, Soukup JM, Gilmour MI, Devlin RB. 1996. Stimulation of human and rat alveolar macrophages by urban air particulates: Effects on oxidant radical generation and cytokine production. Toxicol Appl Pharmacol 141:637–648.

Benson JM, Chang L-Y, Cheng YS, Hahn FF, Kennedy CH, Barr EB, Maples KR, Snipes MB. 1995. Particle clearance and histopathology in lungs of F344/N rats and B6C3F1 mice inhaling nickel oxide or nickel sulfate. Fundam Appl Toxicol 28:232–244.

Bonnell J, Schilling C, Massey P. 1980. Clinical and experimental studies of the effects of pulverized fuel ash: A review. Ann Occup Hyg 23:159–164.

Buettner GR. 1990. Use of ascorbate as test for catalytic metals in simple buffers. Methods Enzymol 186:125–127.

Carter JD, Ghio AJ, Samet JM, Devlin RB. 1997. Cytokine production by human airway epithelial cells after exposure to an air pollution particle is metal-dependent. Toxicol Appl Pharmcol 146:180–188.

Chao CC, Lund LG, Zinn KR, Aust AE. 1994. Iron mobilization from crocidolite asbestos by human lung carcinoma cells. Arch Biochem Biophys 314:384–391.

Chao CC, Park SH, Aust AE. 1996. Participation of nitric oxide and iron in the oxidation of DNA in asbestos-treated human lung epithelial cells. Arch Biochem Biophys 326:152–157.

Chen C, Chock DP, Winkler SL. 1999. A simulation study of confounding in generalized linear models for air pollution epidemiology. Environ Health Perspect 107:217–222.

Chen LC, Miller PD, Amdur MO, Gordon T. 1992. Airway hyperresponsiveness in guinea pigs exposed to acid-coated ultrafine particles. J Toxicol Environ Health 35:165–174.

Costa DL, Dreher KL. 1997. Bioavailable transition metals in particulate matter mediate cardiopulmonary injury in healthy and compromised animal models. Environ Health Perspect 105:1053–1060.

Devlin RB, McKinnon KP, Noah T, Becker S, Koren HS. 1994. Ozone-induced release of cytokines and fibronectin by alveolar macrophages and airway epithelial cells. Am J Physiol 266:L612–L619.

Dockery DW, Pope CA III, Xu X, Spengler JD, Ware JH, Fay ME, Ferris BG Jr, Speizer FE. 1993. An association between air pollution and mortality in six US cities. N Engl J Med 329:1753–1759.

Dockery DW, Speizer FE, Stram DO, Ware JH, Spengler JD, Ferris BG Jr. 1989. Effects of inhalable particles on respiratory health of children. Am Rev Respir Dis 139:587–594.

Dockery DW, Ware JH, Ferris BG, Speizer FE, Cook NR, Herman SM. 1982. Changes in pulmonary function associated with air pollution episodes. J Air Pollut Control Assoc 32:937–942.

Doll R. 1990. Report of the international committee on nickel carcinogenesis in man. Scand J Work Environ Health 16:1–82.

Donaldson K, Brown DM, Mitchell C, Dineva M, Beswick PH, Gilmour P, MacNee W. 1997. Free radical activity of PM_{10}: Iron-mediated generation of hydroxyl radicals. Environ Health Perspect 105:1285–1289.

Downey GP, Bumbay RS, Doherty DE, LaBrecque JF, Henson JE, Henson PM, Worthen GS. 1988. Enhancement of pulmonary inflammation by PGE2: Evidence for a vasodilator effect. J Appl Physiol 64:728–741.

Dreher KL, Jaskot RH, Lehmann JR, Richards JH, McGee JK. 1997. Soluble transition metals mediate residual oil fly ash induced acute lung injury. J Toxicol Environ Health 50:285–305.

Dusseldorp A, Kruize H, Brunekreef B, Hofschreuder P, de Meer G, van Oudvorst AB. 1995. Associations of PM_{10} and airborne iron with respiratory health of adults living near a steel factory. Am Rev Respir Crit Care Med 152:1932–1939.

Dye JA, Adler KB, Richards JH, Dreher KL. 1997. Epithelial injury induced by exposure to residual oil fly-ash particles: Role of reactive oxygen species? Am J Respir Cell Mol Biol 17:625–633.

Eborn SK, Aust AE. 1995. Effect of iron acquisition on induction of DNA single-strand breaks by erionite, a carci-

nogenic mineral fiber. Arch Biochem Biophys 316:507–514.

Electric Power Research Institute. 1979. Evaluation of the George Neal No 3 Electrostatic Precipitator. Electric Power Research Institute, Palo Alto CA.

Environmental Protection Agency (US). 1994. National Air Quality and Emissions Trends Report, 1993. EPA Report EPA-454/R-94-026, NTIS Document PB95-159893. National Technical Information Service, Springfield VA.

Fang R. 1999. Induction of Ferritin Synthesis in Human Lung Epithelial Cells (A549) Treated with Iron-containing Particulates and Iron Mobilization from These Particulates [dissertation]. Utah State University, Logan UT.

Fang R, Aust AE. 1997. Induction of ferritin synthesis in human lung epithelial cells treated with crocidolite asbestos. Arch Biochem Biophys 340:369–375.

Frampton MW, Ghio AJ, Samet JM, Carson JL, Carter JD, Devlin RB. 1999. Effects of aqueous extracts of PM(10) filters from the Utah valley on human airway epithelial cells. Am J Physiol 277:L960–L967.

Fubini B, Giamello E, Mollo L, Zanetti G, Eborn SK, Aust AE. 1999. Zeolites as model solids for investigations on the role of iron at the solid-liquid interface in particulate toxicity. Res Chem Intermediates 25:95–109.

Garrett NE, Campbell JA, Stack HF. 1981. The utilization of the rabbit alveolar macrophage and Chinese hamster ovary cell for evaluation of the toxicity of particulate materials. Environ Res 24:345–365.

Gavett S, Madison SL, Dreher KL, Winsett DW, McGee JK, Costa DL. 1997. Metal and sulfate composition of residual oil fly ash determines airway hyperreactivity and lung injury in rats. Environ Res 72:162–172.

Ghio AJ, Carter JD, Richards JH, Brighton LE, Lay JC, Devlin RB. 1998. Disruption of normal iron homeostasis after bronchial instillation of an iron-containing particle. Am J Physiol 18:L396–L403.

Ghio AJ, Stonehuerner J, Dailey LA, Carter JD. 1999a. Metals associated with both the water-soluble and insoluble fractions of an ambient air pollution particle catalyze an oxidative stress. Inhalation Toxicol 11:37–49.

Ghio AJ, Stoneheurner J, McGee JK, Kinsey JS. 1999b. Sulfate content correlates with iron concentrations in ambient air pollution particles. Inhalation Toxicol 11:293–307.

Ghio AJ, Stonehuerner J, Pritchard RJ, Piantadosi CA, Quigley DR, Dreher KL, Costa DL. 1996. Humic-like substances in air pollution particulates correlate with concentrations of transition metals and oxidant generation. Inhalation Toxicol 8:479–494.

Gladney ES, Perrin DR, Robinson RD, Trujillo PE. 1984. Multitechnique determination of elemental concentrations in NBS urban air particulate SRM 1648 and evaluation of its use for quality assurance. J Radioanal Nucl Chem Articles 83:379–386.

Gordon J. 1991. Use of vanadate as protein-phosphotyrosine phosphatase inhibitor. Methods Enzymol 201:477–482.

Gormley IP, Collings P, Davis JMG, Ottery J. 1979. An investigation into the cytotoxicity of respirable dusts from British colleries. Br J Exp Pathol 60:526–536.

Gulumian M, van Wyk JA. 1987. Hydroxyl radical production in the presence of fibres by a Fenton-type reaction. Chem Biol Interact 62:89–97.

Hadnagy W, Seemayer N. 1994. Inhibition of phagocytosis of human macrophages induced by airborne particulates. Toxicol Lett 72:23–31.

Halliwell B, Gutteridge JMC. 1999. Free Radicals in Biology and Medicine. Oxford University Press, New York NY.

Hansen LD, Silberman D, Fisher GL. 1981. Crystalline components of stack-collected, size-fractionated coal fly ash. Environ Sci Technol 15:1057–1062.

Hardy JA, Aust AE. 1995. Iron in asbestos chemistry and carcinogenicity. Chem Rev 95:97–118.

Hart RW, Kendig O, Blakeslee J, Mizuhira V. 1980. Effect of cellular ingestion on the elemental ratio of asbestos. In: The In Vitro Effects of Mineral Dusts (Brown RC, Chamberlain M, Davies R, Gormley IP, eds). Academic Press, Orlando FL, pp 191–199.

Hatch GE, Boykin E, Graham JA, Lewtas J, Pott F, Loud K, Mumford JL. 1985. Inhalable particles and pulmonary host defense: In vivo and in vitro effects of ambient air and combustion particles. Environ Res 36:67–80.

Health Effects Institute. 1995. Particulate Air Pollution and Daily Mortality: Replication and Validation of Selected Studies (The Phase I Report of the Particle Epidemiology Evaluation Project). Health Effects Institute, Cambridge MA.

Health Effects Institute. 1997. Particulate Air Pollution and Daily Mortality: Analysis of the Effects of Weather and Multiple Air Pollutants (The Phase I.B Report of the Par-

ticle Epidemiology Evaluation Project). Health Effects Institute, Cambridge MA.

Holian A, Hamilton RF Jr, Morandi MT, Brown SD, Li L. 1998. Urban particle-induced apoptosis and phenotype shifts in human alveolar macrophages. Environ Health Perspect 106:127–132.

Holmes A, Morgan A. 1967. Leaching and constituents of chrysotile and asbestos in vivo. Nature 215:441–442.

Hornbeck P. 1994. Antibody-sandwich ELISA to detect soluble antigens. In:Current Protocols in Immunology (Coico R, Coligan JE, Kruisbeek AM, Margulies DH, Shevach EM, Strober W, eds) pp 2.1.9–2.1.11. John Wiley & Sons, New York NY.

Houck JE, Goulet JM, Chow JC, Watson JG, Pritchett LC. 1990. Chemical characterization of emission sources contributing to light extinction. Air & Waste Management Association, Pittsburgh PA.

Hu AA. 2000. Collection and Characterization of Coal Fly Ash for Toxicology [thesis]. University of Utah, Salt Lake City UT.

Huffman GP, Huggins FE. 1978. Mossbauer studies of coal and coke: Quantitative phase identification and direct determination of pyritic and iron sulphide sulphur content. Fuel 57:592.

Huffman GP, Huggins FE, Dunmyre GR. 1981. Investigation of the high-temperature behaviour of coal ash in reducing and oxidizing atmoshperes. Fuel 60:585–597.

Imbert V, Peyron JF, Farahi Far D, Mari B, Auberger P, Rossi B. 1994. Induction of tyrosine phosphorylation and T-cell activation by vanadate peroxide, an inhibitor of protein tyrosine phosphatases. Biochem J 297:163–173.

Kamp DW, Graceffa P, Pryor WA, Weitzman SA. 1992. The role of free radicals in asbestos-induced disease. Free Radic Biol Med 12:293–315.

Kennedy T, Ghio AJ, Reed W, Samet J, Zagorski J, Quay J, Carter J, Dailey L, Hoidal JR, Devlin RB. 1998. Copper-dependent inflammation and nuclear factor-KB activation by particulate air pollution. Am J Respir Cell Mol Biol 19:366–378.

Kiell A, Hadnagy W, Seemayer NH, Behrendt H, Tomingas R. 1993. Inhalation studies with airborne particulates in rodents: Cytotoxic and genotoxic effects on alveolar macrophages and bone marrow cells. In: Advances in Controlled Clinical Inhalation Studies (Mohr U, ed). Springer-Verlag, New York NY.

Knecht EA, Moorman WJ, Clark JC, Lynch DW, Lewis TR. 1985. Pulmonary effects of acute vanadium pentoxide inhalation in monkeys. Am Rev Respir Dis 132:1181–1185.

Kodavanti UP, Jaskot RH, Costa DL, Dreher KL. 1997. Pulmonary proinflammatory gene induction following acute exposure to residual oil fly ash: Roles of particle associated metals. Inhalation Toxicol 9:679–701.

Lay JC, Bennett WD, Ghio AJ, Bromberg PA, Costa DL, Kim CS, Koren HS, Devlin RB. 1999. Cellular and biochemical response of the human lung after intrapulmonary instillation of ferric oxide particles. Am J Respir Cell Mol Biol 20:631–642.

Linak WP. 1985. The Effect of Coal Type, Residence Time, and Combustion Configuration on the Submicron Aerosol Composition and Size Distribution from Pulverized Coal Combustion (dissertation). The University of Arizona, Tucson AZ.

Linak WP, Wendt JOL. 1994. Trace metal transformation mechanisms during coal combustion. Fuel Processing Technology 39:173–198.

Linn WS, Avol EL, Anderson KR, Shamoo DA, Peng RC, Hackney JD. 1989. Effect of droplet size on respiratory responses to inhaled sulfuric acid in normal and asthmatic volunteers. Am Rev Respir Dis 140:161–166.

Liu WK, Wong MH, Tam FY. 1986. Comparison of hemolytic activities of coal fly ash and its soluble and insoluble fractions. Environ Res 40:459–469.

Lund LG, Aust AE. 1990. Iron mobilization from asbestos by chelators and ascorbic acid. Arch Biochem Biophys 278:60–64.

Lund LG, Aust AE. 1991. Mobilization of iron from crocidolite asbestos by certain chelators results in enhanced crocidolite-dependent oxygen consumption. Arch Biochem Biophys 287:91–96.

Lund LG, Aust AE. 1992. Iron mobilization from crocidolite asbestos greatly enhances crocidolite-dependent formation of DNA single-strand-breaks in phi X174 RFI DNA. Carcinogenesis 13:637–642.

May WE, Benner BA Jr, Wise SA, Schuetzle D, Lewtas J. 1992. Standard reference materials for chemical and biological studies of complex environmental samples. Mutat Res 276:11–22.

McCain J, Gooch J, Smith W. 1975. Results of field measurements of industrial particulate sources and electro-

static precipitator performance. J Air Pollut Control Assoc 25:117–121.

McElroy MW, Carr RC, Ensor DS, Markowski GR. 1982. Size distribution of fine particles from coal combustion. Science 215:13–19.

Minotti G, Aust SD. 1987. The requirement for iron (III) in the initiation of lipid peroxidation by iron (II) and hydrogen peroxide. J Biol Chem 262:1098–1104.

Moolgavkar SH, Luebeck GE. 1996. A critical review of the evidence on particulate air pollution and mortality. Epidemiology 7:420–428.

Moolgavkar SH, Luebeck EG, Hall TA, Anderson EL. 1995. Air pollution and daily mortality in Philadelphia. Epidemiology 6:476–484.

Mumford JL, Lewtas J. 1982. Mutagenicity and cytotoxicity of coal fly ash from fluidized-bed and conventional combustion. J Toxicol Environ Health 10:565–586.

Neville M, Quann RJ, Haynes BS, Sarofim AF. 1981. Vaporization and condensation of mineral matter during pulverized coal combustion. In: Eighteenth Symposium (International) on Combustion, pp 1267–1274. The Combustion Institute, Pittsburgh PA.

Neville M, Sarofim AF. 1982. The stratified composition of inorganic submicron particles produced during coal combustion. In: Nineteenth Symposium (International) on Combustion, pp 1441–1449. The Combustion Institute, Pittsburgh PA.

Perl ER. 1976. Sensitization of Nociceptors and Its Relation to Sensation. Raven Press, New York NY.

Pope CA III. 1989. Respiratory disease associated with community air pollution and a steel mill, Utah Valley. Am J Public Health 79:623–628.

Pope CA III. 1991. Respiratory hospital admissions associated with PM_{10} pollution in Utah, Salt Lake, and Cache Valleys. Arch Environ Health 46:90–97.

Pope CA III, Dockery DW. 1992. Acute health effects of PM_{10} pollution on symptomatic and asymptomatic children. Am Rev Respir Dis 145:1123–1128.

Pope CA III, Hill RW, Villegas GM. 1999. Particulate air pollution and daily mortality on Utah's Wasatch Front. Environ Health Perspect 107:567–573.

Pritchard RJ, Ghio AJ. 1993. Oxidant generation, alveolitis and infection increase with ionizable iron concentrations on air pollution particulates. Am Rev Respir Dis 147:A13.

Pritchard RJ, Ghio AJ, Lehmann JR, Winsett DW, Tepper JS, Park P, Gilmour MJ, Dreher KL, Costa DL. 1996. Oxidant generation and lung injury after particulate air pollutant exposure increase with concentrations of associated metals. Inhalation Toxicol 8:457–477.

Quann RJ, Sarofim AF. 1982. Vaporization of refractory oxides during pulverized coal combustion. In: Nineteenth Symposium (International) on Combustion, pp 1429–1440. The Combustion Institute, Pittsburgh PA.

Ratafia-Brown JA. 1994. Overview of trace element partitioning in flames and furnaces of utility coal-fired boilers. Fuel Processing Technol 39:137–154.

Reddel RR, Ke Y, Gerwin BI, McMenamin MG, Lechner JF, Su RT, Brash DE, Park JB, Rhim JS, Harris CC. 1988. Transformation of human bronchial epithelial cells by infection with SV40 or adenovirus-12 SV40 hybrid virus, or transfection via strontium phosphate coprecipitation with a plasmid containing SV40 early region genes. Cancer Res 48:1904–1909.

RMCOEH (Rocky Mountain Center for Occupational and Environmental Health). 1996. Cancer, Cardiovascular and Chronic Obstructive Pulmonary Mortality and Ambient Air Pollution: A Study of 11 California Counties, 1963 to 1992, Using Monthly Data. RMCOEH, Park City, Utah.

Samet JM, Graves LM, Quay J, Dailey LA, Devlin RB, Ghio AJ, Wu W, Bromberg PA, Reed W. 1998. Activation of MAPKs in human bronchial epithelial cells exposed to metals. Am J Physiol 275:L551–L558.

Samet JM, Reed W, Ghio AJ, Devlin RB, Carter JD, Dailey LA, Bromberg PA, Madden MC. 1996. Induction of prostaglandin H synthase 2 in human airway epithelial cells exposed to residual oil fly ash. Toxicol Appl Pharmacol 141:159–168.

Samet JM, Stonehuerner J, Reed W, Devlin RB, Dailey LA, Kennedy TP, Bromberg PA, Ghio AJ. 1997. Disruption of protein tyrosine phosphate homeostasis in bronchial epithelial cells exposed to oil fly ash. Am J Physiol 272:L426–L432.

Sarofim AF, Howard JB, Padia AS. 1977. The physical transformation of mineral matter in pulverized coal under simulated combustion conditions. Comb Sci Technol 16:187–204.

Schaich KM. 1990. Preparation of metal-free solutions for studies of active oxygen species. Methods Enzymol 186:121–125.

Schieven GL, Kirihara JM, Myers DE, Ledbetter JA, Uckun FM. 1993. Reactive oxygen intermediates activate NF-κB

in a tyrosine kinase-dependent mechanism and in combination with vanadate activate the p561ck and p59fyn tyrosine kinases in human lymphocytes. Blood 82:1212–1220.

Schilling CJ, Tams IP, Schilling RSF, Nevitt A, Rossiter CE, Wilkinson B. 1988. A survey into the respiratory effects of prolonged exposure to pulverised fuel ash. Br J Ind Med 45:810–817.

Schneider W. 1984. Hydrolysis of iron(III)-chaotic olation versus nucleation. Comments Inorg Chem 3:205–223.

Schreider JP, Culbertson MR, Raabe OG. 1985. Comparative pulmonary fibrogenic potential of selected particles. Environ Res 38:256–274.

Schwartz J. 1994a. PM_{10}, ozone, and hospital admissions for the elderly in Minneapolis-St Paul, Minnesota. Arch Environ Health 49:366–374.

Schwartz J. 1994b. Air pollution and daily mortality: A review and meta analysis. Environ Res 64:36–52.

Schwartz J. 1994c. Total suspended particulate matter and daily mortality in Cincinnati, Ohio. Environ Health Perspect 102:186–189.

Schwartz J, Dockery DW, Neas LM. 1996. Is daily mortality associated specifically with fine particles? J Air Waste Manag Assoc 46:927–939.

Schwartz J, Morris R. 1995. Air pollution and hospital admissions for cardiovascular disease in Detroit, Michigan. Am J Epidemiol 142:23–35.

Shendrikar AD, Ensor DS, Cowen SJ, Woffinden GJ, McElroy MW. 1983. Size-dependent penetration of trace elements through a utility baghouse. Atmos Environ 17:1411–1421.

Siegl WO, Zinbo M, Korniski TJ, Richert JFO, Chladek E, Paputa MC, Peck, Weir JE, Schuetzle D, Jensen TE. 1994. Air Toxics: A comparison of the gas- and particle-phase emissions from a high-emitter vehicle with those from a normal-emitter vehicle. SAE Paper 940581. Society of Automotive Engineers, Warrendale PA.

Smith KL, Smoot LD, Fletcher TH, Pugmire RJ. 1994. The structure and reaction processes of coal. In: The Plenum Chemical Engineering Series (Luss D, ed). Plenum Press, New York NY.

Smith KR, Aust AE. 1997. Mobilization of iron from urban particulates leads to generation of reactive oxygen species in vitro and induction of ferritin synthesis in human lung epithelial cells. Chem Res Toxicol 10:828–834.

Smith KR, Veranth JM, Hu AA, Lighty JS, Aust AA. 2000. Interleukin-8 levels in human lung epithelial cells are increased in response to coal fly ash and vary with bioavailability of iron, as a function of particle size and source of coal. Chem Res Toxicol 13:118–125.

Smith KR, Veranth JM, Lighty JS, Aust AE. 1998. Mobilization of iron from coal fly ash was dependent upon the particle size and the source of coal. Chem Res Toxicol 11:1494–1500.

Smith WL, DeWitt DL. 1995. Biochemistry of prostaglandin endoperoxide H synthase-1 and synthase-2 and their differential susceptibility to nonsteroidal antiinflammatory drugs. Semin Nephrol 15:179–194.

Spinti JCP. 1997. An Experimental Study of the Fate of Char Nitrogen in Pulverized Coal Flames (dissertation). University of Utah, Salt Lake City UT.

Standiford TJ, Kunkel SL, Basha MA, Chensue SW, Lynch JPI, Toews GB, Westwick J, Strieter RM. 1990. Interleukin-8 gene expression by a pulmonary epithelial cell line. J Clin Invest 86:1945–1953.

Stringer B, Imrich A. 1996. Lung epithelial cell (A549) interaction with unopsonized environmental particulates: Quantitation of particle-specific binding and IL-8 production. Exp Lung Res 22:495–508.

Stultz SC, Kitto JB. 1992. Steam: Its Generation and Use with Catalogue of the Manufactures of the Babcock and Wilcox Company. Babcock & Wilcox, New York NY.

Takeuchi T, Morimoto K. 1994. Crocidolite asbestos increased 8-hydroxydeoxyguanosine levels in cellular DNA of a human promyelocytic leukemia cell line, HL60. Carcinogenesis 15:635–639.

Veranth JM, Smith KR, Aust AE, Dansie SL, Griffith JB, Hu AA, Huggins ML, Lighty JS. 2000a. Coal fly ash and mineral dust for toxicology and particle characterization studies: Equipment and methods for PM2.5- and PM1-enriched samples. Aerosol Sci Technol 32:127–141.

Veranth JM, Smith KR, Hu AA, Lighty JS, Aust AE. 2000b. Mobilization of iron from coal fly ash was dependent upon the particle size and the source of coal: Analysis of rates and mechanisms. Chem Res Toxicol 13:382–389.

Veranth JM, Smith KR, Huggins F, Hu AA, Lighty JS, Aust AE. 2000c. Mössbauer spectroscopy indicates that iron in an aluminosilicate glass phase is the source of the bioavailable iron from coal fly ash. Chem Res Toxicol 13:161–164.

Weitzman SA, Graceffa P. 1984. Asbestos catalyzes hydroxyl and superoxide radical generation from hydrogen peroxide. Arch Biochem Biophys 228:373–376.

Weitzman SA, Weitberg AB. 1985. Asbestos-catalysed lipid peroxidation and its inhibition by desferroxamine. Biochem J 225:259–262.

Wesselius LJ, Smirnov IM, Nelson ME, O'Brien-Ladner AR, Flowers CH, Skikne BS. 1996. Alveolar macrophages accumulate iron and ferritin after in vivo exposure to iron or tungsten dusts. J Lab Clin Med 127:401–409.

Zar HJ. 1996. Biostatistical Analysis, 3rd ed, pp 338–343. Prentice Hall, Upper Saddle River NJ.

Zeng T. 1998. Transformation of Iron and Trace Elements During Coal Combustion (dissertation). Massachusetts Institute of Technology, Cambridge MA.

APPENDIX A. Processing of Coal and Recovery of Coal Samples

PARENT COALS

The Utah, Illinois, and North Dakota coals used in the study are described in the Methods and Study Design section and in Table 1.

Parent coals were sent to Vortec Products Company (Long Beach CA) to be pulverized. Screen analysis was used to determine the size distribution of the pulverized coals (Table A.1). These experimental data indicate that the Utah and Illinois coals had similar size distributions: about 70% of the coal was smaller than 200 mesh (American Society for Testing and Materials standard E11-01). The North Dakota coal was quite different: a coarser material, with only 43% of the sample smaller than 200 mesh.

Composite samples of each pulverized coal were sent to Huffman Laboratories (Golden CO) for ultimate and proximate analysis by standard ASTM methods (Table 1). The sulfur concentrations in the North Dakota and Illinois coals (1.01% and 1.07%) were approximately the same, whereas the sulfur concentration in Utah coal (0.52%) was lower. The moisture content in the North Dakota coal (27.65%) was much higher than in the Utah and Illinois coals (2.5% and 4.47%). In addition, the heating value of North Dakota coal (7,532 BTU/hr) was lower than the heating value of the Utah and Illinois coals (12,338 BTU/hr and 12,748 BTU/hr, respectively).

The Utah, Illinois, and North Dakota coals used in the experiments described in this Report were new batches of the same coals used in studies conducted in 1997. Ultimate and proximate analyses indicated that coal composition varied slightly between batches (see coal analysis data in Smith and colleagues [1998]). The sulfur and ash contents in the new Illinois coal (1.07% and 5.81%) were notably lower than that of the old coal (3.82% and 11.78%). The moisture content of the new North Dakota coal (27.65%) was considerably higher than that of the old coal (8.21%). These differences emphasize that coal can vary substantially even within a mine and that coal must be characterized with each acquisition.

U-FURNACE DESCRIPTION

A laboratory scale multifuel furnace, which simulates the time and gas temperature history of a full-scale coal-fired boiler, was used to burn pulverized coals. Furnace details are described elsewhere (Spinti 1997). A brief description of the equipment is given below.

The 30-kW furnace (the U-furnace), shown in Figure A.1, has seven sections constructed in a U configuration. Temperature measurements can be obtained at ports located in each section. The burner used in this experiment was a premix burner that was designed at the University of Utah Combustion Laboratory. The burner allows

Table A.1. Screen Analysis of Pulverized Coal[a]

Tyler Mesh US No.	Opening (μm)	% Material Retained on Screen: Utah Bituminous	Illinois No. 6 Bituminous	North Dakota Lignite
Lid				
115/120	125	6.96 ± 0.01	10.90 ± 0.19	32.08 ± 0.73
170/170	88	11.93 ± 0.02	12.66 ± 0.08	16.08 ± 0.17
200/200	74	9.81 ± 0.54	8.38 ± 0.10	9.10 ± 0.16
250/230	63	9.94 ± 0.37	7.04 ± 0.23	4.43 ± 0.29
325/325	44	19.88 ± 0.03	14.50 ± 0.14	10.17 ± 0.13
400/400	37	9.32 ± 1.21	8.55 ± 0.21	5.74 ± 0.45
Pan	0	32.17 ± 0.23	37.97 ± 0.53	22.31 ± 0.75

[a] Screen analysis was conducted using a Ro-Tap shaker with 8-in diameter sieves. Approximately 40 g of coal was shaken for 15 min. Data are mean ± SD (N = 3).

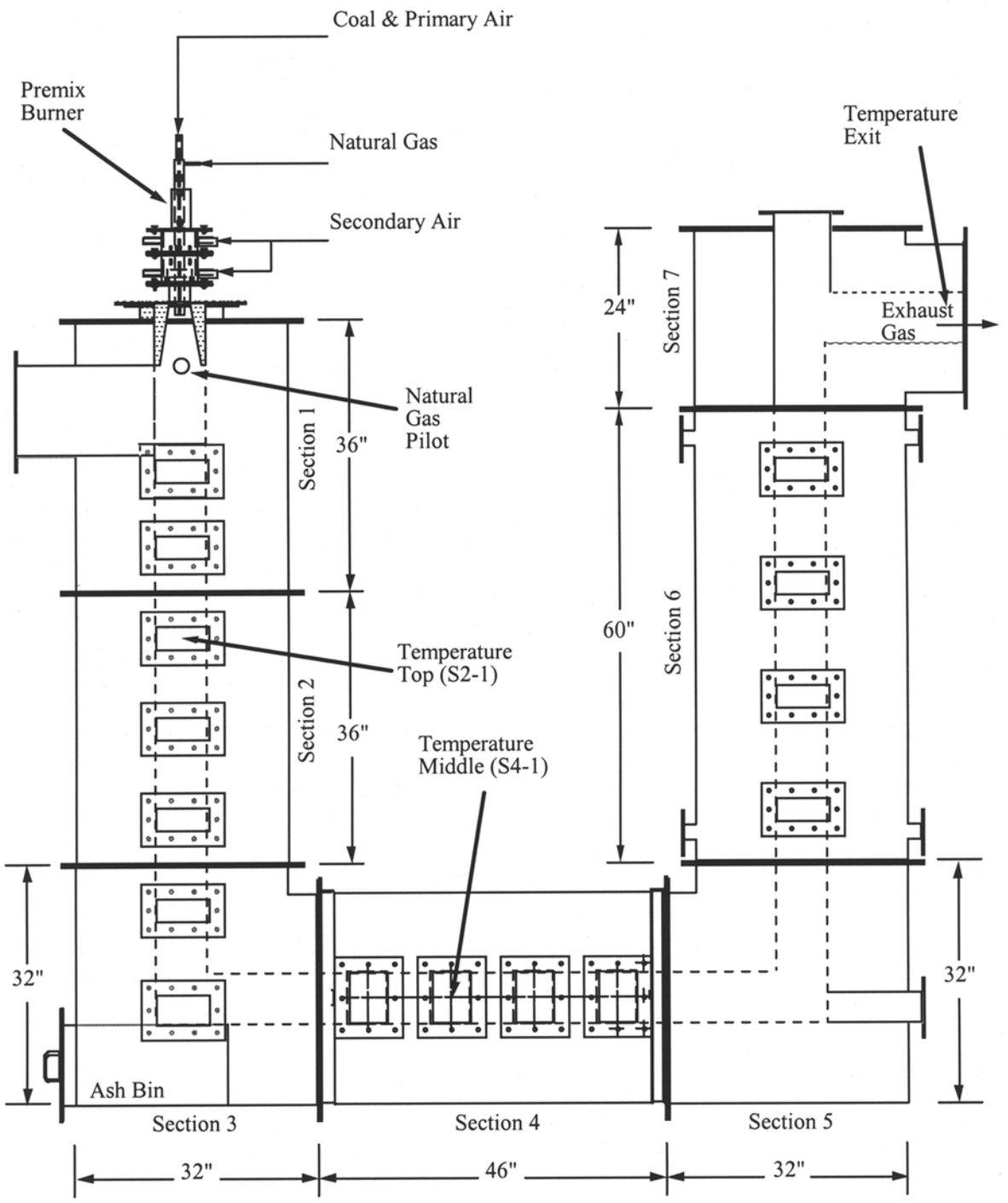

Figure A.1. Multifuel, 30-kW furnace (U-furnace).

complete mixing of fuel and air before fuel enters the combustion chamber of the furnace. The combustion chamber is 287.4 in long with a diameter of 6.30 in. The primary air stream, comprising approximately 85% of the total air requirement, was preheated to 204°C. A volumetric feeder manufactured by K-Tron International (Pitman NJ) was used to feed the coal to the furnace. The feeder was placed on a scale that was used to monitor the weight change of the feeding system. The secondary air stream, which comprised the remainder of the total air requirement and was not preheated, carried the coal from the feeder to the burner located approximately 3.6 m above the coal feeding system.

Furnace conditions monitored during each run included coal feed rate, air feed rate, furnace temperatures, and composition of flue gas. Coal feed rate was calculated from the weight change of the coal feeding system. Air feed rate was adjusted for approximately 15% excess air to achieve a 3% oxygen concentration in the exhaust gas. The furnace temperature was measured at section 2, port 1 (S2-1), section 4, port 1 (S4-1), and the exit of the furnace. Composition of the exiting flue gas (percentages of O_2 and CO_2, as well as parts per million nitrogen oxides [NO_x]) was recorded by a continuous, online data acquisition system.

PARTICLE COLLECTION SYSTEM

The particle collection system was designed and constructed to collect submicron particles from the entire exhaust flow from the U-furnace. The 35 m^3/hr collection train was located 3.4 m downstream of the U-furnace (Figure A.2). Collection equipment included a 20-jet preseparator, virtual impactor, array of filter housings, two heat exchangers (downstream and upstream), rotary vacuum pump, eductor vacuum pump, flow controllers, and two temperature controllers. All lines upstream of the preseparator were wrapped with heating tape and insulation and were preheated to 85°C to prevent initial condensation. The heat exchangers contained 0.9 m (3 ft) of warm water at 40°C to 45°C to prevent initial condensation and to cool the gas stream.

The major components of the collection apparatus were the 20-jet preseparator and the virtual impactor (Figure A.2). The 20-jet preseparator removed coarse particles and the virtual impactor concentrated the flow containing fine particles. The fine particles in the concentrated gas stream were collected on four PTFE filters, which were removed regularly to recover submicron particles.

The preseparator, a 20-jet conventional inertial impactor, was designed to separate out particles with an aerodynamic diameter greater than 1 μm. The preseparator we used consisted of three sections: top, middle, and bottom. The top section contained one inlet port at the top and 20 outlet ports at the bottom. This section distributed the gas flow to the next, middle section. The middle section consisted of 20 removable nozzles hanging from the top plate and four exit ports at the bottom. The 20 nozzles increased the velocity of the gas for inertial impaction. Changing the diameter of the removable nozzles varied the cut size of the collection equipment. In most cases, oversized particles were collected on a substrate in the middle section. The bottom section served as the connection between the preseparator and the virtual impactor. Dimensional drawings of the 20-jet preseparator are documented elsewhere (Veranth 1998).

An oiled polyester-felt substrate in the middle section of the preseparator was used in most cases to retain oversized particles and to minimize particle bounce. Severely hydrotreated paraffinic oil (12.5 mL; CMP 19A high vacuum pump oil; Cambridge Mill Products, Malvern OH) was poured onto the substrate directly under the jets. The oil was then allowed to saturate the surrounding areas of the substrate. Oversized particles were collected on this oiled substrate, forming columns of ash and oil directly under the jets. Ash columns were removed periodically to avoid clogging the jets. The amount of oversized particles collected depended mostly on what coal was being burned. The preseparator was typically cleaned after 1 to 1.5 hours of run time.

Oiled substrate was not used in the preseparator when collecting the Illinois PM_1 fraction. Because Illinois coal produced low amounts of ash, the oiled substrate retained most of the submicron particles and made the oiled substrate impractical. In addition, Illinois ash was sticky and oversized particles tended not to bounce after impact, even in the absence of substrate. (See mass distribution of Illinois PM_1 fraction in Particle Collection section, page 10.)

Mounted directly below the 20-jet preseparator was a single-slit virtual impactor designed by Sioutas and colleagues (1994) (Harvard School of Public Health; manufactured by Clematis Machine and Fixture Co, Waltham MA). As the flue gas passed from the preseparator though the narrow slit, the flow velocity increased. A small fraction of the gas, about 20% of the total flow, was extracted along the streamline of the main flow to concentrate the particles into a smaller flow. The diluted major flow, about 80% of the total flow, was removed perpendicular to the streamline of the main flow by a constant-volume rotary vacuum pump and then exhausted. The coarse fractions, rich in $PM_{2.5–10}$ and $PM_{1–2.5}$, were collected using the cascade impactor. After this initial concentration, the minor flow was directed to a filter array via an eductor vacuum pump. The filter array consisted of four 47-mm polycarbonate

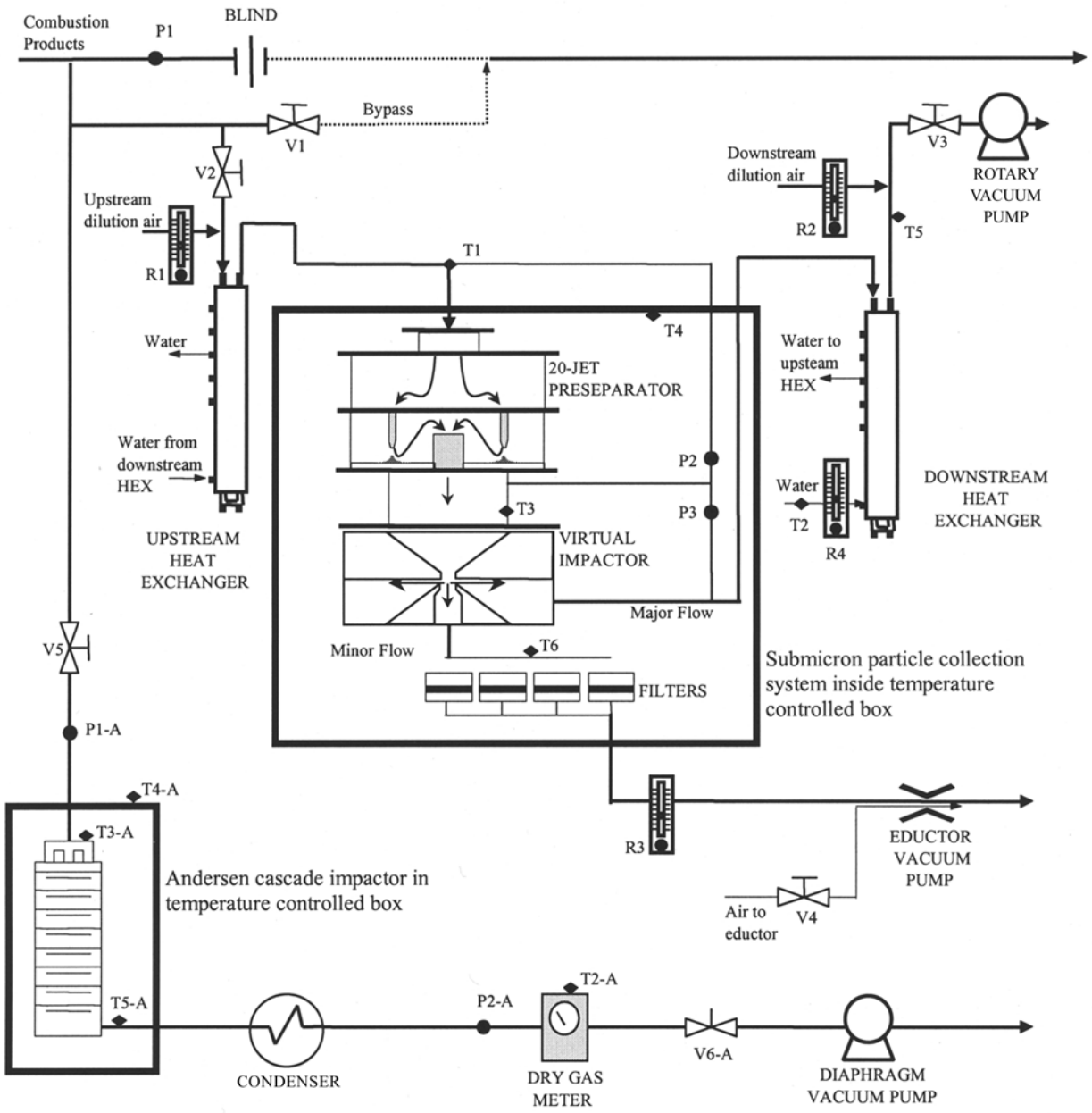

Figure A.2. Collection system for size fractionation of combustion particles.

filter housings in parallel. Submicron particles were collected on 47-mm PTFE filter membranes (Gelman Sciences). The flow rate through the filters was monitored, and when the flow rate decreased to 60% of the original rate, the filters were replaced. Filters were usually changed after 30 to 60 minutes, depending on the coal being burned.

The 20-jet preseparator, virtual impactor, and filter array were kept in an insulated box maintained at 75°C to 90°C, depending on the coal, to maintain isothermal conditions. Adjustments to the dilution air, both upstream of the preseparator and downstream of the virtual impactor, were used to compensate for variation in flow rate of the flue gas, to maintain a constant pressure drop through the preseparator, and to control velocity for inertial impaction.

CASCADE IMPACTOR

The coarse size fractions of CFA samples were collected with a 1-acfm Andersen cascade impactor (Graseby-Andersen). The impactor used in this study was a 10-stage, 1.7 m^3/hr (1 acfm) conventional cascade impactor (Figure 1). The apparatus was set upstream of the submicron particle collection system as shown in Figure A.2. Approximately 5% of the total furnace flow was pulled through the cascade impactor by a diaphragm vacuum pump. The impactor was placed in an insulated, temperature-controlled box to maintain isothermal conditions. Temperatures were recorded at the inlet and outlet of the impactor. The moisture in the gas was removed in the condenser and a dry gas meter measured the flow rate. A control valve, upstream of the pump, controlled the rate of flow through this part of the system.

Particles were collected on dry metal plates to avoid contamination by oil that would interfere with biochemical and toxicologic experiments. Consecutive plates were combined to form samples of particles of various size fractions (see Figure 1). Oiled substrates were used on stages 0 and 4 to prevent particle bounce, which in turn separated particle size fractions more thoroughly. The substrates (Durapore membrane filter GVHP0950; Millipore) were treated with silicon oil (Dow 316 silicon spray; Dow Chemical Co, Midland MI.

In separate runs, the Andersen cascade impactor was also used parallel to the submicron filters as a visual indication of the separation achieved in the 20-jet preseparator. In situations in which a mass distribution was required, oiled substrates were used on all metal plates in the cascade impactor.

EQUIPMENT AND SAMPLE HANDLING

The submicron particles were collected on PTFE filters in the virtual impactor, which were then stored in disposable sterilized polystyrene petri dishes. Loaded filters from the same run were stored together until the sample was recovered. The coarse fractions, rich in particles with diameter greater than 10 μm, were collected using the cascade impactor. Collected material and/or plates from each stage were stored separately in sterilized polystyrene petri dishes until the sample was recovered.

All equipment was handled with care to prevent contamination of samples, which would interfere with toxicology tests. At the end of each day, the 20-jet preseparator, virtual impactor, filter housings, and cascade impactor were cleaned with warm water and Liqui-Nox detergent (SPI Supplies, West Chester PA) and were allowed to air-dry overnight. The filter housings and collection plates of the cascade impactor, which contacted the samples directly, were then disinfected by wiping with a 70% ethanol solution to prevent contamination by microbes. Filters and substrates were handled with latex gloves or clean tweezers. Care was taken to minimize dust contamination by covering filters and substrates during preparation.

The equipment handling and cleaning procedures were validated with endotoxin and microbial contamination tests. A sample of the collected particles and a sample of the equipment rinse water were sent to Utah State University for testing. The samples were tested for endotoxins by the *Limulus* amebocyte lysate assay (Sigma Chemical Co). The samples were also incubated in the cell culture medium for 72 hours to measure contamination by microbes. The

results indicated that the samples were free of endotoxins and did not contain microbial contamination sufficient to affect toxicology studies.

Equipment was also cleaned between coals. The furnace was dry-cleaned rather than wet-washed to prevent the refractory from cracking. The U-furnace was turned off and the bottom ash was removed from the ash bin. Slag formed near the ash bin was also dislodged and removed. The remaining bottom ash was removed with compressed air and a vacuum cleaner. The exit pipe, 6 inches in diameter, was wiped on the exterior with a cloth towel and the interior was cleaned out with compressed air. Any remaining CFA was reentrained into the air stream and vented. All pipes in the collection train 1 to 1.5 inches in diameter upstream of the preseparator, including the tube side of the heat exchangers, were flushed with water. The collection train was then flushed with air and allowed to dry overnight. After equipment had been cleaned, the furnace was brought back to normal operating temperature using natural gas as the fuel. Background particle concentrations were determined to quantify the mass of particles from the previous run that was reentrained into the flue gas. Background samples were taken after the equipment was cleaned, between coals, and also between runs. While the furnace burned on natural gas, the flue gas was diverted to the collection train. The background samples (two consecutive 30-minute natural gas blanks) were collected at an average rate of 0.05 mg/min on glass fiber filters placed in the cleaned submicron filter array (Table A.2). Some of the particulate collected during the natural gas runs might have been from the U-furnace walls. To test this hypothesis, another two 30-minute natural gas blanks were run through the furnace after a day's run on North Dakota coal but before the furnace and pipes were cleaned; the background samples were then collected. As shown in Table A.2, mass was collected on the filter during these two runs at 0.47 mg/min for the first 30 minutes and 0.09 mg/min for the next 30 minutes. In contrast, submicron CFA was collected during CFA production runs on North Dakota coal at a rate of 3 to 6 mg/min (Table A.2). Since the pipes were cleaned between each coal, contamination of the sample with ash remaining in the furnace from the previous coal was estimated as less than 2%.

REFERENCES TO APPENDIX A

Sioutas C, Koutrakis P, Burton R. 1994. A high-volume small cutpoint virtual impactor for separation of atmospheric particulate from gaseous pollutants. Particle Sci Technol 12:207–222.

Smith KR, Veranth JM, Lighty JS, Aust AE. 1998. Mobilization of iron from coal fly ash was dependent upon the particle size and the source of coal. Chem Res Toxicol 11:1494–1500.

Spinti JCP. 1997. An Experimental Study of the Fate of Char Nitrogen in Pulverized Coal Flames (dissertation). University of Utah, Salt Lake City UT.

Veranth JM. 1998. Particle Emissions from Practical Combustion Systems (dissertation). University of Utah, Salt Lake City UT.

Table A.2. Material Collected During Natural Gas Flushes and Coal-Fired Runs

Weight (g)	Time (min)	Collection (mg/min)
Material Left in the System After Furnace Has Been Cleaned (furnace operated on natural gas)		
0.0016	32	0.05
0.0011	30	0.04
Material Left in the System After Previous Day's Run on North Dakota Coal (furnace operated on natural gas)		
0.0140	30	0.47
0.0028	31	0.09
Submicron Material Collected While Furnace Burned on North Dakota Coal		
0.2230	60	3.72
0.1211	42	2.88
0.1644	40	4.11
0.1015	29	3.50
0.1838	30	6.13
0.2601	45	5.78

APPENDIX B. Results of Additional Statistical Analyses

Table B.1. ANOVA Analysis

Source of Variance	Degrees of Freedom	Sum of Squares	Mean Squares	F Value	*P* Value
Effect of CFA on MDA Formation					
Size class	3	21,300	7,100	24.43	<0.001
Source	2	12,800	6,380	21.94	<0.001
Size class × Source	6	12,100	2,010	6.93	<0.001
Residual	36	10,500	291		
Effect of CFA Iron Mobilization from CFA by Citrate					
Size class	2	2,990	1,490	475.47	<0.001
Source	2	448	224	71.34	<0.001
Size class × Source	4	298	74.5	23.73	<0.001
Residual	18	56.5	3.14		
Effect of CFA on Concentration of Ferritin in A549 Cells					
Size class	3	2.29	0.762	189.73	<0.001
Source	2	1.19	0.594	147.86	<0.001
Size class × Source	6	0.441	0.0734	18.28	<0.001
Residual	24	0.0964	0.00402		
Effect of 10 μg/cm^2 CFA on IL-8 Concentration in Medium from A549 Cells[a]					
Size class	3	2.89	0.964	71.11	<0.001
Source	2	1.91	0.954	70.35	<0.001
Size class × Source	6	1.22	0.203	14.95	<0.001
Residual	24	0.325	0.0136		
Effect of 20 μg/cm^2 CFA on IL-8 Concentration in Medium from A549 Cells[a]					
Size class	3	7.53	2.51	238.91	<0.001
Source	2	4.91	2.45	233.42	<0.001
Size class × Source	6	1.78	0.296	28.17	<0.001
Residual	24	0.252	0.0105		
Effect of 40 μg/cm^2 CFA on IL-8 Concentration in Medium from A549 Cells[a]					
Size class	3	8.56	2.85	206.69	<0.001
Source	2	7.61	3.81	275.94	<0.001
Size class × Source	6	1.63	0.272	19.74	<0.001
Residual	24	0.331	0.0138		

[a] Data were $\log_e$-transformed prior to analysis.

Table B.2. Linear Regression of Effect of FAC on Ferritin Concentration in A549 Cells

Source of Variance	Degrees of Freedom	Sum of Squares	Mean Squares	F Value	*P* Value
Total	23	4.76			
Linear regression	1	4.59	4.59		
Residual	22	0.17	0.00768		
Among groups	7	4.69	0.670		
Linear regression	1	4.59	4.59	1,044.87	<0.001
Deviations from linearity	6	0.10	0.0164	3.74	0.016
Within groups	16	0.0703	0.00439		

Table B.3. Parameter Estimates for Linear Regression of Ferritin on FAC

Parameter	Estimate	SE[a]
Intercept	0.0736	0.0222
FAC	0.134	0.00414

[a] Standard errors are based on within-group variability.

Table B.4. Piecewise Linear Regression of Effect of FAC on IL-8 Production by A549 Cells

Source of Variance	Degrees of Freedom	Sum of Squares	Mean Squares	Asymptotic F Value	*P* Value
Regression	4	3,370,000	842,000	343.83	<0.001
Residual	20	23,800	1,190		
Uncorrected Total	24	3,390,000			
Corrected Total	23	1,250,000			

Table B.5. Parameter Estimates for Piecewise Linear Regression of Effect of FAC on IL-8 Production by A549 Cells

Parameter	Estimate	Asymptotic Standard Error	Asymptotic 95% Confidence Limits
Intercept	109	18.2	70.8, 147
Slope for first segment	−0.667	14.1	−30.0, 28.7
Slope adjustment for second segment	84.7	3.48	77.4, 91.9
Breakpoint	2.59	0.346	1.87, 3.31

APPENDIX C. Methods for Mathematical Analysis of Iron Mobilization Rate

The data on the rate of iron mobilization from CFA by citrate were mathematically analyzed to test whether the observed differences among size fractions could be explained by purely physical differences, in particular the change in surface area/mass ratio with decreasing diameter. This analysis has been published (Veranth et al 2000).

DATA

The data on iron mobilization from CFA used in this study (Figure 11) were obtained from the same experimental series as reported by Smith and colleagues (1998). The detailed particle size distribution data were determined for mathematical analysis by SEM examination of the collected samples using methods described elsewhere (Veranth 1998; Veranth et al 2000).

Mathematical analysis of fluid-solid and liquid-solid heterogeneous mass transfer and chemical reactions has been extensively studied by chemical engineers and extractive metallurgists because predicting the rates of heterogeneous interactions is important for the design of industrial-scale equipment. These methods of analyzing heterogeneous processes have also been applied to biological and biochemical systems such as drug delivery (Stenberg et al 1986; Polakovic et al 1999) and bacterial leaching of metals from ore (Blancarte-Zurita et al 1986; Asai et al 1992). Many of these studies involved reactions in the extracellular medium. However, the mathematical analysis is based on fundamental physics and is equally applicable to fine particles in vitro, to particles in the extracellular fluid, and to intracellular transfer from particles taken up by the cell through either endocytosis or phagocytosis. The basic form of the analysis can be summarized as a material balance for each chemical species:

$$\text{In} - \text{out} + \text{generation} - \text{consumption} = \text{Accumulation}.$$

When the molar concentration of the mobile species is low, the mass transport is usually considered a combination of convection plus the Fick law of diffusion in three dimensions. The changes in individual chemical species are linked by stoichiometry and the reaction rates are a function of local concentration of the reactants, which may include active sites on the solid surface. This analysis results in a system of coupled nonlinear partial differential equations with specified initial and boundary conditions. Analytic solutions to these general equations have been found for limiting cases in which various terms can be approximated as constants or can be neglected as being numerically insignificant. The rigorous derivation of these transport and chemical reaction equation solutions are available in standard texts and references (Bird et al 1960; Wen 1968; Levenspiel 1998). To apply the general heterogeneous mass transfer and chemical reaction theory to the specific case of iron mobilization from CFA, certain assumptions were necessary. The mobilization of iron was assumed to comprise the following steps: (1) transport of the chelator to the surface of the particle; (2) transport of the chelator from the particle surface to the iron within the particle; (3) binding of the iron to the chelator; (4) release of the iron from the solid phase mineral; (5) transport of iron from the initial location in the solid to the solid-liquid interface; and (6) transport of the iron-chelator complex from the particle surface to the bulk fluid.

Four limiting mechanisms were selected for this study on the basis of physical reasoning, preliminary calculations, and the ability of the mathematical models pertaining to the selected mechanisms to make quantitative predictions that could be tested with available data. The key assumptions, the equations relating iron mobilization rate to time, the nature of the approach to steady state, and a citation for the equations are given in Table C.1 for each mechanism. Two mechanisms, solid-liquid equilibrium and depletion of active species, are listed together because the rate of a first-order reaction approaching equilibrium and the rate of a first-order reaction in which one reactant is being depleted are indistinguishable. The idealized cases in which liquid-phase diffusion and solid-phase diffusion limit mass transfer are illustrated in Figure C.1. This schematic shows the concentrations of the chelator and the iron as functions of the radius from the center of the particle out to the bulk fluid. The major resistance in one case is the liquid film surrounding the particle and in the other case a growing layer of depleted material between the particle surface and the unreacted core. An example of mass transfer limited by liquid-phase diffusion is the dissolution of homogeneous particles of a soluble species in an unagitated solvent. The heterogeneous surface reaction model (Table C.1; not illustrated in Figure C.1) is applicable to chemical reactions in which the rate constant is based on the unreacted surface area in contact with the liquid; the available surface decreases as the reaction proceeds. This limiting case applies to both shrinking particles and to constant-size particles in which the depleted surface layer is highly porous. Heterogeneous surface reactions that are first order in the solid-phase species concentration occur in situations, such as those involving catalysts, in which only a portion of the surface consists of active sites and the active site, once reacted, is unavailable for future reaction. The solid-phase diffusion

Table C.1. Mechanisms Considered in Mathematical Analysis of Iron Mobilization Rate[a,b]

Mechanism			
Solid-Liquid Equilibrium / Depletion of Active Species	Liquid-Phase Diffusion	Heterogeneous-Surface Reaction	Solid-Phase Diffusion
Assumptions			
• First-order rate in difference between C_M and C_{Me} • First-order rate in concentration of solid component	• Constant-size particle • Solid surface in equilibrium with liquid medium • Porous particle	• Shrinking unreacted surface • Constant or shrinking particle • Transport fast compared to reaction time	• Constant-size particle • Fast transport in liquid • Unreacted core in equilibrium with mobile species inside particle
Rate Law			
$X = 1 - e^{-t/\tau}$	$X = \frac{t}{\tau}$	$\frac{t}{\tau} = 1 - (1-X)^{1/3}$	$\frac{t}{\tau} = 1 - 3(1-X)^{2/3} + 2(1-X)$
Characteristic Time			
$\tau = \frac{1}{k_r}$	$\tau = \frac{\rho_M R}{3bk_g C_A}$	$\tau = \frac{\rho_M R}{6bk_{rs} C_A}$	$\tau = \frac{\rho_M R^2}{6bD_e C_A}$
Approach to Steady State			
Asymptotic	Constant rate until completion	Decreasing rate but complete in finite time	Decreasing rate but complete in finite time
Comments			
	Quasi-steady particle size	Temperature-sensitive	Shrinking core limiting case
Citation[a]			
Chapt 3, Eq 12 (rearranged)	Chapt 12, Eqs 9 and 11	Chapt 12, Eqs 22 and 23	Chapt 12, Eqs 17 and 18b

[a] Adapted with permission from Levenspiel (1972).

[b] b = stoichiometric coefficient, C_A = molar concentration of reactant in liquid, C_M = concentration of arbitrary species, C_{Me} = equilibrium concentration of M in liquid, D_e = effective diffusivity in solid, k_g = film coefficient for mass transfer, k_{rs} = heterogeneous surface reaction rate constant, R = particle radius, ρM = molar density of mobile metal species in particle, τ = characteristic time = (time per time for complete reaction), X = conversion (moles reacted per mole of initial).

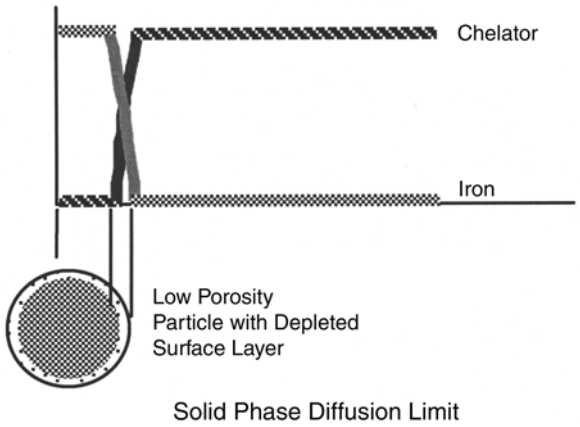

Figure C.1. Concentration versus radius for two ideal cases of diffusion-limited mass transfer from solid spherical particles.

(shrinking-core) model (Table C.1) approximates a process in which mass transfer across a depleted layer on the surface of a constant-size particle is much slower than both mass transfer in the liquid and the reaction by which the mobile ions/molecules are formed at the unreacted surface.

MODELING MOBILIZATION OF IRON

The particle-size statistics determined by SEM examination are listed in Table C.2. The differences between the mass median aerodynamic diameter, the mean volume diameter, the mean surface diameter, and the number mean diameter per particle sample are discussed in the textbook by Hinds (1982). The geometric mean and geometric standard deviation (GSD) provide a convenient way to mathematically describe the size distribution of polydisperse aerosols. The amount of iron mobilized in 24 hours by the citrate chelator is given in both Table C.2 and Table 8.

The iron mobilization measured experimentally and the corresponding model predictions are compared in Figure C.2. The graphs for the liquid diffusion, surface reaction, and solid diffusion models each have a characteristic locus when expressed in terms of conversion versus normalized time. The raw data for nanomoles of iron mobilized versus time for three size fractions of the three coals were expressed in terms of conversion (X vs normalized time [t/τ]). The data were transformed to represent conversion by dividing the amount of iron mobilized at each time point by the estimated total for that sample. Time was normalized by dividing actual time by the extrapolated time for complete reaction based on the last three measurements. Of the three models considered, the solid diffusion model provided the best fit to the experimental data (see Figure C.2). In addition, the model fit to the data was tested quantitatively by plotting the appropriate rate law for X versus normalized time and comparing the resulting data points to a straight line using an R^2 statistic.

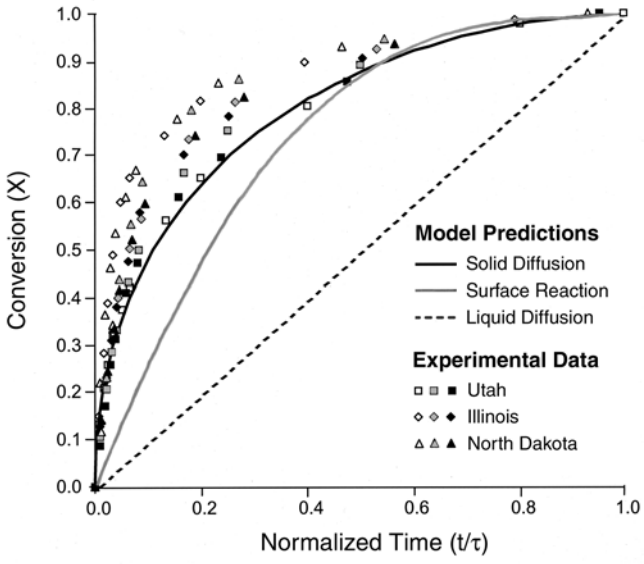

Figure C.2. Measured mobilization of iron from CFA and the predictions of three models. Values for iron mobilization (taken from Figure 11) for three sizes of CFA from three sources were compared with the predictions of three models: liquid diffusion controlled mobilization, surface reaction controlled mobilization, and solid diffusion controlled mobilization. The standard error of the conversion is estimated to be 8% due to uncertainty in both the individual iron mobilization measurements and the extrapolated final value.

Table C.2. Size Statistics for Polydisperse Aerosol Samples[a]

Sample	Mass Median Aerodynamic Diameter	Volume Geometric Mean Diameter	GSD	Surface (Sauter) Mean Diameter	Number Mean Diameter	Iron Mobilized over 24 Hours (nmol/mg)
Utah						
$PM_{>10}$	10.0	6.3	1.7	5.4	1.6	22.0
$PM_{2.5–10}$	4.9	3.5	1.5	3.2	1.4	40.2
$PM_{2.5}$	2.6	1.8	2.0	1.4	0.5	56.7
Illinois						
$PM_{>10}$	9.1	5.9	1.6	5.1	1.2	24.0
$PM_{2.5–10}$	4.7	3.3	1.5	3.0	1.6	27.9
$PM_{2.5}$	1.9	1.3	1.7	1.1	0.5	43.3
North Dakota						
$PM_{>10}$	4.2	2.9	1.8	2.4	1.2	22.3
$PM_{2.5–10}$	4.2	2.7	1.4	2.6	1.6	24.6
$PM_{2.5}$	2.1	1.5	1.7	1.3	0.7	44.1

[a] Diameters are given in microns except for geometric standard deviation (GSD).

The case of solid-phase diffusion with limited mass transfer provided the best fit between model predictions and measurements (Figure C.2). This result suggests that actual mobilization of iron from CFA involved transport of mass within the particle at a rate slower than those of the other steps. The liquid-phase diffusion model with controlled mass transfer in our study implies a constant rate of conversion versus normalized time, which does not agree with the experimental measurements. Also, the rate of iron mobilization was about six orders of magnitude slower than what would be expected based on values published in the literature for diffusion of ions in liquid. The apparent diffusivity of the iron calculated from the Utah $PM_{2.5}$ collected at 1 to 2 hours was 1.5×10^{-11} cm^2/second, whereas typical values of diffusivity in aqueous solution are approximately 1×10^{-5} cm^2/second (Weast et al 1988). Transport in the liquid film surrounding the particle is much faster than transport during other stages of iron mobilization. The liquid-phase controlled-diffusion case can be conclusively ruled out under the conditions of these experiments. The heterogeneous surface reaction model predicts a lower conversion at early times than was observed, but this case cannot be ruled out due to the uncertainty introduced by needing to estimate final values from the available data. The mass transfer and surface reaction limited cases all result in models that predict the iron mobilization going to completion in finite time. The chemical equilibrium case and the depletion of active species case both predict an exponential approach to steady state (neither shown in Figure C.2). A reasonable fit to the data can be obtained by arbitrarily adjusting the time constant in the exponential equation, but the available data are insufficient to test whether either of these mechanisms describe the actual iron mobilization process.

The North Dakota $PM_{2.5}$ fraction, shown in Figure C.3, was actually a bimodal mixture of 0.5- to 3-µm spheres and clusters of ultrafine particles. Although this was the only bimodal CFA sample, all other samples were also slightly polydisperse, as indicated by the GSD data in Table C.2. (The GSD for the North Dakota $PM_{2.5}$ sample in Table C.2 is for the large particle mode only and does not include the ultrafine primary particles.) Because the predicted mass transfer rate for the solid-phase diffusion case depends inversely on the square of the physical diameter (D_p^{-2}), the smallest particles in a polydisperse sample could react to completion while the largest particles remain largely unreacted.

We also investigated whether the deviations from predictions of the solid-phase diffusion model were an effect of the polydisperse samples. The conversion for a monodisperse aerosol (GSD = 1.0) and for a polydisperse aerosol (linear mass distribution from 1 to 14 µm) were calculated

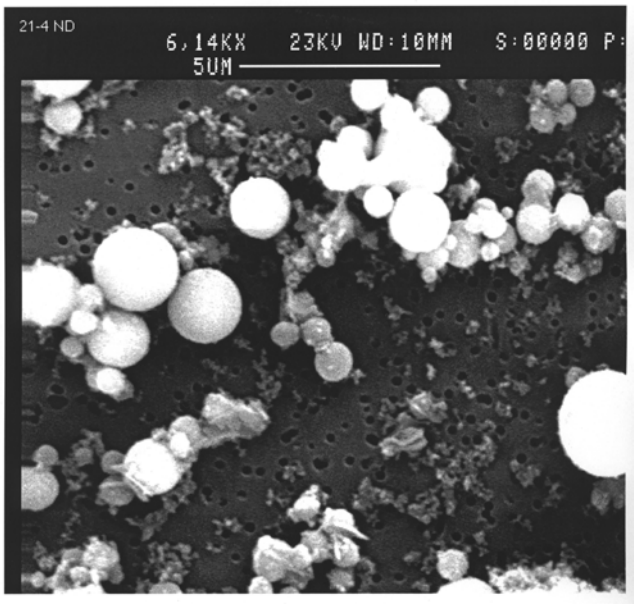

Figure C.3. SEM of North Dakota CFA $PM_{2.5}$ at ×5000. The spherical particles are residual ash formed by coalescence of molten mineral inclusions in the parent coal, and the clusters are aggregates of ultrafine particles formed by vaporization and condensation. The black circles are pores in the polycarbonate substrate.

using the solid-phase diffusion rate law equation (Table C.1), assuming that the volume medians of two aerosols are equal. Time was normalized by the time for complete reaction of the monodisperse aerosol. The apparent conversion of the polydisperse aerosol was normalized to match conversion of the monodisperse aerosol: $\tau = 1$. (This normalization reflected the way in which the experimental data were interpreted in Figure C.2.) Figure C.4 shows that calculated results for a polydisperse aerosol given higher initial conversion and a slow continuing increase compared to a monodisperse aerosol. The initial data points in Figure C.4 generally fall above the predictions for the solid diffusion model shown in Figure C.2. The iron mobilization data for 12 and 24 hours suggest a continual slow increase rather than a constant value. These data support the hypothesis that initial iron mobilization values may be due to the smallest particles in a polydisperse CFA sample.

The conversion at fixed time versus particle size is the most sensitive test for distinguishing between the solid-phase diffusion and heterogeneous surface reaction cases. The models predict that the rate of the solid diffusion controlled mass transfer varies with D_p^{-2}, whereas the rate of the heterogeneous surface reaction varies with D_p^{-1}. For example, if iron mobilization from particles of invariant composition were controlled by solid-phase diffusion, iron mobilized from a 2.5-µm particle in 1 hour would be the same as iron mobilized from a 10-µm particle in 16 hours, that is, 1 × hour. This prediction was tested by

replotting the iron mobilization data for each coal against time adjusted by the ratio of the surface mean diameter of that fraction to the surface mean diameter of the small particle fraction for that coal. Iron mobilization was normalized such that the small particle fraction mobilization at 24 hours was 1.0. The curves for three size fractions were expected to coincide if the measured iron mobilization rate from CFA fit the solid diffusion model exactly. The results for the three Utah CFA size fractions adjusted by D_p^{-1} and D_p^{-2} are shown in Figure C.5. Although adjusting the time scale using the solid diffusion model improves the agreement between the three size fractions, the results for all three coal types are ambiguous (Illinois and North Dakota not shown). The empirical best fit is a fractional exponent between −1 and −2, which implies that neither solid diffusion nor surface reaction is a complete description of the actual iron mobilization process.

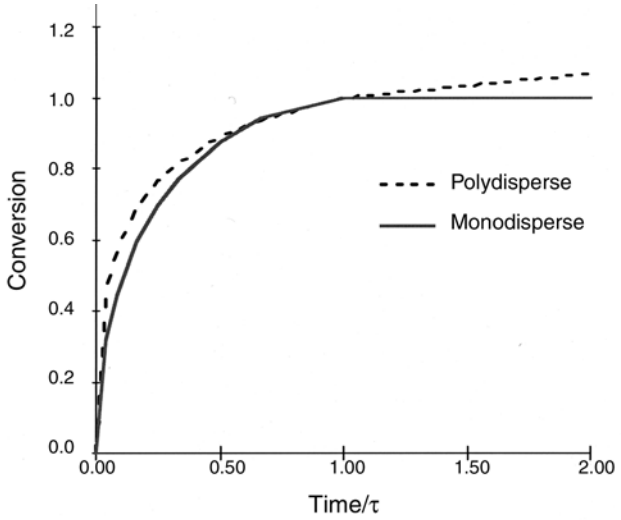

Figure C.4. Iron mobilization calculated for a monodisperse and a polydisperse aerosol with same median aerodynamic diameter. The calculations, based on the solid diffusion controlled model, show that more iron is mobilized from the polydisperse aerosol than from the monodisperse aerosol at early times.

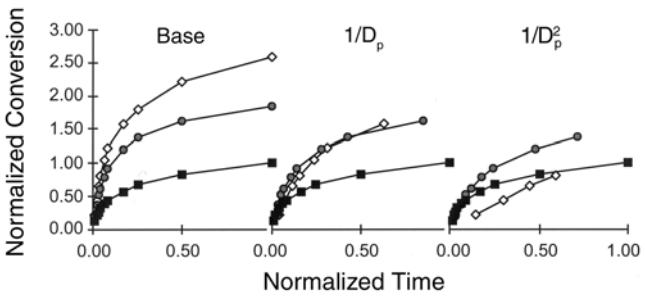

Figure C.5. Iron mobilization versus time for three normalized Utah CFA fractions. The fractions were normalized so the mobilization of the smallest = 1 at time = 1. Base = uncorrected data replotted from Smith and colleagues (1998). $1/D_p$ and $1/D_p^2$ = time rescaled by surface-weighted mean physical diameter ($PM_{>10}$, ■; $PM_{2.5–10}$, ●; $PM_{2.5}$, ◇). For particles of invariant composition, the solid diffusion mass transfer model predicts that the rates from different size fractions should coincide if time is rescaled by $1/D_p^2$.

REFERENCES TO APPENDIX C

Asai S, Konishi Y, Yoshida L. 1992. Kinetic model for batch bacterial dissolution of pyrite particles by *Thiobacillus ferroxidans*. Chem Eng Sci 47:133–139.

Bird RB, Stewart WE, Lightfoot EN. 1960. Transport Phenomena. John Wiley & Sons, New York NY.

Blancarte-Zurita MA, Branion RMR, Lawrence RW. 1986. Application of a shrinking particle model to the kinetics of microbial leaching. Elsevier Science Publishing Co, New York NY.

Hinds WC. 1982. Aerosol Technology: Properties, Behavior, and Measurement of Airborne Particles. John Wiley & Sons, New York NY.

Levenspiel O. 1998. Chemical Reaction Engineering. John Wiley & Sons, New York NY.

Polakovic M, Gorner T, Gref R, Dellacherie E. 1999. Lidocaine loaded biodegradable nanospheres: II. Modeling of drug release. J Controlled Release 60:169–177.

Smith KR, Veranth JM, Lighty JS, Aust AE. 1998. Mobilization of iron from coal fly ash was dependent upon the particle size and the source of coal. Chem Res Toxicol 11:1494–1500.

Stenberg M, Stiblert L, Nygren H. 1986. External diffusion in solid-phase immunoassays. J Theor Biol 120:129–140.

Veranth JM. 1998. Particle Emissions from Practical Combustion Systems (dissertation). University of Utah, Salt Lake City UT.

Veranth JM, Smith KR, Aust AE, Dansie SL, Griffith JB, Hu AA, Huggins ML, Lighty JS. 2000. Coal fly ash and mineral dust for toxicology and particle characterization studies: Equipment and methods for PM2.5- and PM1-enriched samples. Aerosol Sci Technol 32:127–141.

Weast RC, Astle MJ, Beyer WH. 1988. Handbook of Chemistry and Physics. CRC Press, Boca Raton FL.

Wen CY. 1968. Noncatalytic heterogeneous solid fluid reaction models. Indust Eng Chem 60:34–54.

ABOUT THE AUTHORS

Ann E Aust is a professor of biochemistry in the Chemistry and Biochemistry Department at Utah State University, Logan, Utah. She received her BS in biophysical science at the University of Houston and her PhD in biochemistry in the Biochemistry Department at Michigan State University. Her primary research interests are to elucidate the mechanism(s) by which particulate materials, such as asbestos and urban air particulates, cause cancer and other lung disorders. Of primary interest has been to understand the role played by iron in the particles in eliciting these biological effects.

James C Ball is a research scientist in the Chemistry and Environmental Sciences Department of Ford Research in Dearborn, Michigan. He received his BS in chemistry from California State Polytechnical University, Pomona, California, and his PhD in bioorganic chemistry from the University of New Mexico. He spent two years as a postdoctoral fellow in the laboratory of Veronica Maher and Justin McCormick investigating cytotoxicity by methylated purines. Since 1982 he has been with Ford Motor Company investigating the biochemical toxicology of vehicle emissions. His interests include the genotoxicity of nitroarenes, optically active mutagenic compounds, and the role of carbocations as intermediates in the carcinogen-DNA reaction from both an experimental and a theoretical view. His latest interests are chiefly in the area of mechanistic particle toxicology.

Autumn A Hu received her BS and MS in chemical and fuels engineering from the University of Utah. She is currently working with the Combustion Group in the Chemical and Fuels Engineering Department at the University of Utah.

JoAnn S Lighty is the associate dean for academic affairs, College of Engineering, and professor, Department of Chemical and Fuels Engineering, University of Utah. She received her BS and PhD in chemical engineering at the University of Utah. Her primary research interests are incineration, fate of metals and organics during thermal treatment, fluidized bed combustion, biomass combustion, air pollution problems along the US/Mexico border, and the characterization of fine PM from combustion systems.

Kevin R Smith is a postdoctoral fellow in the Institute of Toxicology and Environmental Health at the University of California, Davis, California. He received his BS in chemistry at Weber State University, Ogden, Utah. He contributed to the research in this final report while a doctoral student at Utah State University, Logan, Utah, where he received his PhD in biochemistry. His research interests include the mechanisms of damage to the respiratory system by urban air PM. Specifically, he is interested in toxicity of particles from the combustion of fuel additives and transition fuels that contain metal.

Ann M Straccia is a research scientist in the Chemistry and Environmental Sciences Department of Ford Research in Dearborn, Michigan. She received her BS in chemistry from the University of Michigan. She spent several years investigating the properties and use of a thermoreversible gel to reduce tissue adhesion after surgery. Recently, she studied the generation of reactive oxygen species and the thermal release of nitric oxide from ambient air particles. Her interests include biocompatible polymers, particle toxicology, the surface chemistry of materials, and atmospheric particle morphology.

John M Veranth is an academic research assistant professor of chemical and fuels engineering at the University of Utah. He received his BS and MS in Mechanical Engineering from the Massachusetts Institute of Technology. He received an MBA and his PhD in chemical engineering from the University of Utah. His research interests are industrial-scale combustion and control of air pollution with emphasis on the formation of fine particles at high temperatures, aerosol sampling and characterization, and particle health effects.

Willie C Young is a research scientist in the Chemistry and Environmental Sciences Department of Ford Research. He received his BA in history from Talladega College in Alabama and his MA in biology from Atlanta University in Georgia. Since 1977, he has worked at Ford Motor Company and has developed emission control devices, investigated the mutagenicity of diesel particles and halomethylarenes, and characterized bacteria from water-based manufacturing fluids. Most recently, he has measured the ability of small particles to generate reactive oxygen species.

OTHER PUBLICATIONS RESULTING FROM THIS RESEARCH

Ball BR, Smith KR, Veranth JM, Aust AE. 2000. Bioavailability of iron from coal fly ash: Mechanisms of mobilization and of biological effects. Inhalation Toxicol 12:209–225.

Ball JC, Straccia AM, Young WC, Aust AE. 2000. The formation of reactive oxygen species catalyzed by neutral, aqueous extracts of NIST ambient particulate matter and diesel engine particles. J Air Waste Manag Assoc 50(11):1897–1903.

Smith KR, Veranth JM, Hu AA, Lighty JS, Aust AE. 2000. Interleukin-8 levels in human lung epithelial cells are increased in response to coal fly ash and vary with bioavailability of iron, as a function of particle size and source of coal. Chem Res Toxicol 13:118–125.

Veranth JM, Smith KR, Aust AE, Dansie SL, Griffith JB, Hu AA, Huggins ML, Lighty JS. 2000. Coal fly ash and mineral dust for toxicology and particle characterization studies: Equipment and methods for $PM_{2.5}$- and PM_1-enriched samples. Aerosol Sci Technol 32:127–141.

Veranth JM, Smith KR, Hu AA, Lighty JS, Aust AE. 2000. Mobilization of iron from coal fly ash was dependent upon the particle size and the source of coal: Analysis of rates and mechanisms. Chem Res Toxicol 13:328–389.

Veranth JM, Smith KR, Huggins F, Hu AA, Lighty JS, Aust AE. 2000. Mössbauer spectroscopy indicates that iron in an aluminosilicate glass phase is the source of the bioavailable iron from coal fly ash. Chem Res Toxicol 13:161–164.

Smith KR, Veranth JM, Lighty JS, Aust AE. 1998. Mobilization of iron from coal fly ash was dependent upon the particle size and the source of coal. Chem Res Toxicol 11:1494–1500.

ABBREVIATIONS AND OTHER TERMS

A549	cultured human lung epithelial (cells)
acfm	actual cubic feet per minute
ANOVA	analysis of variance
As	arsenic
ASTM	American Society for Testing and Materials
BEAS	SV-40 transformed human bronchial epithelial (cells)
cDNA	complementary DNA
CFA	coal fly ash
CO_2	carbon dioxide (used once)
DF	*N*-[5-[3-[(5-aminopentyl)hydroxycarbamoyl]propionamido]-pentyl]-3-[[5-(*N*-hydroxyacetamido)pentyl]carbamoyl]propionohydroxamic acid, or desferrioxamine B
DMSO	dimethyl sulfoxide
DMTU	dimethylthiourea
EIA	enzyme immunoassay
ELISA	enzyme-linked immunosorbent assay
EPA	Environmental Protection Agency (US)
ERK	extracellular receptor kinase (used once)
FAC	ferric ammonium citrate
Fe_2O_3	hematite
Fe_3O_4	magnetite
FeS_2	pyrite
$FeSO_4$	ferrous sulfate
ferrozine	3-(2-pyridyl)-5,6-diphenyl-1,2,4-triazine-*p,p′*-disulfonic acid

GAPDH	glyceraldehyde-3-phosphate dehydrogenase
GSD	geometric standard deviation
HCl	hydrochloric acid
H_2O_2	hydrogen peroxide
ICP-MS	inductively coupled plasma mass spectrometry
IL	interleukin [IL-1, IL-1β, IL-6, IL-8]
INAA	instrumental neutron activation analysis
iNOS	inducible nitric oxide synthase
JNK	c-Jun NH_2-terminal kinase
LDH	lactate dehydrogenase
MAPK	mitogen-activated protein kinase
MDA	malondialdehyde
mRNA	messenger RNA
NaCl	sodium chloride
$NaHCO_3$	sodium bicarbonate
NF-κB	nuclear factor-κB
NIST	National Institute of Standards and Technology (US)
NO	nitric oxide
NO_x	nitrogen oxides
O_2	oxygen
PGE_2	prostaglandin E_2
$PGF_{2\alpha}$	prostaglandin $F_{2\alpha}$
PM	particulate matter
PM_1	particulate matter less than 1 μm in aerodynamic diameter
PM_{10}	particulate matter less than 10 μm in aerodynamic diameter
$PM_{>10}$	particulate matter greater than 10 μm in aerodynamic diameter
$PM_{2.5}$	particulate matter less than 2.5 μm in aerodynamic diameter
$PM_{2.5–10}$	particulate matter greater than 2.5 μm but less than 10 μm in aerodynamic diameter
PTFE	polytetrafluoroethylene (Teflon)
R^2	coefficient of determination for multivariate analysis
ROFA	residual oil fly ash
ROS	reactive oxygen species
RT-PCR	reverse transcriptase–polymerase chain reaction
SEM	scanning electron microscopy
SRM	NIST Standard Reference Material (SRM 1648, 1649, 1650, 2975)
TiO_2	titanium dioxide
TGF-β	tumor growth factor-β
TMTU	tetramethylthiourea
TNF	tumor necrosis factor

COMMENTARY
Health Review Committee

INTRODUCTION

Ambient particulate matter (PM*) comes from many sources and varies in size, chemical composition, and other physical and chemical properties depending on the source of the particles and the changes the particles undergo in the atmosphere. Inhalation of PM has been associated with both acute and chronic health effects. Concerns about these effects derive primarily from epidemiologic studies that show an association between short-term increases in particle concentration and increases in daily morbidity and mortality from respiratory and cardiovascular diseases (Samet et al 1995, 1997, 2000; reviewed by Ostro 1993; Dockery and Pope 1994; Moolgavkar and Luebeck 1996; US Environmental Protection Agency [EPA] 1996; HEI 1999). One area of toxicologic PM research targeted initially in HEI's Strategic Plan for 1994 to 1998 (HEI 1994) and again in HEI's most recent Strategic Plan (HEI 2000) focuses on the question of which components or attributes of the ambient PM mixture may be important in causing toxicity.

In 1996, HEI issued RFA 96-1, *Mechanisms of Particle Toxicity: Fate and Bioreactivity of Particle-Associated Compounds*. In response, Dr Ann Aust of Utah State University submitted an application titled "Particle Characteristics Responsible for Effects on Human Lung Epithelial Cells." Aust and colleagues hypothesized that transition metals bound to inhaled PM are released within lung epithelial cells and catalyze the formation of reactive oxygen species (ROS). (Transition metals exist in two or more valence states and can participate in oxidation and reduction reactions.) ROS can stimulate epithelial cells to produce inflammatory mediators, some of which attract inflammatory cells that contribute to lung inflammation and injury. Aust and colleagues proposed to study the mobilization of metals (with a focus on iron) from particles and to determine whether they produce oxidative stress (via formation of hydroxyl free radicals) that induces synthesis of inflammatory mediators.

The investigators proposed to study particles from size-fractionated coal fly ash (CFA) generated from three types of coal, exhaust from gasoline and diesel engines, natural soils, and ambient Utah air. The HEI Research Committee thought that the proposal addressed the goals of RFA 96-1 in that the proposal focused on the role of particle-associated metals and particle size in causing effects that might lead to lung inflammation. External reviewers thought that Aust and her research team had substantial expertise in the research they proposed. The strengths of the proposal were considered the use of particles whose size and chemical composition were well-characterized and the correlation of chemical measures of both metal content and bioavailability with physiologic effects. The Research Committee agreed in large part with the external panel's evaluation and thought that the in vitro experiments would be useful for investigating the specific hypotheses; thus, the Committee recommended the study for funding.[†]

This Commentary is intended to aid HEI's sponsors and the public by highlighting the strengths of the study and placing the report in scientific perspective.

SCIENTIFIC BACKGROUND

Combustion of coal or oil to generate electricity produces particulate inorganic byproducts called *fly ash*. Metals in the fuels vaporize at the high combustion temperatures and as the temperature falls they condense, predominantly on the surface of the submicron particles. Thus, the metals may be present on ultrafine and smaller fine particles at a higher relative proportion by weight than on larger fine particles and coarse particles (Linak and Wendt 1994; EPA 1996). (Coarse particles are defined as those greater than 2.5 μm in aerodynamic diameter, fine particles as those 0.1 to 2.5 μm aerodynamic diameter, and ultrafine particles as those less than 0.1 μm in aerodynamic diameter.)

Iron is the predominant transition metal in CFA. As discussed in the Introduction of the Investigators' Report, fuel oil contains lower levels of crustal elements (aluminum, silica, and calcium) than coal, and therefore, its combustion produces much less ash. Fuel oil ash does, however, contain the transition metals vanadium (the highest in concentration), nickel, and iron. Fly ash from fuel combustion contributes more than 2.5×10^5 tons of PM annually to the United States ambient PM burden

*A list of abbreviations and other terms appears at the end of the Investigators' Report.

This document has not been reviewed by public or private party institutions, including those that support the Health Effects Institute; therefore, it may not reflect the views of these parties, and no endorsements by them should be inferred.

[†] Dr Aust's 18-month study, *Particle Characteristics Responsible for Effects on Human Lung Epithelial Cells,* began in August 1997. Total expenditures were $147,209. The draft Investigators' Report from Dr Aust and colleagues was received for review in April 2000. A revised report, received in September 2001, was accepted for publication in October 2001. During the review process, the HEI Health Review Committee and the investigators had the opportunity to exchange comments and to clarify issues in both the Investigators' Report and in the Review Committee's Commentary.

(EPA 1993). As mentioned, inhaled particle-bound transition metals could pose a health hazard if they were to become bioavailable within lung cells. Currently, the EPA is concerned that bound metals might leach into groundwater and threaten public health if CFA is disposed of improperly. The EPA does not regulate CFA as a hazardous substance under the Resource Conservation and Recovery Act because combustion waste is exempt from federal regulation (Chem Eng News 2000). However, the agency plans to conduct a major scientific analysis of combustion waste that will help decide its policy in the future (EPA 2000).

Because fly ashes contain potentially cytotoxic and genotoxic metals, they are useful models for study of a possible association between PM-bound metals and adverse health effects (Ghio and Samet 1999). The remainder of this Scientific Background describes studies that have associated pathologic effects with exposure to residual oil fly ash (ROFA) and CFA that contain transition metals.

EFFECTS OF TRANSITION METALS ASSOCIATED WITH FLY ASH

Studies performed predominantly in EPA laboratories and with collaborating institutions suggest that soluble transition metals may play a role in the pulmonary injury induced by ROFA; fewer studies have utilized CFA. Commentary Tables 1 and 2 summarize in vivo and in vitro studies of lung inflammation and injury (primarily of ROFA and its associated transition metals). The in vivo studies described in Commentary Table 1 used intratracheal instillation to expose laboratory animals to ROFA or CFA. This method of exposure is a useful way to investigate pollutant effects, but the results do not necessarily represent those from inhalation exposures. The first five studies summarized in Commentary Table 1 share the finding that ROFA-induced lung pathology can be reproduced by the bioavailable transition metals associated with ROFA (Costa and Dreher 1997; Dreher et al 1997; Kodavanti et al 1997, 1998; Madden et al 1999). The study by Kodavanti and colleagues (1998) is unique because they collected ROFA samples from ten different locations within a power plant. Because the samples differed in metal composition, the investigators were able to demonstrate that the lung response to ROFA samples depends on the metals, such as nickel, iron, and vanadium, that the ROFA contained. Pritchard and coworkers (1996) demonstrated similar lung responses to a variety of particulate samples with transition metal content.

Several investigators demonstrated production of ROS catalyzed by metal or ROFA in vitro (eg, Ghio et al 1999 and Becker et al 1996 in Commentary Table 2). Kadiiska and coworkers (1997) extended these results to an in vivo system by demonstrating production of reactive free radicals in the lung after exposure to ROFA or associated metals. Other findings indicate that exposure to vanadium is associated with oxidative stress (Liochev and Fridovich 1991; Shi et al 1996). Gilmour and colleagues (2000) reported that ROFA or its associated transition metals affect the antigen priming process and the secondary immune responses after antigen challenge. The increases in messenger RNA (mRNA) of inflammatory mediators in that study suggest that pulmonary inflammation played a role in the process. In two non-EPA studies, Esaka and colleagues (1995) made the important observation that transition metals from instilled CFA apparently become bioavailable and probably travel in the blood to other organs. Srivastava and coworkers (1990) demonstrated that potentially harmful CFA-associated transition metals pass through the placenta to fetal organs.

Results of the in vitro studies summarized in Commentary Table 2 have two major themes. First, production of inflammatory mediators increases in lung epithelial cells exposed to ROFA or its associated metals (Carter et al 1997; Stringer and Kobzik 1998; Dye et al 1999; Jiang et al 2000) and in epithelial cells exposed to metal-containing ambient particles (Ghio et al 1999). Second, exposure to metals or ROFA increases ROS production by alveolar macrophages (Becker et al 1996; Kodavanti et al 1998) and epithelial cells (Ghio et al 1999; Madden et al 1999). The relations among metal exposure, ROS production, and subsequent inflammation was shown by Carter and coworkers (1997): a metal chelator (which inhibits ROS production) or an antioxidant (which inhibits the activity of ROS) decreased the production of inflammatory mediators.

STUDIES OF CFA

The toxicity and occupational health hazards associated with CFA have been reviewed by Borm (1997) and are discussed in the Introduction of the Investigators' Report. Borm (1997) and Aust and colleagues (this Research Report) point out that, in contrast to ROFA, there are few data that describe how CFA affects the production of proinflammatory cytokines, growth factors, or ROS. The study by Aust and coworkers is a solid step toward filling this gap.

TECHNICAL EVALUATION

This study was performed by an experienced group of investigators with demonstrated excellence in the field of metal-catalyzed oxidative stress and particle-associated injury. The study was of high scientific quality, was well conceived and executed, and adds substantially to our knowledge of the biological properties of particles. The abundance of some particles that were tested allowed the investigators to separate them by size and, in the case of

Commentary Table 1. In Vivo Studies of Fly Ash and Transition Metal Toxicity

Agent	Recipient of Intratracheal Instillation	Results	Reference
ROFA, metal salts	Rats	ROFA induced the appearance of inflammatory cells in BALF. Both solubilized metals from ROFA and a solution of iron, nickel, and vanadium reproduced the injury.	Dreher et al 1997
ROFA, metal salts	Rats	ROFA-induced inflammation, edema, and fibrosis (histopathology) reproduced by solution of iron, nickel, and vanadium. Nickel alone caused greater inflammation than vanadium or iron alone.	Kodavanti et al 1997
ROFA, metal salts	Rats	ROFA-induced increases in BALF protein and LDH associated with nickel and iron content. ROFA-induced neutrophil recruitment associated with vanadium content.	Kodavanti et al 1998
DOFA, ROFA, CFA	Rats	Inflammatory responses (DOFA > ROFA > CFA) related to amount of bioavailable transition metals, not mass of instilled PM.	Costa and Dreher 1997
ROFA, metal salts	Rats	ROFA-induced appearance of acetaldehyde (indicator of lung lipid oxidation) in lung lavage fluid reproduced by solution of iron or vanadium.	Madden et al 1999
ROFA, CFA, desert dust, volcanic ash, ambient air particles	Rats	Eight solubilized transition metals were differentially associated with particulates. Neutrophil influx, lavage protein levels, and airway reactivity increased with the content of soluble metals. Bacterial challenge after particle instillation increased mortality as a function of particle soluble metal content.	Pritchard et al 1996
ROFA, metal salts	Rats	Presence of ESR free radical signals in lung tissue induced by ROFA; a mixture of vanadium, nickel and iron sulfates; and vanadium or iron alone.	Kadiiska et al 1997
ROFA, metal salts, house dust mite allergen	Rats	Pretreatment with ROFA or a mixture of transition metal salts caused a transient increase in inflammatory responses 2 days after allergen sensitization. Antibody and lymphoproliferative immune responses increased in ROFA-treated animals during sensitization and subsequent antigen challenge. ROFA or metal salt mixture increased [mRNA] of inflammatory mediators in sensitized animals.	Gilmour et al 2000
CFA (1–5 μm in aerodynamic dynameter)	Mice	Manganese and nickel appeared in the lung and decreased with time. Later nickel appeared in the kidneys and manganese in the liver.	Esaka et al 1995
CFA (nonfractionated)	Pregnant rats (for 6 consecutive days, beginning on day 14)	On day 20, significant amounts of nine transition metals were found in differing amounts in placenta and in fetal liver, lung, heart, and kidney.	Srivastava et al 1990

Commentary Table 2. In Vitro Studies of Fly Ash and Transition Metal Toxicity

Agent	System	Results	Reference
Ambient Utah particles	Cell-free, human bronchial epithelial cells	Aqueous metal-containing extracts of particles or the insoluble metal-containing residue caused the production of ROS in the cell-free system. Epithelial cells exposed to both fractions released IL-8. Iron had the highest concentration of all metals in both fractions.	Ghio et al 1999
ROFA, ambient particles, diesel dust	Human and rat alveolar macrophages	Exposure to ROFA increased ROS formation more than exposure to ambient particles; diesel dust had no effect.	Becker et al 1996
ROFA, metal salts	Human bronchial epithelial cells	Cells exposed to ROFA containing vanadium, nickel, and iron produced IL-8, IL-6, and TNF-α and their mRNAs. These reactions were inhibited by a metal chelator or an antioxidant. Vanadium (but not iron or nickel) alone caused similar reactions.	Carter et al 1997
ROFA	Mouse lung epithelial cells	Cells primed by an inflammatory mediator (TNF-α) increased IL-8 synthesis after exposure to ROFA; an antioxidant reduced this response.	Stringer and Kobzik 1998
ROFA, metal salts	Rat tracheal epithelial cells	ROFA, vanadium, or nickel plus vanadium increased cell permeability, detachment, and death. ROFA or vanadium increased gene expression of inflammatory markers.	Dye et al 1999
ROFA, vanadium	Guinea pig tracheal epithelial cells	ROFA exposure increased mucin secretion and mucin gene expression. Mucin secretion was inhibited by an antioxidant. Vanadium also provoked mucin secretion.	Jiang et al 2000
ROFA	Rat alveolar macrophages	Exposure to ROFA with vanadium increased ROS formation more than exposure to ROFA with iron and vanadium.	Kodavanti et al 1998
ROFA	Human airway epithelial cells	ROFA increased oxidation of cell lipids as indicated by acetaldehyde production.	Madden et al 1999

CFA, to conduct detailed physical and chemical analyses. A limitation of the study is that the investigators used stored particles rather than fresh ones. Resuspending the particles may have changed their physical or chemical properties, which may have in turn affected their biological reactivity.

SPECIFIC AIMS

The long-term objectives of the investigators' research is to identify the mechanism(s) by which PM in ambient air may contribute to respiratory disease and to identify the characteristics of the particles that are responsible for specific biological effects. The aims specific to this study were to determine the following:

1. whether iron associated with CFA becomes bioavailable in human lung epithelial cells and whether the bioavailability of iron is related to (a) the source of the coal, (b) the amount of iron or the speciation (chemical form) of iron in CFA, or (c) the size of the CFA particles;
2. whether the amount of iron mobilized from CFA by a biological chelator, citrate, can be used in a cell-free system as an in vitro indicator of the relative amount of bioavailable iron in the CFA;
3. whether mediators of pulmonary inflammation are produced in human lung epithelial cells exposed to CFA and whether the production of mediators is related to (a) the source of the coal, (b) the size of the respirable CFA particles, or (c) the amount of bioavailable iron in the particles;
4. whether the generation of hydroxyl radical in a cell-free system by CFA can be used as an in vitro indicator of the amount of bioavailable iron or the production of mediators of pulmonary inflammation in human lung epithelial cells; and
5. whether particles from diesel or gasoline exhaust or ambient air particles collected in Salt Lake City, Utah, generate hydroxyl radical, and whether this is related to the amount of transition metal present in the particles.

STUDY DESIGN AND METHODS

The investigators' central hypothesis was that transition metals associated with inhaled PM become bioavailable within human lung epithelial cells and catalyze reactions leading to oxidative stress and inflammatory injury. The research focused on the relation between the transition metal content and the ability of the particles to generate ROS, such as the hydroxyl free radical, and induce the formation of inflammatory mediators. (Hydroxyl radicals are thought to cause oxidative stress within cells, which in turn induces inflammatory processes.) The investigators focused on iron content and mobilization because iron is the predominant transition metal in CFA. In addition to ashes from three different coal sources (Utah, Illinois, and North Dakota) with different chemical constituents, the investigators studied particles from gasoline and diesel engine exhaust, urban Salt Lake City air, natural soils, and mine tailings.

A strength of this study is that the sample sizes of most particles were sufficient to allow the investigators to collect material on different stages of a cascade impactor to separate the particles by size (with the exception of the gasoline and diesel exhaust particles). The CFAs were separated into PM_1, $PM_{2.5}$, $PM_{2.5–10}$, and $PM_{>10}$ (PM less than 1 µm, less than 2.5 µm, greater than 2.5 µm but less than 10 µm, and greater than 10 µm in aerodynamic diameter, respectively). Particles from desert dust were separated into PM_1 and $PM_{2.5}$ and particles from urban air into $PM_{2.5–10}$ and $PM_{2.5}$. The investigators removed PM_1 and $PM_{2.5}$ samples from filters by sonication in ethanol, whereas the larger particles were brushed from the filters. The investigators analyzed the metal composition of each size class of CFA particle by neutron absorption analysis and used inductively coupled plasma mass spectrometry (ICP-MS) to analyze the metal content of buffer extracts of the particles. The surface area of each size class of CFA particle was determined by a technique employing adsorption of nitrogen gas on the particle surface; these surface areas were compared with estimates of surface area obtained by scanning electron microscopy (SEM). The investigators used Mössbauer spectroscopy to identify the chemical forms of iron present in the CFA particles.

Aust and colleagues used phosphate buffer–soluble particle extracts to quantify the production of ROS by transition metals in vitro. The assay was based on the metal-catalyzed production of hydroxyl free radical, which oxidizes 2-deoxyribose in the assay medium to malondialdehyde (MDA). They quantified the level of MDA produced by adding 2-thiobarbituric acid to the assay medium, forming a colored reaction product that was measured spectrophotometrically. Desferrioxamine B, which forms a complex with transition metals and removes them from further reaction, was tested for its ability to inhibit ROS formation. The investigators used a spectrophotometric assay for total iron (Fe^{2+} and Fe^{3+}) to probe for bioavailable iron released from the particles in vitro by citrate, a physiologic metal chelator found in cells. Aust and coworkers examined the effect of low (2.5), near neutral (7.5), and high (10.1) pH on iron mobilization from particles using ICP-MS.

After determining the physical and chemical characteristics of the particles, the investigators evaluated the biological effects of the release of transition metals in a cultured human lung epithelial cell line (A549 cells), characteristic of alveolar epithelial type II cells. They employed an assay developed by Aust and coworkers to quantify the production of the iron storage protein ferritin (an indicator of intracellular iron release from particles), the inflammatory mediator interleukin (IL)-8, and mRNA for IL-8, by A549 cells exposed to CFA particles. Cell culture was usually carried out for 24 hours (except for the mRNA experiments, which were only 4 hours in duration) at particle concentrations of 20 µg/cm^2 (except for the IL-8 experiments, which used concentrations of 10, 20, or 40 µg/cm^2).

RESULTS AND INTERPRETATION

PHYSICAL AND CHEMICAL PROPERTIES OF PARTICLES

For the PM_1-enriched fraction of CFA, approximately 50% of the CFA particles were less than 1 µm in mean aerodynamic diameter and their surface area was larger proportionately than that of the coarser particles. The surface area of each size class of particle determined by nitrogen adsorption was two to four times larger than that measured by SEM, suggesting that the particles may contain micropores that adsorbed nitrogen measured but could not be detected by the magnification used for SEM imaging of the particles. In theory, recovering smaller particles from filters by sonication (in contrast to brushing the larger particles from filters) might fracture them and affect measurements of surface area. However, the results of pilot experiments indicated that sonication had no significant effect on surface area (A Aust, personal communication, 2001). The submicron particle fraction contained both single particles and aggregates of ultrafine particles.

The predominant metals in CFA were magnesium, aluminum, sodium, potassium, calcium, and the transition metals iron and titanium. Illinois CFA contained the greatest percentage of iron by weight and North Dakota

CFA the lowest. Iron was enriched in the CFA PM_1 samples compared with the coarser fractions from the same ash. The investigators demonstrated that phosphate buffer extracts of particles from all sources generated ROS. Particles from gasoline engine combustion had a greater ability to generate ROS than did particles from diesel engine combustion and were in the same range as that of ROS produced by CFA PM_1 and $PM_{2.5}$. Illinois and Utah CFA PM_1 generated more ROS than the larger particles did. This finding may reflect greater iron bioavailability of PM_1 compared with the coarser fractions and a greater iron bioavailability of the Illinois and Utah CFAs relative to North Dakota CFA. Again, the question of whether sonication of the smaller particles fractured them and made iron more readily soluble is mitigated by the pilot experiments described previously. The finding that desferrioxamine B inhibited ROS formed by all four size fractions of CFA suggests that transition metals were responsible for ROS production.

Citrate (pH 7.5) mobilized iron from particles from all sources with the exception of gasoline combustion particles. The latter source was not tested for iron mobilization because of very limited amounts of these particles. Only low levels of iron were mobilized from diesel exhaust particles. Citrate was chosen for further experiments because it was considered a physiologically relevant model chelator that is found in cells. The amount of iron mobilized from CFA $PM_{2.5}$ by citrate was greater than that mobilized from the coarser particles. Mobilization also depended on the source of coal. For example, more iron was mobilized from Utah CFA $PM_{2.5}$ than from Illinois CFA $PM_{2.5}$, even though the Illinois sample contained almost three times the amount of iron. Although North Dakota CFA $PM_{2.5}$ contained only one-fifth the amount of iron contained in Illinois CFA $PM_{2.5}$, the amount of iron mobilized from the two samples was similar. Thus, a key finding was that the total iron content of the particles was not closely correlated with bioavailable iron.

An acidic (pH 2.5) aqueous solution mobilized iron from CFA $PM_{2.5}$. In contrast, at pH 7.5 (in 50 mM NaCl), citrate was needed to mobilize iron. These findings demonstrate that consideration of pH and the chelator is important when determining the bioavailability of metals from PM.

Iron was present in several forms in the CFA particles. CFA PM_1 contained a larger fraction of total iron in the aluminosilicate phase than did CFA $PM_{>10}$. The remaining iron in CFA was in the form of mixed oxides. The investigators found that iron was removed from the aluminosilicates but not from the oxides. Thus, the iron associated with the aluminosilicates appeared to be the source of the iron mobilized from CFA.

Crustal dust, a component of urban PM, contained iron oxides but not iron associated with aluminosilicates. The finding that almost no iron could be mobilized by citrate from crustal dust supports the conclusion that the aluminosilicate fraction is the source of mobilized iron. Samples of ambient $PM_{2.5}$ collected from Salt Lake City, Utah, over 5-day periods within a month exhibited wide variation in the amount of iron that was mobilized by citrate.

BIOLOGICAL EFFECTS OF PARTICLES

Ferritin levels increased in A549 cells exposed to CFA. Because ferritin is an iron storage protein, this finding indicates that bioavailable iron was released by the particles. The amount of ferritin produced was inversely related to the size of the particles and depended on the source of coal (Utah > Illinois > North Dakota). This latter finding agrees with the amounts of iron mobilized by citrate from the size-fractionated CFA particles in the cell-free system. Diesel exhaust particles also induced ferritin synthesis by A549 cells. Cytochalasin D inhibited ferritin production by A549 cells exposed to CFA, indicating that endocytosis of the particles (uptake into cells) was required before iron was mobilized and ferritin synthesis was induced. The greater ferritin production by the smaller particles may have been caused by differential endocytosis: larger particles (either naturally occurring or formed by aggregation) may have been endocytosed less efficiently than smaller particles and therefore produced less ferritin. The investigators concede that particle size might affect endocytosis although their study was not designed to address this issue. However, iron mobilization was inversely proportional to particle size in both human lung cells and in cell-free solutions, where endocytosis is not a factor. In addition, the only CFA particles that showed aggregation were the North Dakota $PM_{2.5}$ samples. Thus, Aust and colleagues concluded that differential particle endocytosis does not play a major role in the differences observed in ferritin production (A Aust, personal communication, 2001). However, mechanisms of endocytosis of particles need further study.

Exposure to CFA increased synthesis of the inflammatory mediator IL-8 by A549 cells. Like ferritin, the levels of IL-8 produced related inversely to the size of the particles and depended on the source of coal (Utah > Illinois > North Dakota). The investigators reported a strong correlation between ferritin production and IL-8 levels, supporting their hypothesis that iron release plays a role in induction of the inflammatory process. CFA also induced formation of IL-8 mRNA by A549 cells. The role of transition metals in this process was demonstrated by the finding that desferrioxamine inhibited IL-8 mRNA formation. Dimethylthiourea and dimethyl sulfoxide, antioxidants that scavenge hydroxyl free radicals (Ghio and Samet 1999), inhibited IL-8 production by A549 cells exposed to CFA. This

important finding indicates that metal-induced oxidative stress in cultured lung epithelial cells can provoke synthesis of an inflammatory mediator, which can then attract inflammatory cells to the lung.

DISCUSSION

Aust and colleagues demonstrated a plausible connection among the intracellular release of transition metals from particles (with a focus on size-fractionated CFA), oxidative stress caused by ROS production, and lung inflammation. Their results show that iron was also mobilized from diesel-engine emission particles, but their stock of gasoline-engine emission particles was low, precluding similar studies. Although the authors focused on the possible effects of particles on respiratory disease, their results may also be applicable to effects on cardiovascular disease (eg, Godleski et al 2000).

The investigators found that extracts of all particles studied induced ROS production. However, the smallest CFA particles (PM_1), which were enriched in iron compared with the coarser particles, caused greater ROS production than the coarse fractions. Although the agent that caused ROS production was not definitively identified, the investigators obtained indirect evidence that transition metals released from the particles were likely responsible. The results concerning ROS production were extended by the finding that citrate solubilized iron from particles, a process that was also greater for smaller CFA particles than for coarser fractions. The speciation (chemical form) of iron in CFA particles affects its solubilization and bioavailability. Iron present as mixed oxides is insoluble (Fang 1999); however, iron ionically associated with silicates is reactive and capable of being mobilized (Hardy and Aust 1995). Aust and coworkers' finding that the smaller CFA particles were enriched in aluminosilicates (and that iron associated with aluminosilicates was the source of bioavailable iron) agrees with their results concerning ROS production and iron solubilization by citrate.

The investigators successfully demonstrated that human lung epithelial cells exposed to CFA particles in cell culture produced ferritin and that ferritin production was contingent on CFA particles entering the cells. Because ferritin (an iron storage protein) is produced in response to the presence of iron in cells, this finding provides evidence that iron was released from the particles within the cells. Aust and colleagues established that transition metals released from particles induce oxidative stress and that iron release from particles occurs intracellularly. They then linked these findings with the inflammatory process by demonstrating that cultured human lung epithelial cells exposed to CFA particles produced the inflammatory mediator IL-8 and that its production was reduced by antioxidants. Hetland and coworkers (2000) have shown that the same human lung epithelial cell line used in this study produces IL-8 and IL-6 in the presence of iron-containing stone quarry particles of 8 to 10 µm aerodynamic diameter.

The investigators' findings bring significant insight and creativity to the study of particle-associated lung injury by metal-catalyzed oxidative stress and subsequent lung inflammation. This study provides new and useful information regarding differences in particle activity as a function of size. The investigators made the important observation that, in agreement with ROS production and iron mobilization by citrate, smaller particles more actively produced ferritin (and thus contained more bioavailable iron) and IL-8 than larger particles. The results across the various particles tested are internally consistent and strengthen the conclusion that smaller particles may contain higher levels of bioavailable transition metals. The investigators' observations that the total iron content of particles correlated with neither the amount of iron mobilized by citrate nor the effects of CFA particles on epithelial cells support their proposal that a critical determinant of a particle's pathologic effects is its amount of bioavailable iron. The greater biological activity of the smaller CFA particles would tend to support the epidemiologic evidence for adverse health effects of $PM_{2.5}$ (Dockery et al 1993; Pope et al 1995) and suggests what may be a credible mechanism by which injury may occur. However, these results were obtained in vitro. To extend them to the situation in vivo, Aust and colleagues will measure ferritin levels in lung tissue and lavage fluid from rats exposed to CFA by inhalation in a new study supported by HEI. Further studies in humans would also provide additional credibility.

Reactions catalyzed by soluble transition metals are not the only mechanism that can cause lung inflammation. For example, inflammation may be caused by reactive gases and free radicals bound by fine and ultrafine particles transported deep into the lung. In addition, researchers have proposed that genotoxic polycyclic aromatic hydrocarbons associated with inhaled diesel exhaust particles, most of which are less than 1 µm in aerodynamic diameter, become bioavailable (Sun et al 1984; Bond et al 1986; Gerde et al 2001). If so, they have the potential to produce DNA mutations in lung cells.

SUMMARY AND CONCLUSIONS

This study by Aust and colleagues was of high scientific quality, was well conceived and executed, and adds substantially to our knowledge of the biological properties of

particles. The investigators studied particles from fly ash produced from three sources of coal, gasoline and diesel engine exhaust, natural soils and metallurgic mine tailings, and Salt Lake City air. The abundance of CFA sampled allowed the investigators to fractionate the particles into four size classes (PM_1, $PM_{2.5}$, $PM_{2.5–10}$, and $PM_{>10}$) and to conduct detailed physical and chemical analyses of each class before proceeding to study the particles' biological effects in cultured human lung epithelial cells.

The investigators demonstrated a plausible in vitro connection among the intracellular release of transition metals from particles (with a focus on size-fractionated CFA particles), oxidative stress caused by ROS production, and lung inflammation. Using a cell-free system, they found that both ROS production catalyzed by transition metals and solubilization of iron were greater for small particles than for coarser fractions. The solubilized iron was associated with aluminosilicates rather than oxides. The smaller CFA particles were enriched in aluminosilicates.

Aust and colleagues demonstrated that cultured human lung epithelial cells exposed to CFA particles synthesized ferritin, a protein that is produced in response to the presence of iron in cells, and that ferritin production depended on the uptake of the particles by the cells. Thus, iron released intracellularly from particles, as demonstrated by ferritin synthesis, had the capacity to produce ROS, which in turn caused oxidative stress that can trigger the inflammatory process. The finding that cultured human lung epithelial cells exposed to CFA produced the inflammatory mediator IL-8 links the release of iron (or other PM-associated transition metals) with lung inflammation and possible injury. To extend their in vitro results, to the in vivo situation, Aust and colleagues will measure ferritin levels in lung tissue and lavage fluid from rats exposed to CFA in a new study supported by HEI. Other components or properties of particles have been proposed to cause lung injury as well; therefore, there may be multiple mechanisms by which inhaled particles produce adverse health effects. Further research to identify particle characteristics (and sources) responsible for PM toxicity is important for developing increasingly effective and appropriate air quality regulations, as noted in HEI Perspectives, *Understanding the Health Effects of Components of the Particulate Matter Mix: Progress and Next Steps* (HEI 2002).

ACKNOWLEDGMENTS

The Health Review Committee thanks the ad hoc reviewers for their help in evaluating the scientific merit of the Investigators' Report. The Committee is also grateful to Maria Costantini for her oversight of the study, to Bernard Jacobson for his assistance in preparing its Commentary, and to Sally Edwards, Ruth Shaw, Jenny Lamont, and Quentin Sullivan for their roles in publishing this Research Report.

REFERENCES

Becker S, Soukup JM, Gilmour MI, Devlin RB. 1996. Stimulation of human and rat alveolar macrophages by urban air particulates: Effects on oxidant radical generation and cytokine production. Toxicol Appl Pharmacol 141:637–648.

Bond JA, Sun JD, Medinsky MA, Jones RK, Yeh HC. 1986. Deposition, metabolism, and excretion of 1-[^{14}C] nitropyrene and 1-[^{14}C] nitropyrene coated on diesel exhaust particles as influenced by exposure concentration. Toxicol Appl Pharmacol 85:102–117.

Borm PJA. 1997. Toxicity and occupational health hazards of coal fly ash (CFA). A review of data and comparison to coal mine dust. Ann Occup Hyg 41:659–676.

Carter JD, Ghio AJ, Samet JM, Devlin RB. 1997. Cytokine production by human airway epithelial cells after exposure to an air pollution particle is metal-dependent. Toxicol Appl Pharmacol 146:180–188.

Chemical and Engineering News. 2000. EPA declines to list coal ash as hazardous. 78:38.

Costa DL, Dreher KL. 1997. Bioavailable transition metals in particulate matter mediate cardiopulmonary injury in healthy and compromised animal models. Environ Health Perspect 105 (Suppl 5):1053–1060.

Dockery DW, Pope CA III. 1994. Acute respiratory effects of particulate air pollution. Annu Rev Public Health. 15:107–132.

Dockery DW, Pope CA III, Xu X, Spengler JD, Ware JH, Fay ME, Ferris BG Jr, Speizer FE. 1993. An association between air pollution and mortality in six US cities. N Engl J Med 329:1753–1759.

Dreher KL, Jaskot RH, Lehmann JR, Richards JH, McGee JK, Ghio AJ, Costa DL. 1997. Soluble transition metals mediate residual oil fly ash induced acute lung injury. J Toxicol Environ Health 50:285–305.

Dye JA, Adler KB, Richards JH, Dreher KL. 1999. Role of soluble metals in oil fly ash-induced airway epithelial injury and cytokine gene expression. Am J Physiol 277 (Lung Cell Mol Physiol 21):L498–L510.

Environmental Protection Agency (US). 1993. National Air Quality and Emissions Trends Report, 1993. EPA 454/R-94-026. Office of Air Quality Planning and Standards, Research Triangle Park NC.

Environmental Protection Agency (US). 1996. Air Quality Criteria for Particulate Matter, Vol I. EPA/600/P-95/001af. Office of Research and Development, Washington DC.

Environmental Protection Agency (US). 2000. Wastes from Coal Burning to be Addressed. Headquarters Press Release, April 25. EPA, Washington DC.

Esaka F, Takahashi S, Sato H, Kubota Y, Kikuchi T, Furuya K. 1995. Concentrations of metal elements in mouse organs after intratracheal administration of coal fly ash. J Toxicol Sci 20:103–108.

Fang R. 1999. Induction of Ferritin Synthesis in Human Lung Epithelial Cells (A549) Treated with Iron-Containing Particulates and Iron Mobilization from These Particulates [dissertation]. Utah State University, Logan UT.

Gerde P, Muggenburg BA, Lundborg M, Tesfaigzi Y, Dahl AR. 2001. Respiratory Epithelial Penetration and Clearance of Particle-Borne Benzo[*a*]pyrene. Research Report 101. Health Effects Institute, Cambridge MA.

Ghio AJ, Samet JM. 1999. Metals and air pollution particles. In: Air Pollution and Health (Holgate ST, Samet JM, Koren HS, Maynard RL, eds), pp 635–651. Academic Press, San Diego CA.

Ghio AJ, Stonehuerner J, Dailey LA, Carter JD. 1999. Metals associated with both the water-soluble and insoluble fractions of an ambient air pollution particle catalyze an oxidative stress. Inhalation Toxicol 11:37–49.

Gilmour MI, Selgrade MJK, Lambert AL. 2000. Enhanced allergic sensitization in animals exposed to particulate air pollution. Inhalation Toxicol 12 (Suppl 3):373–380.

Godleski JJ, Verrier RL, Koutrakis P, Catalano P. 2000. Mechanisms of Morbidity and Mortality from Exposure to Ambient Air Particles. Research Report 91. Health Effects Institute, Cambridge MA.

Hardy JA, Aust A. 1995. Iron in asbestos chemistry and carcinogenicity. Chem Rev 95:97–118.

Health Effects Institute. 1994. HEI Strategic Plan for Vehicle Emissions and Fuels 1994–1998. Health Effects Institute, Cambridge MA.

Health Effects Institute. 1999. Research on Particulate Matter (HEI Research Program Summary). Health Effects Institute, Cambridge MA.

Health Effects Institute. 2000. HEI Strategic Plan for the Health Effects of Air Pollution 2000–2005. Health Effects Institute, Cambridge MA.

Health Effects Institute. 2002. Understanding the Health Effects of Components of the Particulate Matter Mix: Progress and Next Steps. HEI Perspectives. Health Effects Institute, Boston MA.

Hetland RB, Refsnes M, Myran T, Johansen BV, Uthus N, Schwarze PE. 2000. Mineral and/or metal content as critical determinants of particle-induced release of IL-6 and IL-8 from A549 cells. J Toxicol Environ Health, Part A, 60:47–65.

Jiang NF, Dreher KL, Dye JA, Li YH, Richards JH, Martin LD, Adler KB. 2000. Residual oil fly ash induces cytotoxicity and mucin secretion by guinea pig tracheal epithelial cells via an oxidant-mediated mechanism. Toxicol Appl Pharmacol 163:221–230.

Kadiiska MB, Mason RP, Dreher KL, Costa DL, Ghio AJ. 1997. *In vivo* evidence of free radical formation in the rat lung after exposure to an emission source air pollution particle. Chem Res Toxicol 10:1104–1108.

Kodavanti UP, Hauser R, Christiani DC, Meng ZH, McGee J, Ledbetter A, Richards J, Costa DL. 1998. Pulmonary responses to oil fly ash particles in the rat differ by virtue of their specific soluble metals. Toxicol Sci 43:204–212.

Kodavanti UP, Jaskot RH, Costa DL, Dreher KL. 1997. Pulmonary proinflammatory gene induction following acute exposure to residual oil fly ash: Roles of particle-associated metals. Inhalation Toxicol 9:679–701.

Linak WP, Wendt JOL. 1994. Trace metal transformation mechanisms during coal combustion. Fuel Processing Technol 39:173–198.

Liochev SI, Fridovich I. 1991. The roles of O_2^-, HO• and secondarily derived radicals in oxidation reactions catalyzed by vanadium salts. Arch Biochem Biophys 291:379–382.

Madden MC, Thomas MJ, Ghio AJ. 1999. Acetaldehyde (CH_3CHO) production in rodent lung after exposure to metal-rich particles. Free Radic Biol Med 26:1569–1577.

Moolgavkar SH, Luebeck EG. 1996. A critical review of the evidence on particulate air pollution and mortality. Epidemiology 7:420–428.

Ostro B. 1993. The association of air pollution and mortality: Examining the the case for inference. Arch Environ Health 48:336–342.

Pope CA III, Thun MJ, Namboodiri MM, Dockery DW, Evans JS, Speizer FE, Heath CW. 1995. Particulate air pollution as a predictor of mortality in a prospective study of US adults. Am J Respir Crit Care Med 151:669–674.

Pritchard RJ, Ghio AJ, Lehmann JR, Winsett DW, Tepper JS, Park P, Gilmour MI, Dreher KL, Costa DL. 1996. Oxidant generation and lung injury after particulate air pollutant exposure increase with the concentrations of associated metals. Inhalation Toxicol 8:457–477.

Samet JM, Zeger SL, Birhane K. 1995. The association of mortality and particulate air pollution. In: Particulate Air Pollution and Daily Mortality: Replication and Validation of Selected Studies (The Phase I.A Report of the Particle Epidemiology Evaluation Project). Health Effects Institute, Cambridge MA.

Samet JM, Zeger SL, Dominici F, Curriero F, Coursac I, Dockery DW, Schwartz J, Zanobetti A. 2000. The National Morbidity, Mortality, and Air Pollution Study, Part II. Morbidity and Mortality from Air Pollution in the United States. Research Report 94. Health Effects Institute, Cambridge MA.

Samet JM, Zeger SL, Kelsall JE, Xu J, Kalkstein LS. 1997. Air pollution, weather, and mortality in Philadelphia. In: Particulate Air Pollution and Daily Mortality: Analysis of the Effects of Weather and Multiple Air Pollutants (The Phase I.B Report of the Particle Epidemiology Evaluation Project). Health Effects Institute, Cambridge MA.

Shi X, Jiang H, Mao Y, Ye J, Saffiotti U. 1996. Vanadium(IV)-mediated free radical generation and related 2'-deoxyguanosine hydroxylation and DNA damage. Toxicology 106:27–38.

Srivastava VK, Chauhan SS, Srivastava PK, Shukla RR, Kumar V, Misra UK. 1990. Placental transfer of metals of coal fly ash into various fetal organs of rat. Arch Toxicol 64:153–156.

Stringer B, Kobzik L. 1998. Environmental particulate-mediated cytokine production in lung epithelial cells (A549): Role of preexisting inflammation and oxidant stress. J Toxicol Environ Health 55:31–44.

RELATED HEI PUBLICATIONS: PARTICULATE MATTER

Report Number	Title	Principal Investigator	Publication Date*
Research Reports			
105	Pathogenomic Mechanisms for Particulate Matter Induction of Acute Lung Injury and Inflammation in Mice	GD Leikauf	2001
104	Inhalation Toxicology of Urban Ambient Particulate Matter: Acute Cardiovascular Effects in Rats	R Vincent	2001
96	Acute Pulmonary Effects of Ultrafine Particles in Rats and Mice	G Oberdörster	2000
91	Mechanisms of Morbidity and Mortality from Exposure to Ambient Air Particles	JJ Godleski	2000
HEI Communications			
5	Formation and Characterization of Particles: Report of the 1996 HEI Workshop		1997
HEI Perspectives			
	Airborne Particles and Health: HEI Epidemiologic Evidence		June 2001
	Understanding the Health Effects of Components of the Particulate Matter Mix: Progress and Next Steps		April 2002

** Reports published since 1990, with exceptions.*
Copies of these reports can be obtained from the Health Effects Institute and many are available at www.healtheffects.org.

HEALTH
EFFECTS
INSTITUTE

Charlestown Navy Yard
120 Second Avenue
Boston MA 02129-4533 USA
+1-617-886-9330
www.healtheffects.org

RESEARCH
REPORT

Number 110
December 2002